

**A SURVEY OF THE MAINLAND AND ISLAND BELTS,  
THUNDER BAY SILVER DISTRICT, ONTARIO:  
FLUID INCLUSIONS, MINERALOGY,  
AND SULFUR ISOTOPES**

by

ELIZABETH ANNE JENNINGS



Submitted in partial fulfillment  
of the requirement for the degree of

MASTER OF SCIENCE.

Faculty of Arts and Science  
Lakehead University  
Thunder Bay, Ontario, Canada

May, 1987

ProQuest Number: 10611752

All rights reserved

INFORMATION TO ALL USERS

The quality of this reproduction is dependent upon the quality of the copy submitted.

In the unlikely event that the author did not send a complete manuscript and there are missing pages, these will be noted. Also, if material had to be removed, a note will indicate the deletion.



ProQuest 10611752

Published by ProQuest LLC (2017). Copyright of the Dissertation is held by the Author.

All rights reserved.

This work is protected against unauthorized copying under Title 17, United States Code  
Microform Edition © ProQuest LLC.

ProQuest LLC.  
789 East Eisenhower Parkway  
P.O. Box 1346  
Ann Arbor, MI 48106 - 1346

Permission has been granted to the National Library of Canada to microfilm this thesis and to lend or sell copies of the film.

The author (copyright owner) has reserved other publication rights, and neither the thesis nor extensive extracts from it may be printed or otherwise reproduced without his/her written permission.

L'autorisation a été accordée à la Bibliothèque nationale du Canada de microfilmer cette thèse et de prêter ou de vendre des exemplaires du film.

L'auteur (titulaire du droit d'auteur) se réserve les autres droits de publication; ni la thèse ni de longs extraits de celle-ci ne doivent être imprimés ou autrement reproduits sans son autorisation écrite.

ISBN 0-315-39588-5

## ABSTRACT

The Thunder Bay Silver District is composed of two curvilinear groups of veins, the Mainland and Island Belts. The veins can be mineralogically divided into the barren, silver-bearing, and S-element association veins.

During the present study, fluid inclusion, sphalerite composition, and sulfur isotopic composition were investigated, as well as some aspects of the mineralogy of the veins. Fluid inclusions in quartz, calcite, and fluorite indicate temperatures ranging from 70°–450°C during vein deposition could be found in veins of both geographical and all mineralogical groups. Fluid inclusions in sphalerite indicate ore minerals were deposited between 80°–120°C at all locations. Salinity of the hydrothermal solutions was highly variable, 1–30 equiv. wt. % NaCl. The dominant salt in solution was CaCl<sub>2</sub>.

Fe content in sphalerite indicates a log  $a_{S_2}$  of -18 to -25 during ore deposition at all deposits except Spar Island. At Spar Island copper sulfide mineralogy suggests log  $a_{S_2}$  of -14 to -18. Sphalerite often contained trace quantities of Cd.

Sulfur isotopic composition of sulfides and barite ranged from -9.7 to +12.2%, with two anomalous values (near +30%) from supergene samples. Paired data indicate isotopic non-equilibrium during deposition of sulfides.

The consistency of fluid inclusion, sulfur activity, and sulfur isotopic data suggest both depositional environment and hydrothermal fluid source were similar for all veins in the Thunder Bay district. Heterogeneity of the deposits, particularly the presence or absence of Ag, Ni, Co, and As may be due to the evolution of the fluids between their inception and entry into the depositional environment.

The source of the fluids is unknown, although their original sulfur isotopic composition is inferred to be fairly low (+4.7%), suggesting a magmatic source of sulfur is possible.

TABLE OF CONTENTS

Abstract .....	i
Table of Contents .....	ii
List of Figures .....	iv
List of Tables .....	vi
Acknowledgements .....	1
Introduction .....	2
Regional Geology .....	6
Vein Geology .....	15
Vein Classification .....	15
Previous Work .....	20
Rabbit and Silver Mountain Groups .....	21
Little Pig Vein - West Beaver Mine .....	23
No. 2 Vein - West Beaver Mine .....	24
Big Harry Vein .....	24
Rabbit Mountain Mine .....	25
Porcupine (Creswel) Mine .....	26
Silver Creek .....	27
Badger Mine .....	28
Keystone (Climax) Mine .....	28
Silver Mountain .....	29
Port Arthur Group .....	31
Silver Harbour (Beck) Mine .....	32
Algoma Mine .....	33
3A Mine .....	33
Shuniah Mine .....	34
Thunder Bay Mine .....	35
Island Belt .....	35
Silver Islet .....	36
Jarvis Island .....	39
Victoria Island .....	40
Spar Island .....	41
Edward Island .....	42
Fluid Inclusions .....	43
Introduction .....	43
Experimental Technique .....	50
Results - Freezing .....	51
Results - Heating .....	61
Temperature Correction Due to Pressure .....	88

	111
<b>Mineralogical Investigations</b> .....	<b>92</b>
Introduction .....	92
Experimental Technique .....	92
Microprobe Results .....	93
Discussion .....	103
X-ray Diffraction .....	106
<b>Sulfur Isotopic Composition</b> .....	<b>108</b>
Introduction .....	108
Experimental Technique .....	109
Results .....	109
Discussion .....	112
<b>Physical and Chemical Conditions of Ore Deposition</b> .....	<b>117</b>
<b>Vein Genesis</b> .....	<b>125</b>
Genesis of Veins of the Five-element Association .....	125
Models of Formation of the Thunder Bay District Veins .....	128
Application of Fluid Inclusion and Sulfur Isotopic Data to Genetic Models .....	137
<b>Conclusions</b> .....	<b>146</b>
<b>References</b> .....	<b>150</b>
<b>Appendix 1</b> .....	<b>156</b>
<b>Appendix 2</b> .....	<b>158</b>
<b>Appendix 3</b> .....	<b>159</b>

LIST OF FIGURES

Figure	1.	Location of Thunder Bay Silver District .....	3
Figure	2.	Geology of the Thunder Bay Silver District ...	7
Figure	3.	Geology of the Proterozoic rocks of the Lake Superior area .....	14
Figure	4A.	Classification of silver veins in the Thunder Bay District according to Ingall (1888) .....	16
Figure	4B.	Classification of silver veins in the Thunder Bay District according to Bowen (1911) and Oja (1967) .....	16
Figure	5.	Locations of veins sampled during the present study .....	17
Figure	6.	Orientation of veins in Mainland and Island Belts .....	19
Figure	7.	Two-phase (L+V) fluid inclusion in calcite hosted by sphalerite .....	45
Figure	8.	Two-phase (L+V) fluid inclusion showing negative crystal form .....	45
Figure	9.	Field of primary fluid inclusions containing 20-35 volume percent vapour .....	46
Figure	10.	Primary three-phase (L+V+S) fluid inclusion ..	46
Figure	11.	Plane of secondary inclusions in sphalerite ..	49
Figure	12.	Histograms of microthermometric freezing determinations and salinity of fluid inclusions .....	56
Figure	13.	Behaviour of fluid inclusions from the Keystone and Silver Mountain Mines during freezing microthermometry .....	57
Figure	14.	Histogram of microthermometric homogenization temperatures in sphalerite from all mines ....	62
Figure	15.	Histogram of microthermometric homogenization and decrepitation temperatures of inclusions in quartz and fluorite from all mines .....	63
Figure	16.	Histogram of microthermometric homogenization and precipitation temperatures of inclusions in calcite from all mines .....	64

Figure 17.	The relationship between paragenetic sequence and homogenization temperature from Mainland and Island Belt Mines .....	74
	A. West Beaver No. 2 Mine .....	75
	B. West Beaver Little Pig Vein .....	75
	C. Badger .....	76
	D. Porcupine .....	76
	E. Big Harry .....	77
	F. Silver Creek .....	77
	G. Rabbit Mountain .....	78
	H. Keystone (Climax) .....	78
	I. Silver Mountain .....	79
	J. Shuniah .....	80
	K. Silver Harbour (Beck) .....	80
	L. Thunder Bay .....	80
	M. 3A .....	81
	N. Victoria Island .....	82
	O. Jarvis Island .....	82
	P. Spar Island .....	83
	Q. Silver Islet .....	84
Figure 18.	Comparison of homogenization temperatures to trapping temperatures of fluid inclusions assuming 1000m burial .....	91
Figure 19.	Typical textures observed in Silver Islet ore .....	101
Figure 20.	Sulfur activity during sulfide deposition ....	104
Figure 21.	Sulfur isotopic composition of sphalerite-galena pairs .....	113
Figure 22.	Fractionation of sulfur isotopes at varying temperature and oxygen activity conditions ...	121
Figure 23.	Probable fields of ore precipitation (100°C) at Spar Island, Mainland Belt, and Silver Islet .....	122
Figure 24.	Sulfur activity during sulfide deposition at Spar Island .....	124
Figure 25.	Summary plot of lead isotopic composition ....	136
Figure 26.	Relationship between depositional temperature and time at a typical Mainland vein .....	139
Figure 27.	Relationship between depositional temperature and time at Spar Island .....	140
Figure 28.	$T_H$ vs $T_m$ plot .....	143

PLEASE NOTE PAGE vi IS NOT MISSING  
(SEE TABLE OF CONTENTS).

VEUILLEZ NOTER PAGE vi NE MANQUE  
PAS (VOIR TABLE OF CONTENTS).

LIST OF TABLES

Table 1A.	Age Determinations of the Animikie Sediments ...	10
Table 1B.	Age Determinations of Mafic Intrusions .....	10
Table 2.	Calibration of Chaixmeca Stage .....	53
Table 3.	Microthermometric Freezing Data .....	58
Table 4.	Microthermometric Heating Observations .....	66
Table 5.	Microprobe Analyses of Sphalerite Composition ..	95
Table 6.	Microprobe Analyses of Native Silver and Native Arsenic .....	98
Table 7.	Microprobe Analyses of Arsenides and Sulfarsenides from the Island Belt .....	102
Table 8.	Sulfur Isotope Ratio Analyses .....	111
Table 9.	Trace Metals in the Rove Shale .....	133

## ACKNOWLEDGEMENTS

My thanks, first, to Dr. S. A. Kissin, whose guidance and assistance made this project possible. The support and help of many other people throughout this project is also gratefully acknowledged: Dr. A. H. Clarke of Queen's University for the use of the Chaixmeca stage and A. Anderson for his patience teaching me to use it and many useful discussions on fluid inclusion behaviour; Dr. C. Cermignani of the University of Toronto for his help with the electron microprobe; Dr. G. Patterson of the Ministry of Northern Development and Mines for many useful discussions and samples; Dr. F. Wicks of the Royal Ontario Museum for specimens; Dr. T. Griffith of the Lakehead University Instrumentation Laboratory for help with X-ray diffraction studies; and D. Cruthers, A. Hammond, and R. Bennett for help making polished sections. Special thanks to Gail Jennings for patient typing of this manuscript. Financial assistance was obtained from the Ontario Geological Survey to Dr. Kissin (OGRF 300). Research was also supported by the Natural Sciences and Engineering Research Council of Canada operating grant No. A3814 to Dr. Kissin (1984-86). In addition, personal support through a Lakehead Graduate Entrance Scholarship was received.

## INTRODUCTION

The Thunder Bay Silver District lies along the northwest shore of Lake Superior, Ontario, Canada (Figure 1). It lies within the Southern Structural province, hosted by a belt of weakly metamorphosed sediments of Aphebian age, and associated with a series of mafic intrusions of Helikian age.

Silver veins were first discovered in the Thunder Bay area in 1846 when Prince's mine was first worked, although the main interest in this vein was its abundant copper. During the mid 1860s the discovery of veins on the shore of Lake Superior and on a tiny island offshore led to the development of the Silver Islet and Thunder Bay Mines and firmly established the area as an important silver producer.

From 1882 to 1891 a second boom in silver mining in the area occurred when Oliver Daunais discovered silver-bearing veins in the Silver Mountain and Rabbit Mountain areas. During the 1890s a sharp decline in the price of silver effectively ended production from these mines. Attempts to reopen mines during the early 1900s proved unprofitable, although material from some dumps and dredged from the Silver Islet dock area has been processed recently.

A comprehensive summary of vein descriptions was completed

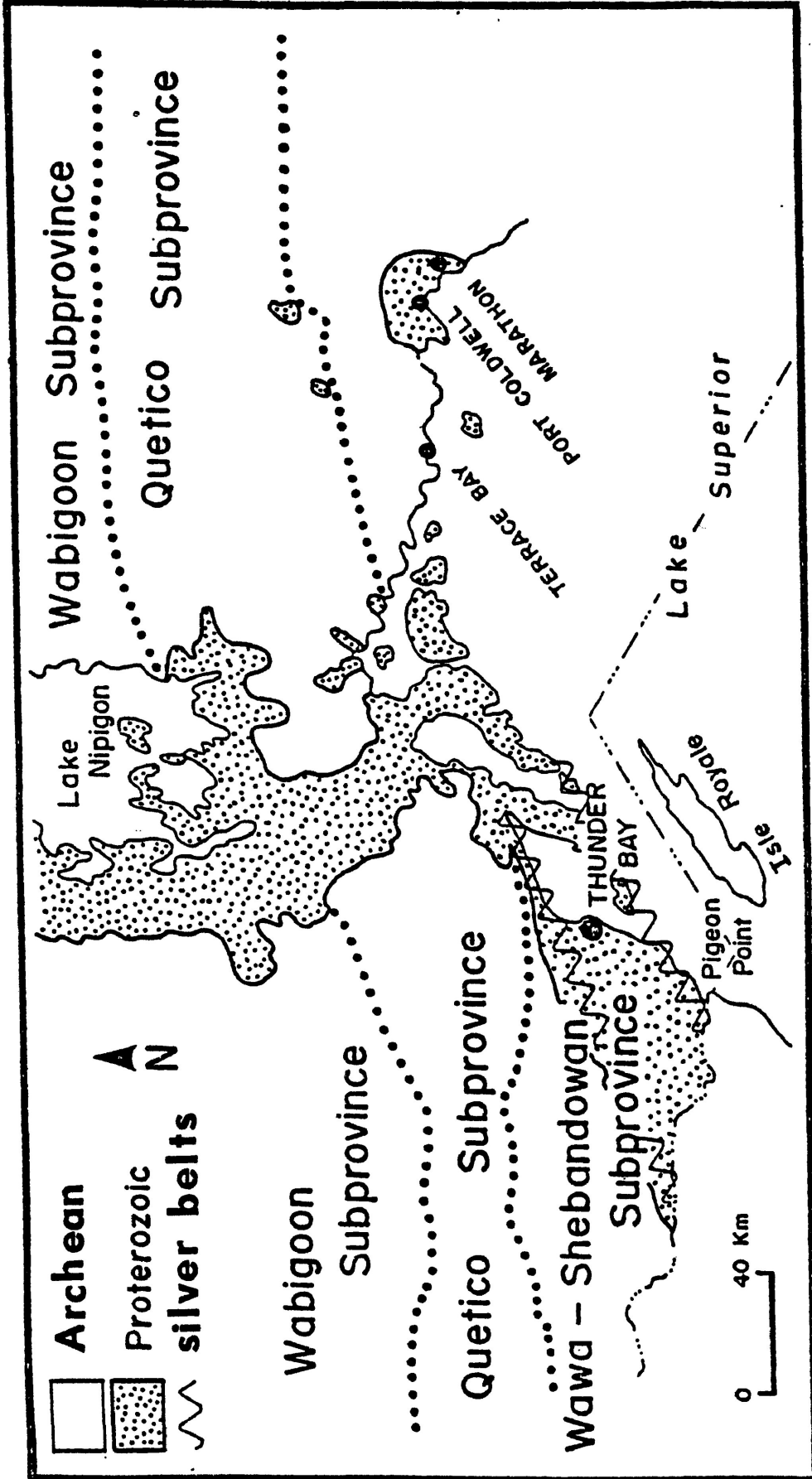


Figure 1: Location of Thunder Bay Silver District. Modified after Franklin et al. (in press).

by Tanton (1931), and has served as a base for most later work. Tanton documented the presence of fluid inclusion in the vein systems at the Silver Islet, Beaver, and Shuniah mines, where pockets of inflammable gas were encountered during mining. The composition of the gas at the Beaver and Shuniah mines was never analyzed; however, at Silver Islet it was found to contain "chlorides of calcium, sodium, magnesium and potassium, calcium carbonate, and calcium sulphate accompanied by inflammable gas... It may have been hydrogen sulphide, which was detected in the mine in 1920, or it may have been a hydrocarbon" (Tanton, 1931).

The mines in the Thunder Bay area were economically important for a brief period of time; however, they are quite significant geologically in that they have quite a variable nature, including veins of the:

- 1) five-element (Ag-Ni-Co-As-Bi) affinity, e.g. the Silver Islet vein,
- 2) simple polymetallic (Ag-Pb-Zn-Cu-Ba) type, e.g. Silver Mountain vein, and
- 3) the base metal (Pb-Zn-Ba) type, e.g. Victoria Island.

The genesis of the five-element association veins is enigmatic (Halls and Stumpfl, 1972), and the similarity of the Silver Islet vein to the ore deposits found in the Cobalt and Great Bear Lake districts is striking. It would be useful, then, to compare

five-element vein genesis to genesis of the less complex veins in the area.

The purpose of this study is to determine the environment of deposition of veins representative of each of the three types itemized, and to deduce from this:

- 1) a genetic model of vein formation, and
- 2) the particular differences in genesis which led to the formation of each of the three distinctive vein types.

To do this, three types of investigation were undertaken and are presented in this thesis:

- 1) a microthermometric study of fluid inclusions in vein material to determine trapping temperatures and fluid salinity,
- 2) an examination of mineralogy and paragenesis of a number of vein systems, including mapping and sample collection, and
- 3) a sulfur isotope study of sphalerite, galena, pyrite, and barite.

The study surveys the complete range of vein types, using as many examples as possible rather than focusing comprehensively on any particular vein.

## REGIONAL GEOLOGY

The Thunder Bay area lies in the Southern structural province, and is composed of Precambrian strata of Archean and Proterozoic age. (Figure 2)

The Archean basement is a steeply dipping assemblage of metamorphosed volcanic and sedimentary strata, intruded by granitoid plutons and batholiths during the Kenoran orogeny. It is unconformably overlain by the Aphebian Animikie Group, comprised of the Rove and Gunflint Formations. The entire area is host to a number of mafic intrusions, including the Logan diabase sills, Pine Point - Mount Mollie gabbro and the Pigeon River diabase dykes (Geul, 1970, 1973).

The Animikie Group is composed of two formations: the older Gunflint Formation and the younger Rove Formation. The geology of these sediments has been described by Goodwin (1956), Franklin (1970, 1982), Morey (1972) and Shegelski (1982). In Canada, the Animikie is exposed between Gunflint Lake, near the Canada-U.S. border, and Thunder Bay, and sporadically as far east as Schreiber, Ontario.

The Gunflint Formation has a maximum thickness of 180m in the Thunder Bay area, 100m in northern Minnesota. Goodwin (1956) subdivided the Gunflint formation into six facies, from bottom to

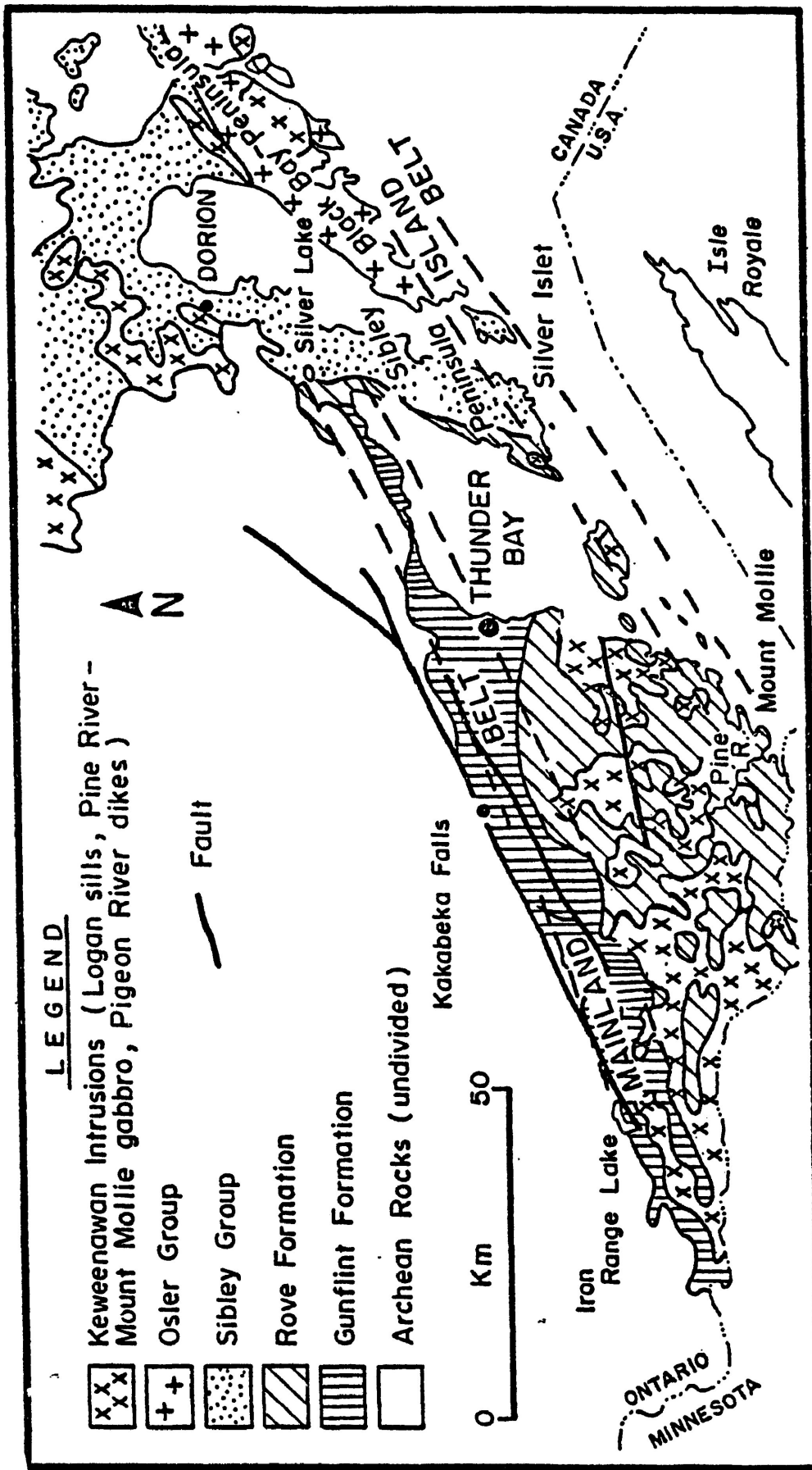


Figure 2: Geology of the Thunder Bay Silver District. Modified after Franklin et al. (in press).

top: the basal conglomerate facies, the algal chert facies, the shale facies, the taconite facies, the chert-carbonate facies and the limestone facies. The lower contact of the Gunflint Formation is unconformable and knife-sharp; it is here that the first facies mentioned, the discontinuous "Kakabeka conglomerate", is found. The following four facies mentioned were thought to represent a depositional cycle found twice in the stratigraphic column. Shegelski (1982) suggested that in fact these "facies" are lens shaped horizons, discontinuous and repeated throughout the region, forming a more complicated stratigraphy. The uppermost unit is composed of limestone and dolostone, which has a gradational contact with the overlying Rove shale.

Goodwin suggested deposition occurred in a restricted basin bordering an open sea. An active volcanic region provided a source for sediments as well as a mechanism for disturbing the basin and causing cyclicity of sedimentation. Shegelski (1982) suggested, instead, a series of partially restricted basins along an intratidal carbonate shelf. Algal cherts are representative of barrier islands, shales of lagoonal areas and mudflats. Grainstones are the product of mixed biochemical and clastic sedimentation; some of them are reworked sediments.

The Rove Formation is up to 600m thick in the Thunder Bay area, but thickens to over 1000m in Minnesota. It has been

divided by Morey (1969) into three facies: the lower argillite, the transitional sequence, and the upper, thin-bedded greywacke facies. In the Thunder Bay area only the lower argillite occurs to any extent. From the base to the top of the Rove Formation, the following units are found: a thin-to-thick-bedded grey argillite showing some primary structures such as crossbedding and grading; a very thin bedded dark grey silty argillite; and a pyritic, carbonaceous, black argillite. The shale commonly contains thin lenses of carbonate and ellipsoidal carbonate concretions up to one meter in diameter.

The shales of the Rove Formation were deposited in relatively quiet waters, indicating a steady subsidence of the basin. Particularly to the south, in Minnesota, the rate of downwarping of the basin was greater than sedimentation rates, so that a gradual increase in slope of the basin margin occurred and the number of deposits resulting from turbidity currents increased. Shegelski noted that the Rove shales could be laterally equivalent to, as well as overlying the Gunflint Formation and that the Rove-Gunflint contact is totally gradational.

Table 1A summarizes radiometric ages determined for the Animikie ages. The actual age of sediment deposition, based on the Nd-Sm method (Stille and Clauer, 1986), is thought to be 2.080Ga. Previous work using K-Ar and Rb-Sr methods had

**TABLE 1A: AGE DETERMINATIONS OF THE ANIMIKIE SEDIMENTS**

<u>AGE (Ga)</u>	<u>SOURCE</u>	<u>METHOD</u>	<u>AUTHOR(S)</u>
1.6±0.5	Gunflint Argillite	K-Ar	Hurley et al 1962)
1.57	Rove } Virginia) Formations Thompson}	Rb-Sr	Peterman (1966)
1.63±.024	Gunflint) Formations Rove }	Rb-Sr	Kovach & Faure (1969)
1.556±.064	Rove Formation	Rb-Sr	Franklin (1978)
2.08±0.25	Gunflint Formation	Sm-Nd	Stille & Claire (1986)

**TABLE 1B: AGE DETERMINATIONS OF THE MAFIC INTRUSIONS**

1.3	Logan Sills	K-Ar	Hanson & Malhotra (1971)
0.9-1.1	Pigeon River Dykes	K-Ar	" "
0.99-1.1	Logan Sills	paleomag- netism	Robertson & Fahrig (1971)
0.73-1.06	Logan Sills	K-Ar	" "
1.109±0.2	Logan Sills	U-Pb	Davis & Sutcliffe (1984)

indicated ages of 1.56 to 1.9Ga, indicating the times of closure of the isotopic systems. Although the sediments appear undeformed, the discrepancy in the age determinations suggest a period of regional metamorphism closing at 1.65Ga (Franklin et al., in press).

Three types of mafic intrusions occur in the Thunder Bay region: the Early Mafic Intrusions, or Logan Sills, the Pigeon River Mafic Dykes, and the Pine River-Mount Mollie Gabbro.

The Early Mafic Intrusions have been described by Blackadar (1956), Geul (1970, 1973), and Weiblen et al. (1972). In the Thunder Bay region they are a series of tholeiitic quartz diabase sills 5-25m thick, but they thicken to the east, in the Lake Nipigon region, to over 100m. They can generally be divided into three zones: the lowest basal or chill zone; the central microcrystalline or subophitic zone; and the upper diabasic, relatively felsic zone. Some diabase is plagioclase porphyritic. Red granophyric phases are found locally at the top of a number of sills; these have been attributed to assimilation of granitic material rather than differentiation of the diabase magma (Blackadar 1956). The grain size and mineralogy of the sills, particularly the presence or absence of quartz and olivine, change abruptly across a typical section of a sill. This suggests a sequence of penecontemporaneous magma intrusions, each pulse not quite solidifying before the next event. These bodies

are characterized by a reverse magnetic polarity.

K-Ar ages of the sills vary from 0.73-1.36Ga (Table 1B), the large variation due to escape of Ar from whole rock samples (Robertson and Fahrig, 1971). Paleomagnetic data supports an age of 0.99-1.16Ga (Robertson and Fahrig, 1971), which is similar to K-Ar age obtained for the Pigeon River dykes.

The Pigeon River Mafic Dykes are a northeast-striking swarm of dykes exposed on the shore of Lake Superior and forming a chain of islands within the lake. They are fine- to medium-grained olivine diabase, and locally, plagioclase porphyritic. Some of these dykes clearly cross-cut the Logan Sills, and all can be distinguished by their normal magnetic polarity.

The Pine River - Mount Mollie gabbro is the youngest of the mafic intrusions with a K-Ar age of 1.0456Ga (Geul, 1973). It is an east-striking, anorthositic to quartz bearing gabbro, interconnected with the layered Crystal Lake gabbro. The presence of deuteric alteration is observed, as evidenced by the presence of biotite, secondary amphibole, saussurite, sericite, and hematite. The gabbro is characterized by normal magnetic polarity.

The Thunder Bay silver district lies within the Southern Province, which has been described by Card et al. (1972). The

Animikie sediments show a regional warping, dipping 2-10° southeast. At local interfaces with mafic intrusions deformation can be more intense.

The structural geology of the area is dominantly related to the formation of the Lake Superior Syncline, which generally coincides with the Mid-Continent Gravity High, during the Keweenawan (Figure 3). Three fault subparallel systems were developed at this time as described by Franklin (1982), the three sets forming arcuate bands subparallel to the axis of the Lake Superior Syncline striking 060° to 070° and dipping steeply south. The two more northerly fracture belts host the silver veins. Movement of these faults is largely normal, but reverse motion was noted at the Porcupine Mine (Franklin, 1970) and is common in the most southerly belt passing through Isle Royale.

Many of the fault zones contain mafic dykes, and movement can often be seen to postdate as well as precede their emplacement.

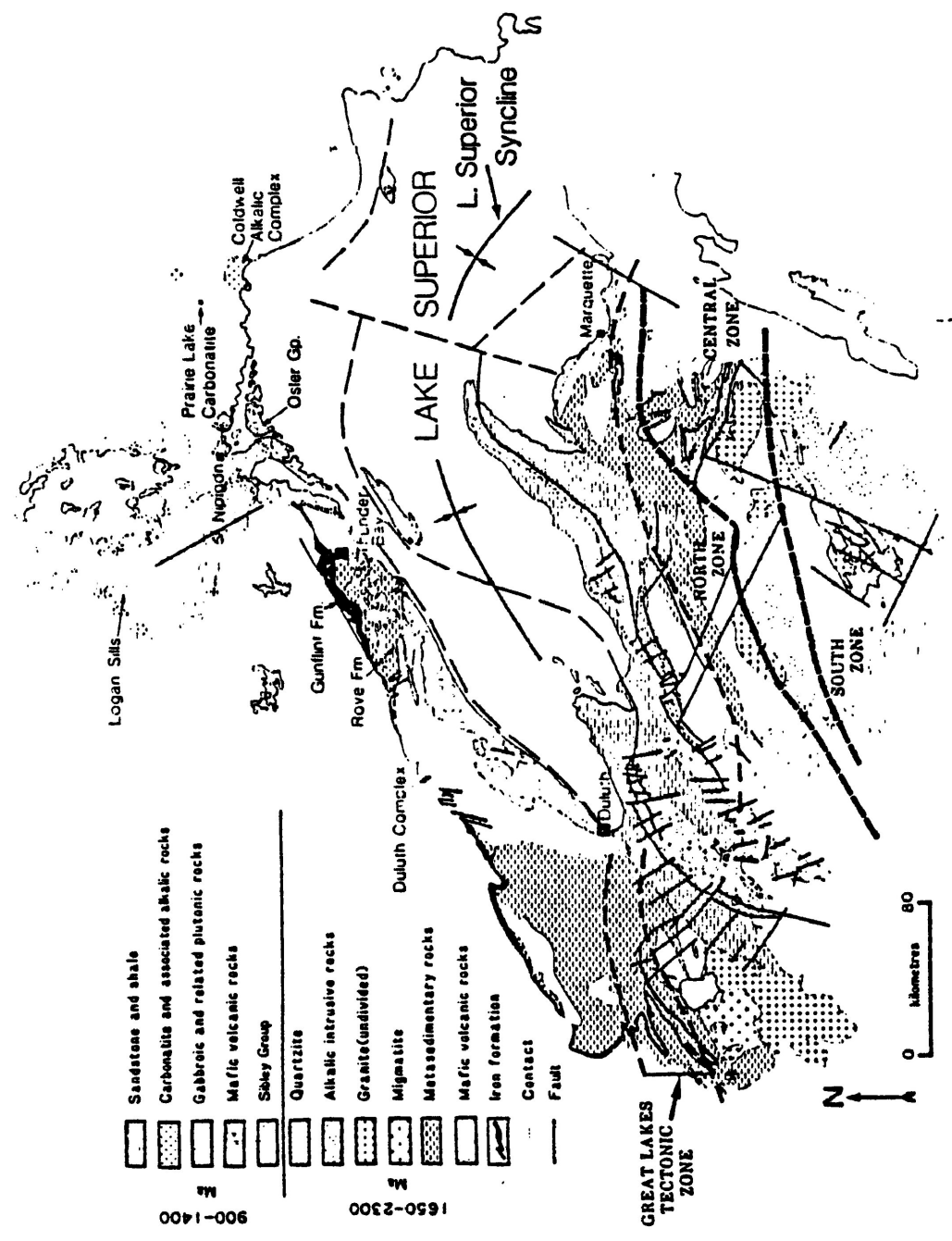


Figure 3: Geology of the Proterozoic rocks of the Lake Superior area (Franklin, 1982).

## VEIN GEOLOGY

### VEIN CLASSIFICATION

Silver-bearing veins of the Thunder Bay area have been described by Ingall (1888), Bowen (1911), Tanton (1931), Oja (1966), Franklin (1970) and Franklin et al. (in press). Ingall (1888) subdivided the veins, on the basis of geographical clusters, into five groups (Figure 4A): the Coast Group, Port Arthur Group, Rabbit Mountain Group, Silver Mountain Group and Whitefish Lake Group. The last group consisted of barren, non-economic veins, but mines located in each of the first four groups mentioned operated during the mid to late 1800s. Bowen (1911) suggested the veins could be divided into only two groups named after their dominant host lithology: the Grey Argillite Belt, indicating the northern system of veins, and the Black Slate Belt indicating those veins found in Lake Superior.

These belts are parallel, curvilinear features, oriented subparallel to the coast of Lake Superior. Mapping has shown no true consistent lithologic difference between the host rocks, prompting Oja (1967) to propose the now accepted classification of Mainland and Island Belts respectively (Figure 4B). The locations of silver veins examined during the current study are presented in Figure 5.

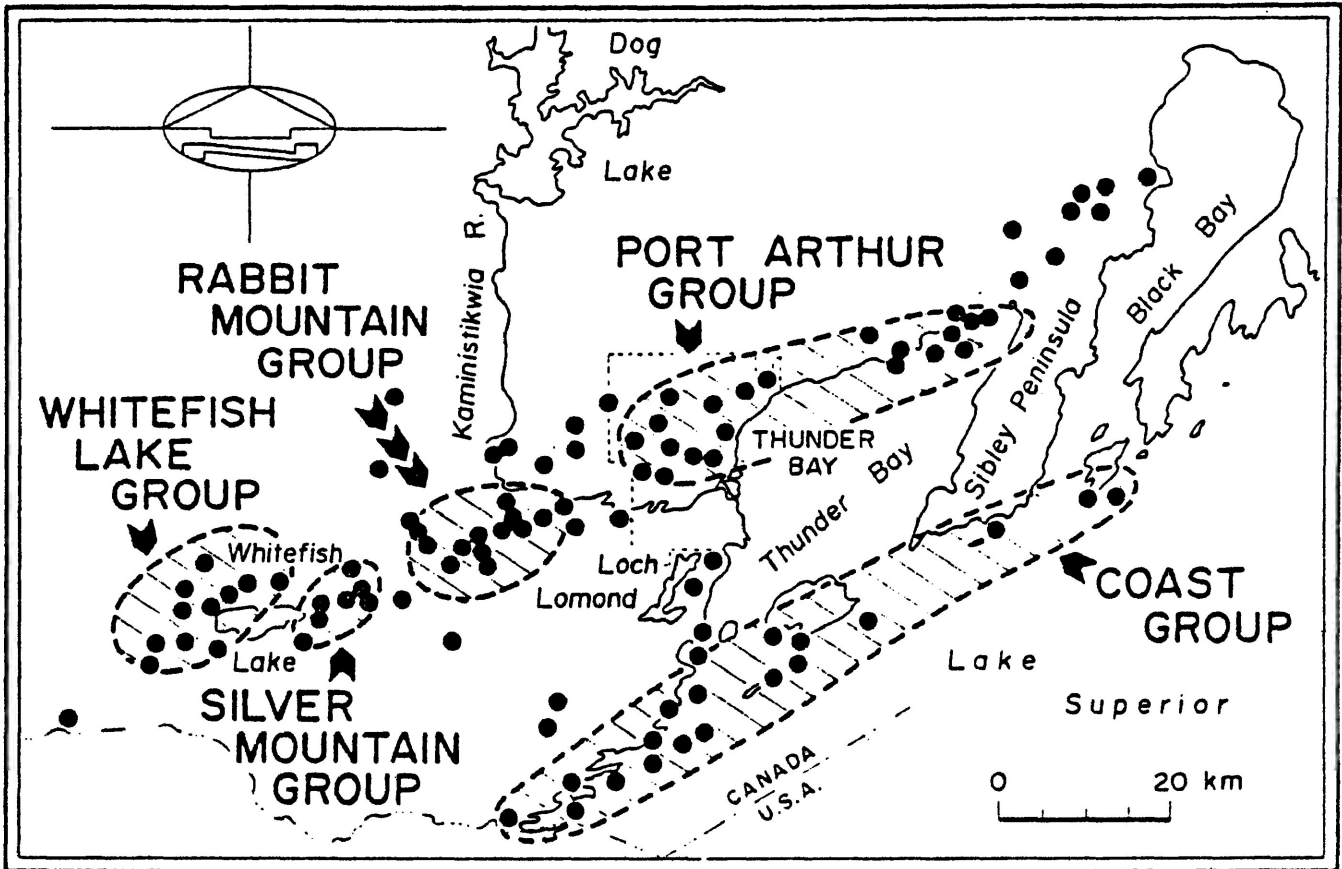


Figure 4A: Classification of silver veins in the Thunder Bay District according to Ingall (1888). Dots represent vein locations after Tanton (1931).

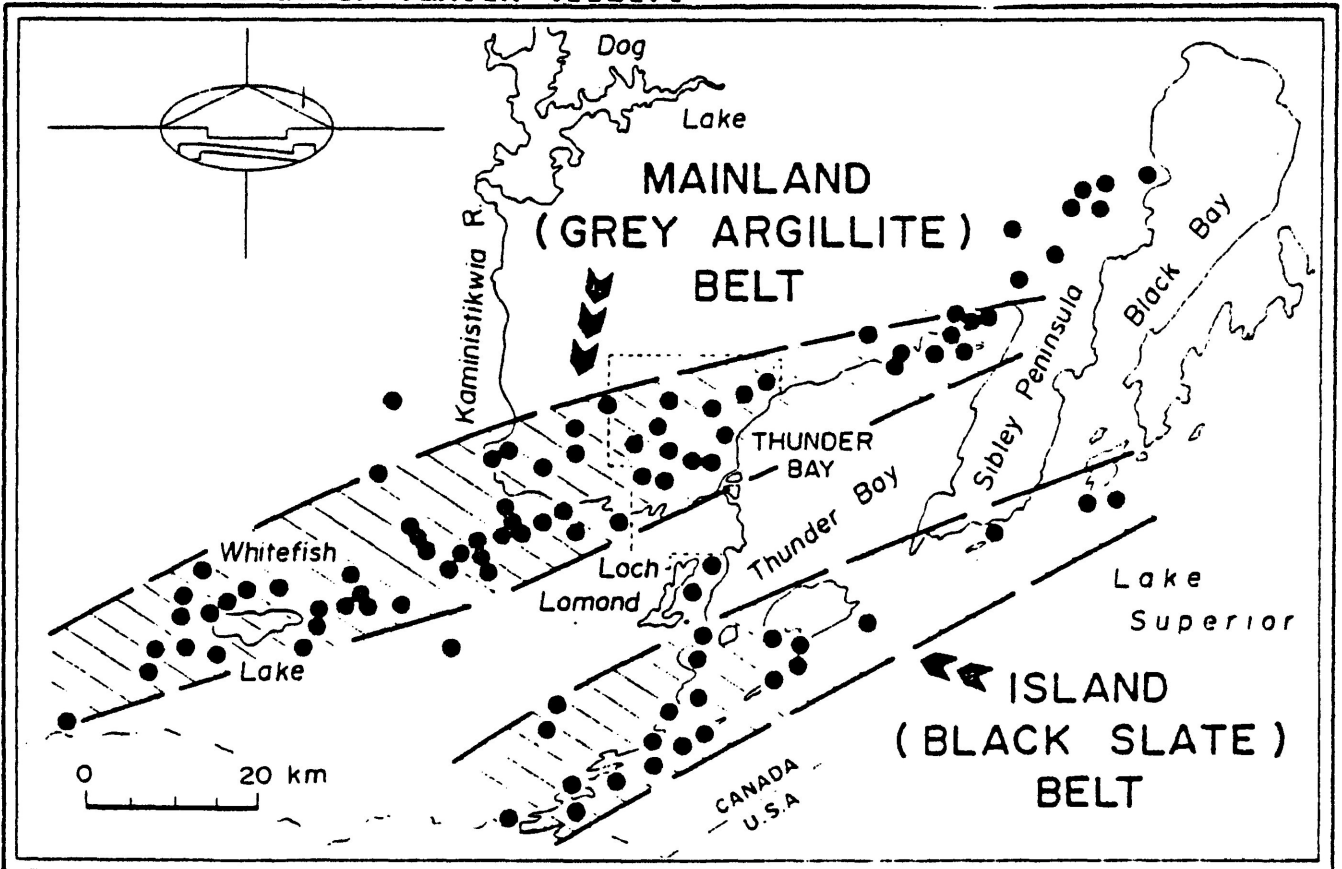


Figure 4B: Classifications of silver veins in the Thunder Bay District according to Bowen (1911) and Oja (1967).

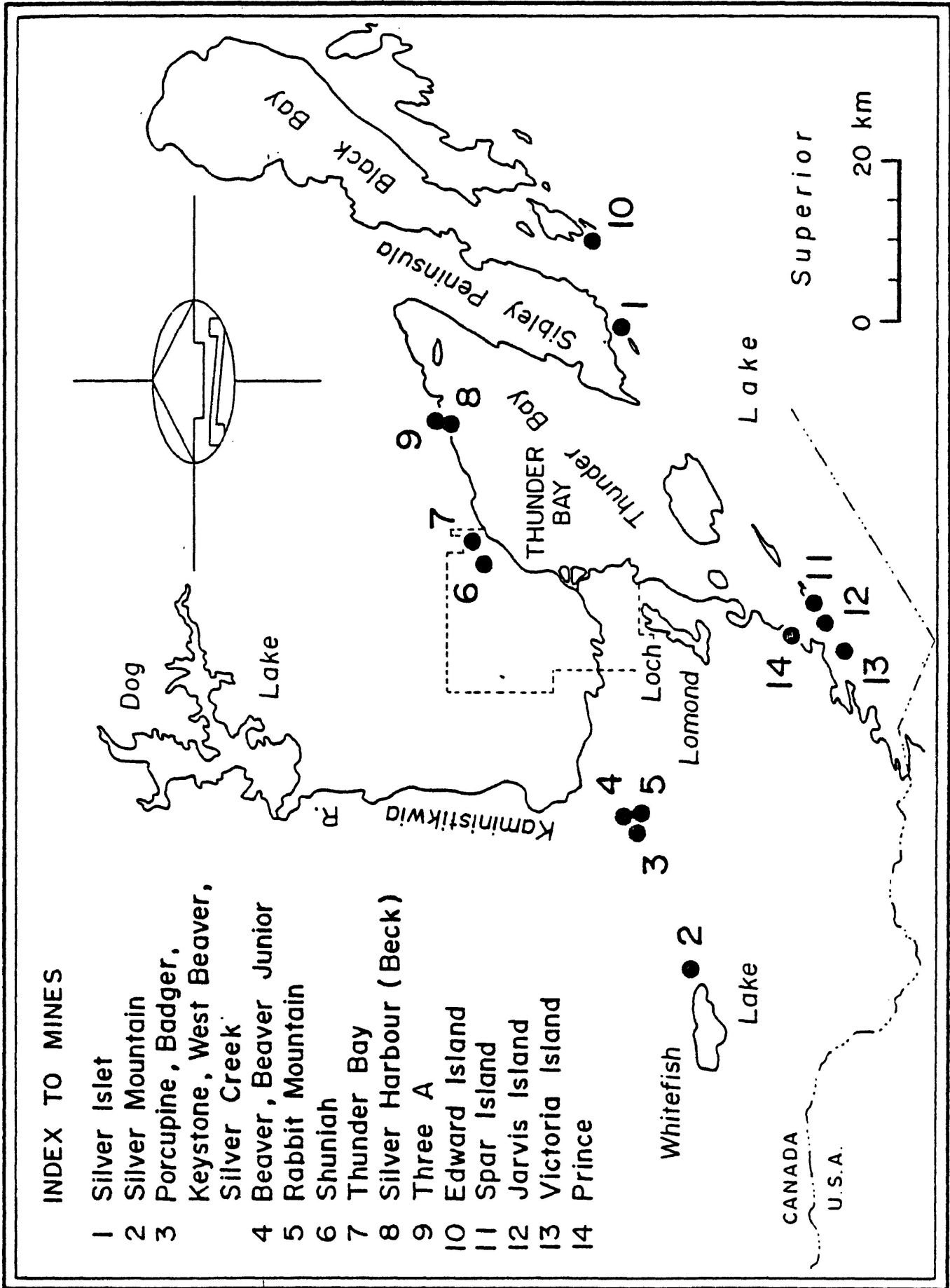


Figure 5: Locations of veins sampled during the present study.

A second type of classification is possible, based on the mineralogy of the veins, and is useful in constructing a genetic model for the vein region. By this scheme the groupings would be the barren veins, the simple silver veins and the five-element associated veins (Ag-Co-Ni-As-Bi).

The majority of veins are anastomosing features that fill faults and shatter zones. They have a curvilinear trend and are of highly variable width. Minerals are commonly euhedral and show open growth type textures such as drusy and comb structures, symmetrical crustification, and rhythmic cycles of deposition. Vugs are common. Replacement features are generally limited to the sulfides and are uncommon except in the Island Belt.

The Mainland and Island Belts have subparallel trends, but the veins within these belts have distinctive orientations. In the Island Belt veins strike north to northwest (Figure 6A), and have a fairly uniform orientation.

In contrast the Mainland veins have a more variable orientation but the majority of Mainland veins strike northeast to east northeast, dipping steeply to the south; examples include the Silver Mountain and Rabbit Mountain veins and the veins of the Port Arthur Group (Figure 6B). In contrast, the Big Harry vein strikes west northwest, the Beaver northwest, and the North Bluff vein strikes west, suggesting these veins may be related to

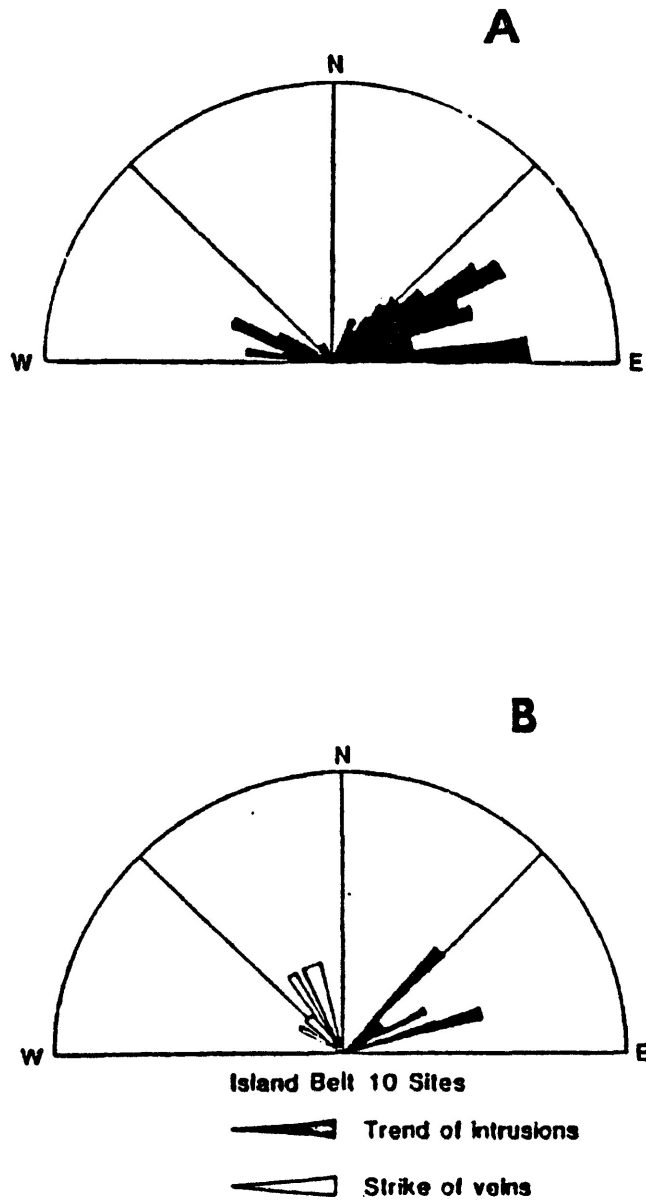


**Figure 6: Orientation of veins in Mainland and Island Belts from Franklin et al. (in press). 6A - 121 Mainland Belt veins; 6B - 10 Island Belt veins.**

a different episode of vein filling than that of most Mainland veins.

### PREVIOUS WORK

Comprehensive descriptive reports on Thunder Bay silver veins were first completed by Ingall (1888) and Tanton (1931). The first recent work was done by Franklin (1970), who presents a summary of significant vein geology, with emphasis on the Creswel (Rabbit Mountain group) claims. A survey of homogenization temperatures done by Franklin et al. (in press) obtained from quartz from the Porcupine Mine indicates the presence of boiling, and depositional temperatures of 200–400°C.

A number of vein systems have been described in H.B.Sc. theses at Lakehead University, examining their mineralogy, structure, and paragenesis. Mines included are the: Rabbit Mountain (Mosley, 1977); West Beaver (Manuala, 1979); Island Belt (Smyk, 1984) and Creswel (Rabbit Mountain Group) (Chambers, 1986). Harvey (1985) tested the lateral secretion model by examining the abundance of metals in Rove shale bordering one of the Rabbit Mountain vein. A number of Pb-isotope analyses have been completed by Franklin et al. (in press), which are presented with a summary of possible genetic models for silver-bearing veins along the north shore of Lake Superior.

## RABBIT AND SILVER MOUNTAIN GROUPS

The Rabbit and Silver Mountain groups are hosted by Rove shale and to a lesser extent the Logan diabase sills. In general veins narrow as they enter the sills, e.g. at the Big Harry Vein; however, there are exceptions to this rule, e.g. the Rabbit Mountain No. 1 Vein. Most of the past producing veins are oriented NE to ENE, dipping steeply south. The main exceptions to this are the Big Harry Vein, have a WNW orientation, and the Beaver Mine Vein, striking NW. The Little Pig Vein, a barren vein, also has a different orientation, striking NW dipping 60° to the SW.

Veins of both groups show an initial phase of fine-grained, drusy, milky to colorless quartz deposition. This is commonly succeeded by bands of green fluorite, either as thin horizons parallel to vein walls or as massive breccia cement. This is followed by the first phase of calcite deposition, which again occurs both as a fracture lining and as breccia cement. Some sphalerite and galena commonly accompany either the transition zone from fluorite to calcite or the calcite deposition. In this position in the paragenetic sequence, sulfides often occur as subhedral to euhedral crystals disseminated in a band parallel to the vein walls. In breccias, sphalerite crystals are often found adjacent to wall rock fragments, while galena is often disseminated through the matrix.

Commonly this first massive calcite deposition phase is interrupted by a period of brittle fracturing/faulting, often oriented subparallel to the initial vein, and observable as a series of wavy, anastomosing fracture surfaces or as brecciation of vein/host material.

This event is often postdated by a combination of sulfide, green and purple fluorite, and calcite deposition, and the initial appearance of silver either as native silver or acanthite. The main post-fracture mineral deposited is calcite, and it is during this stage barite occurs if present in the veins. Pyrite and chalcopyrite may also begin to appear at the point.

The vug-lining stage is dominated by quartz deposition, in colorless, smoky and amethystine forms. This can be accompanied by silver in wire, leaf, and nugget forms, as well as calcite and base metal sulfides, although the latter are uncommon.

With the exception of the Big Harry Vein, all members of these groups fall into the simple silver vein chemical classification. Assay results obtained by Falconbridge at the Big Harry Vein indicate the presence of some arsenide minerals (Cole, 1978).

### Little Pig Vein - West Beaver Mine

The mineralization occurs in a breccia zone 30cm to 1.3m wide, striking 077/70°SE. The vein lies in Rove shale near a Logan sill. The vein is asymmetrical, containing a massive breccia zone, rimmed by encrustations of green, purple, and colorless fluorite, calcite and quartz. Disseminated galena occurs in calcite, along with minor chalcopryrite; sphalerite is found in small quantities throughout the paragenetic sequence; and pyrite with minor chalcopryrite occurs with late stage quartz as vug linings and in ramifying veinlets. The geology of the vein has been described in detail by Manuala (1979), and reviewed by Chambers (1986).

The Little Pig Vein is significant in that no appreciable silver mineralization was found in it, although it seems closely related in all other respects to the nearby No. 2 vein of the West Beaver property. Manuala noted that most veins in the Rabbit Mountain Group are commonly intersected by fracture sets oriented 010° and 300°, but that late stage fracturing of the Little Pig Vein did not occur in these orientations. He suggested the absence of this fracture set is responsible for the lack of silver in this vein system.

### No. 2 Vein - West Beaver Mine

The No. 2 composite vein of the West Beaver Mine is 30-60cm wide, striking 040°, vertically dipping. The vein contains calcite, quartz, fluorite, sphalerite, pyrite, and galena. Tanton (1931) also reported the presence of rose quartz, pyrrhotite, chalcopyrite, and minor acanthite. In general this vein appears to have a granular, massive texture, rather than showing the symmetry and open fracture filling textures common to Mainland veins and evident at the Little Pig Vein, although Tanton mentioned the presence of crustification in samples from the dump. The acanthite is largely found as leaves along late stage calcite cleavage planes. The vein is entirely hosted by the Rove shale, which is shattered in the vein area. Late stage cross-cutting rusty veinlets are common.

### Big Harry Vein

The Big Harry Vein is one of two parallel veins forming the Beaver Junior property. The vein occurs within a fault zone striking 284/85°. The main vein averages 25cm in width, but narrows as it enters diabase from argillite host rock. Quartz, calcite, minor green and purple fluorite are the main gangue minerals found, with barite an important constituent of the neighboring North Bluff Vein. Cole (1978) also reported the presence of plagioclase in an early veinlet near the northern

contact of the vein; however, it was not observed during this study. Ore minerals present include sphalerite, galena, minor pyrite and chalcopyrite, native silver and acanthite. Base metals are found in small quantities throughout the paragenesis; however, native silver is restricted largely to the post-fracturing vein filling, and acanthite is largely associated with the late stage and vug-filling quartz-amethyst-calcite event. Covellite has been observed replacing galena in one sample (Cole 1978).

Cole (1978) tentatively identified allemontite (AsSb) rimming native silver. Further investigation (Kissin, personal communication) has proved this rim to be an Hg-rich silver.

A number of exotic minerals were found in this vein system by Falconbridge Nickel Mines Ltd. (Cole, 1978), and include proustite, pyrargyrite, stephanite, arsenopolybasite, allemontite, and cobaltite. The presence of these minerals suggests the Big Harry Vein has an affinity to the 5-element vein type rather than the simple silver veins. A comprehensive description of this property was completed by Cole (1978).

### Rabbit Mountain Mine

The Rabbit Mountain Mine area contains two parallel veins, one barren, the other rich in native silver and acanthite. The

vein was mined for 35-110m in a long strike, to a depth of 90m; over 50,000 ounces of silver were recovered from it. The veins are situated in a graben like valley, and follow curvilinear faults striking 215-230°, dipping 60-70°NW. The geology of the veins has been described by Mosley (1977).

The main vein is up to 2.2m in width, and composed dominantly of calcite with minor quartz, clear, green, and purple fluorite, and barite. The most abundant sulfide minerals present are sphalerite and pyrite, with smaller quantities of galena, and some chalcopyrite found largely as inclusions within sphalerite. The vein contained three silver rich ore masses, largely composed of argentite, in the shale hosted vein, as well as economic mineralization within the diabase hosted section of the vein.

A fracturing episode is evident in the vein material, and appears to have been a predecessor to all important sulfide and silver deposition.

#### Porcupine (Creswel) Mine

The Porcupine Mine is centered on three fault-filling vein systems (Tanton, 1931), one of which is presently exposed at surface. The latter is oriented 080/80°S, while the other two strike 050° and 060°, dipping steeply to the south. Franklin (1970) noted reverse motion of faults in the Porcupine system,

some movement appears to have postdated vein emplacement.

All veins are of variable width, from 10cm to over 2m. The veins are sandwiched between two diabase sills, hosted by Rove shale. The veins contain calcite, green fluorite, quartz, minor barite and witherite. Sulfides include galena, sphalerite, pyrite, chalcopyrite and possibly pyrrhotite (Tanton, 1931). In the 080/80°S vein argentite and native silver occur along fracture planes, calcite cleavage planes, and in leaf and wire forms in vugs, deposition generally succeeds a fracturing event. No mineralization was reported in the more northeasterly striking veins. Chambers (1986) noted a difference in calcite grain size and sulfide abundance in the post-fracture material. In general vein filling appears to have been symmetrical.

### Silver Creek

The geology of the Silver Creek vein has been described by Chambers (1986). It occurs in a breccia zone of highly variable width, from a few centimeters to over a meter wide. The vein, oriented 065/80°SE, contains calcite, quartz, green fluorite, galena, sphalerite, pyrite, and argentite. Although the presence of a late stage fracturing event is not observable in the present vein exposure, its probable occurrence is indicated by the presence of silver mineralization. Because of the highly variable width of the vein, it is possible the fracturing was

discontinuous.

### Badger Mine

Two veins occur at the Badger mine, the No. 1 vein, up to 2m wide, and the 10cm No. 2 or Porcupine Junior vein. The veins strike 040° and dip steeply to the southeast.

The No. 1 vein is composed dominantly of calcite and quartz, with minor green and purple fluorite, sphalerite, galena, pyrite and argentite. The vein has experienced a later fracturing episode; however, its relationship to silver mineralization has not been established. Observed silver at this mine is associated with the vug-filling stage.

The fissile black shale in the dumps surrounding these mines has been found to contain leaf argentite along the cleavage planes.

### Keystone (Climax) Mine

The Keystone Mine worked three silver bearing veins, the No.1, No. 2, and No. 3. The geology of these veins has been reviewed by Chambers (1986).

The No. 1 and 2 veins are oriented 080°, dipping steeply to

the south, while the No. 3 vein is situated in a fault striking 045°-075° dipping 60°-90° north. The veins average 30cm in width.

The No. 1 and No. 3 veins show a strong secondary fracturing event, accompanied by a pulse of sulfide mineralization, rich in pyrite in the No. 1 vein, and rich in sphalerite, galena and chalcopyrite in the No. 3 vein. Acanthite is the main silver mineral present, which Tanton reported concentrated on the hanging wall side of the vein. This is in accordance with asymmetry of the vein caused by the concentration of post-fracturing gangue and sulfide mineralization on the north side of the vein.

Gangue mineralogy is dominated by calcite and green fluorite, with lesser amounts of milky and colorless quartz, late stage rusty quartz veinlets, and minor purple fluorite. In addition primary clay minerals were found in one sample from the No. 2 vein dump (see Mineralogy section). The veins are hosted by both Rove shale, on the foot wall side of faults, and diabase, on the hanging wall side.

### Silver Mountain

The Silver Mountain Vein system is continuous over two kilometers along strike, and averages 3 meters in width. It is

hosted by Rove shale and Logan diabase. At the west end, the vein varies in orientation from 075° to 090°, dipping steeply north; it is a composite vein, filling a normal fault zone. At the east end of the mountain the vein branches, and fills anastomosing fractures striking from 050° to 041° generally dipping steeply south.

The vein is generally asymmetric, the south wall often composed of a breccia zone, from 10cm-1m in width. Breccia fragments are angular, from 1-20cm in diameter. The cement is generally fine-grained calcite, lined with fine drusy quartz; small vugs (1-2cm in diameter) are common. Minor sphalerite and galena commonly lines the breccia fragments. The breccia zone is commonly lined with green (±purple) fluorite. North of this, a zone of massive, coarse-grained calcite up to 2m in width is common. The north wall of the vein often contacts this calcite zone, but at the west end of the mountain, a 2-30cm zone of massive, bladed barite is common along the north contact.

A fracturing event, subparallel to vein orientation, is well developed through most of the Silver Mountain vein. Post-fracture mineralization is composed of fine (1-10mm) bands of fluorite, sulfide, and calcite deposition. Some argentite is associated with the sulfide deposition, and some native silver with fluorite deposition.

A late-stage, vug-filling event is dominated by quartz and amethyst deposition, accompanied by minor calcite, pyrite, and galena. Native silver and argentite are commonly found along calcite cleavage planes and the fracture planes cross-cutting the vein system. Massive argentite is also found as a vug filling. Present exposure of the vein system contains abundant silver mineralization at a juncture of two fracture-fill veins, where a secondary fracture event is well developed. The silver deposition sites appear to be controlled by the fracture event.

#### PORT ARTHUR GROUP

The veins of the Port Arthur Group are rich in quartz, and poor in calcite in comparison with those of the Silver and Rabbit Mountain groups. Also in contrast to these groups is their host lithology, usually the cherts and argillites of the Gunflint Formation, but also Archean volcanic schist (e.g. 3A mine). The orientation of the veins is highly variable, from N to NE to E in strike, and generally steeply dipping.

The veins are usually networks of discontinuous 1 to 2cm fracture filled veinlets, usually with a simple one or two stage paragenesis. Sulfides are uncommon, and pyrite is the main representative, as opposed to sphalerite and galena in other areas of the Mainland Belt. Barite is a common, although minor,

constituent of the veins. Amethystine, smoky, and rusty red coloured quartz are common.

Ingall (1888) observed the presence of native bismuth at the 3A mine, and Ni, Co, and Au have been reported in assays by Tanton (1931), indicating some of these veins have an affinity to the 5-element vein type.

The only major producer in this group was the Shuniah mine from which 20,000 ounces of silver were mined, although the Thunder Bay, the Beck, and the 3A mines were also producers.

#### Silver Harbour (Beck) Mine

The Silver Harbour vein is hosted by Gunflint chert. Gangue minerals are dominantly quartz and amethyst, accompanied by lesser amounts of calcite and barite. The samples examined show multiple fracture filling, drusy quartz horizons, with the base of quartz crystals amethystine and the tips milky or colorless. The fracture planes at the base of these horizons commonly contain up to 1cm diameter anhedral sphalerite masses. Leaves of Gunflint formation are also found caught between quartz layers. Pyrite is disseminated in quartz and calcite. Very fine-grained galena is associated with coarse bladed barite, commonly as inclusions.

Examination of an adit revealed the presence of 1-2cm chalcedony rich anastomosing veinlets, hosted by Gunflint chert. Chalcedony is white to rusty in colour, minor colorless quartz crystals occur in vugs. Tanton (1931) stated silver mineralization was reported at this vein; however, no evidence of sulfides or silver was observed and no extensive vein exposure was discovered. The network observed at the adit strikes 065°, dipping 80° north.

### Algoma Mine

Samples from the Algoma mine dump were composed of diabase hosting 0.5 to 1.5cm veins. The main mineral observed was colorless, drusy quartz; however, minor purple fluorite and calcite are also present. Tanton (1931) noted that no silver was ever recovered from this vein.

### 3A Mine

The 3A mine is hosted by Archean metavolcanics and occupies a fracture system oriented 058/90°. The main exposure of vein examined averaged 25cm in width and occurs within a shatter zone 30cm-1m wide.

The main gangue minerals present are milky quartz, calcite, and barite. In addition minor pink dolomite was observed.

Sulfides observed include sphalerite, pyrite, chalcopyrite and galena. Ingall (1888) reported the presence of native bismuth in the vein. Tanton (1931) stated assays of vein material indicate the presence of Ni, Co, and Au. Silver mineralization is documented as occurring both as native silver and acanthite, although none was found during the present study.

### Shuniah Mine

The Shuniah was the most productive of the Port Arthur Group mines. It is emplaced in Gunflint cherts and, at lower levels of the vein, in Archean schist. The fault zone is 6m wide, striking 090°, dipping steeply to the south. It has been traced 3km laterally. Tanton (1931) reported "Hydrocarbon gas under great pressure was encountered in some of the vugs in the old mine workings".

Gangue minerals observed include colorless and milky quartz, calcite, and green fluorite. The predominant sulfide presently found in vein exposure is pyrite, although Tanton also reported the presence of sphalerite and galena. In addition native silver and argentite were both recovered; these minerals were particularly concentrated in the uppermost 20m of the worked vein. Manganese oxide encrustations also occur near surface. Both these features are notable as they indicate the importance of supergene processes at this vein.

### Thunder Bay Mine

Two sets of ramifying veins are present at the Thunder Bay Mine, occupying conjugate fracture systems. One, oriented 034° dipping steeply southeast, is predominantly calcite filled. The second is a 2.5m zone oriented 035/65°NW; it is this zone from which silver was recovered. The main gangue mineral filling these fractures is quartz, with lesser amounts of calcite, pink dolomite, and green fluorite. Disseminated sphalerite, galena and pyrite are present in dump material. Tanton also reported the presence of native silver and acanthite.

### ISLAND BELT

In contrast to the two vein groupings into which the Mainland Belt has been divided, the Island Belt is composed of veins of great heterogeneity morphologically, mineralogically and chemically. Smyk (1984) has reviewed the geology of this group of veins. He subdivided them into three groups based on the metal association of each vein. Hence the Silver Islet and Edward Island veins fall into S-element (Ag-Co-Ni-As-Bi) association. Spar, Victoria and Jarvis Islands and the Prince Location have a base metal association (Pb-Zn-Ba±Cu-Ag), and finally the barren veins, such as Pie Island (Pb-Zn-Ba) which contain no associated silver. Because of the great diversity in the geology of these veins, descriptions of individual veins,

rather than a generalization of their morphology and mineralogy, are provided.

### Silver Islet

The Silver Islet ore is hosted by a 80-110m wide gabbro dyke, an extension of the Pine Point - Mount Mollie Gabbro. The dyke strikes 050°, dipping steeply to the southeast. It is crosscut by a fault zone striking 325°, dipping steeply to the northeast, which extends under Lake Superior to Burnt Island. The fault zone also cuts the Rove shale surrounding the intrusive; however, mineralization of the vein is only significant within the gabbro.

The deposit has been described by a number of authors, most recently by Smyk (1984).

The first fluid inclusions at Silver Islet were encountered during mining. MacFarlane (1880) reported that "a miner took a candle to look into the drill-hole, not being aware that there was a large escape of gas with the water. The gas instantly took fire, sending a flame out from the end of the drift for more than 40 feet...". Tanton (1931) reported that also "saline solutions containing chlorides of calcium, sodium, magnesium, and potassium, calcium carbonate, and calcium sulphate accompanied by inflammable gas... The composition...may have been hydrogen

sulphide which was detected in the mine in 1920, or it may have been a hydrocarbon".

The paragenesis of the Silver Islet deposit is very complex and was never fully documented; however, examination of hand specimens has allowed at least a partial reconstruction of depositional sequence, as described below:

#### 1. Main Depositional Phase

- (i) Pink manganiferous dolomite, massive and fine-grained; several pulses of its deposition are demonstrated by cross-cutting veinlets and repeated cementation of rebrecciated gabbroic material near vein borders (Smyk, 1984). Vein contacts sometimes are lined with carbonaceous material.
- (ii) Disseminated anhedral to massive subhedral to euhedral sphalerite, and galena + pyrite, occasionally sphalerite is in found colliform masses; deposition starts toward end of stage 1, continues through stage 3.
- (iii) Medium- to coarse-grained calcite, and medium-grained subhedral to anhedral quartz showing open space filling textures.

## 2. Late-Stage, Vug-Filling Episode

- (i) Medium- to coarse-grained calcite, fine- to coarse-grained quartz including smoky and amethystine varieties; minor sphalerite, galena, and green and purple fluorite. Barite is also reported present in the late stage material (Tanton, 1931).
- (ii) Usually associated with previously deposited sphalerite, native silver, in dendritic masses and wire forms. The native silver forms the cores of rosettes rimmed by cobalt and nickel arsenides and sulfosalts, in this study the presence of nickeline, gersdorffite, bravoite, safflorite, bismuthinite, and tetrahedrite were confirmed.
- (iii) Native arsenic, in colliform masses, containing bands of disseminated sphalerite, and associated with safflorite.
- (iv) Argentite and marcasite disseminated to massive in vug filling material.

## 3. Secondary Enrichment and Remobilization

- (i) Native silver remobilized from the cores of arsenide rosettes is seen to form cross-cutting veinlets. Native silver also occur in wire form in vugs. Argentite and native silver occur along fracture and

cleavage planes.

#### 4. Supergene Alteration

- (i) The presence of such supergene minerals as pyrargyrite, proustite, and witherite has been noted by Tanton (1931). Erythrite and annabergite were observed by the author in all samples containing cobalt and nickel arsenides.

The vein as described by MacFarlane (1880) and Ingall (1888) was of highly variable width and nature. Rich lodes of silver were encountered at fracture intersections and in vugs between large expanses of barren vein. The vein was mined to a depth of ~500m. Mining was halted due to problems of dewatering rather than exhaustion of ore material.

#### Jarvis Island

Jarvis Island contains two mafic dykes, an anorthositic gabbro and an olivine diabase, exposed on the northeast and southwest part of the island respectively. They are overlain by a diabase sill. The host for these intrusions of Rove greywackes and argillites.

The vein lies between the two dykes, it strikes 135°,

dipping  $50^\circ$  to the northeast. The vein is reported to attain a width of up to 4m, presently 3m of exposure is available at the mouth of the main shaft.

The vein shows a ribbing pattern similar to that observed at Spar Island. The southwesternmost rib varies from 20cm-1m and massive barite containing minor pyrite. The next zone northeast is 20cm of calcite containing 10-20% barite. A second, 45cm wide, rib of barite lies between this and the final, northeasternmost zone of massive calcite. Minor purple fluorite was also observed in dump material. Silver was recovered from the mine; however, none was observed during the present investigation. Ingall (1888) reported the presence of carbonaceous material near vein wall contacts.

### Victoria Island

Veins were found at two locations on the shore of Victoria Island, hosted by weakly to intensely sheared diabase and argillite. Veins vary in orientation from a southerly strike ( $186^\circ$ ) to a southeasterly strike ( $135^\circ$ ). Dips are moderate to steep to the west/southwest. Vein width varies from 2-25cm, in the narrower veins mineralogy is simple, containing dominantly euhedral to subhedral calcite with quartz and a red zeolite, perhaps laumontite. In wider veins green fluorite, barite and minor pyrite can also be observed. The presence of apophyllite

has also been documented (Smyk, 1984). A general association between the presence of zeolite and pyrite has been established. No silver mineralization was found in these veins.

### Spar Island

The vein exposed at Spar Island is hosted by a Pigeon River Diabase dyke, actually an olivine bearing gabbro, and is situated in a fault striking  $155^{\circ}$ , dipping vertically. The main vein is 3m wide, and is surrounded by fine stringers of quartz-carbonate.

The vein is composed of a series of symmetrically crustified bands centered on a barite rib. The central rib is composed of pink to white, cross oriented barite, which is the host of the main metal phases. It is rimmed by massive, coarse-grained calcite which in turn is rimmed by massive unoriented barite. The southern contact of the vein is marked by a thin (<2cm) band of euhedral quartz and calcite. At the northern contact the barite rib is adjacent to the gabbro dyke which further to the north (50cm) is cut again by a 40cm quartz-calcite vein.

The silver in this vein occurs at the borders of the central barite rib, in the form native silver and argentite (Smyk, 1984) associated with copper mineralization. Primary copper minerals include chalcocite, bornite, and covellite. Some chalcocite has

been replaced along fractures and cleavage planes by blaubleibender covellite. Bornite is occasionally rimmed by chalcopyrite. Safflorite occurs as minute inclusions ( $\leq 2\mu\text{m}$  in diameter) within these minerals. Supergene alteration of copper minerals to malachite, and to a lesser extent azurite, is pervasive, crystals being deeply embayed or totally replaced.

No multiple, cross-cutting, fracturing events are observed in the vein; however, the general symmetric form of the mineralization suggests a progressive widening of the vein with time.

#### Edward Island

Edward Island was described by Tanton (1931). Two subparallel veins are emplaced in faults striking  $035^\circ$ , in a grey granophyre phase of a diabase dyke. These dykes crosscut coarse sediments of Osler Group.

The vein is zoned, composed of calcite, sphalerite and native arsenic along vein walls, and the central band of calcite, chalcopyrite, galena, arsenopyrite, and minor argentite and silver. The native arsenic occurs in reniform masses to 10cm in diameter.

## FLUID INCLUSIONS

### INTRODUCTION

Preliminary examination of 200 doubly polished thin sections was made to determine the presence and nature of usable fluid inclusions in various minerals. The vein material was excellent for fluid inclusion work, as the bulk of material collected contained some suitable inclusions. The term "suitable" is here used to imply the inclusions were:

- 1) large enough to be seen clearly, usually greater than  $10\mu\text{m}$  in diameter,
- 2) clearly classifiable into the primary, secondary, or pseudosecondary group using the criteria described by Roedder (1984),
- 3) unaffected by post-entrapment volume changes due to stretching or necking,
- 4) contained in a mineral with sufficiently different refractive index than the fluid to allow the inclusion to be clearly visible.

Quartz, calcite, green and purple fluorite and sphalerite all contained usable inclusions. Late stage quartz, in contrast, often contained only very small ( $\leq 1-2\mu\text{m}$ ) inclusions and was therefore not commonly useful. Some problems with double

refraction in calcite, which obscured inclusion boundaries, precluded the usage of some sections. The sheer abundance of small inclusions in some calcite prevented their use, due to the difficulty this caused in their classification.

A few doubly polished sections were made of barite and dolomite; however, these minerals did not host large enough inclusions to be useful. In barite, this problem was further complicated due to the similar refractive indices of the mineral and the trapped fluids.

The majority of inclusions examined were two-phase, liquid plus vapour bubble, in all host minerals at all deposits. Vapour bubble volume was generally on the order of 1-2 percent (Figures 7, 8). In necked inclusions the vapour volume was, of course, highly variable, from 0-100 percent. In some primary inclusions that showed no evidence of secondary volume changes the vapour volume was as great as 35 percent. In samples in which large vapour bubbles were found, a large variation in vapour volume in the inclusion field was generally observed (Figure 9).

A large number of empty (one phase) inclusions were also observed. These often occurred near the surface of the sample, indicating they may have been affected by sample preparation. It should be noted that other inclusions, which were observed prior to and after breaking plates into chips for microthermometric

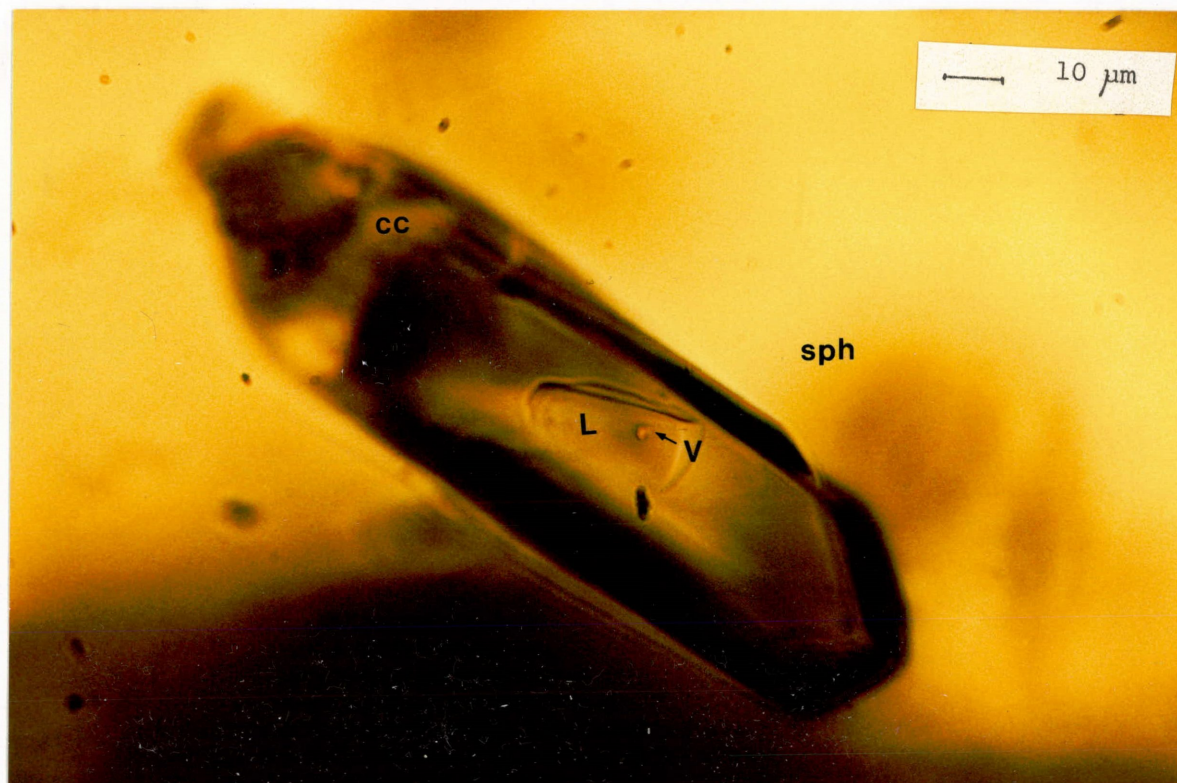


Figure 7: Two-phase (L+V) fluid inclusion in calcite inclusion hosted by sphalerite. (Keystone Mine EA 2).

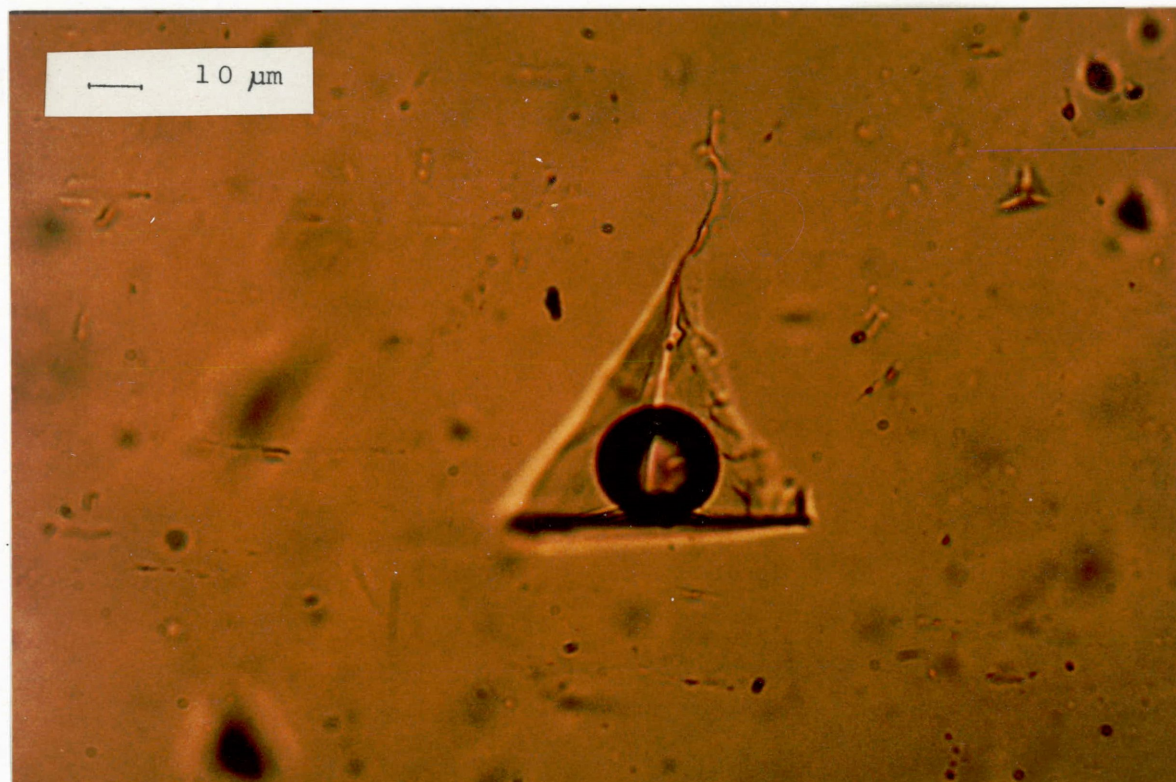


Figure 8: Two-phase (L+V) fluid inclusion showing negative crystal form. Stretching of one corner of the inclusion is observed. (Silver Mountain SM 2A)



Figure 9: Field of primary fluid inclusions containing 20-35 volume percent vapour. (Rabbit Mountain RM 8)

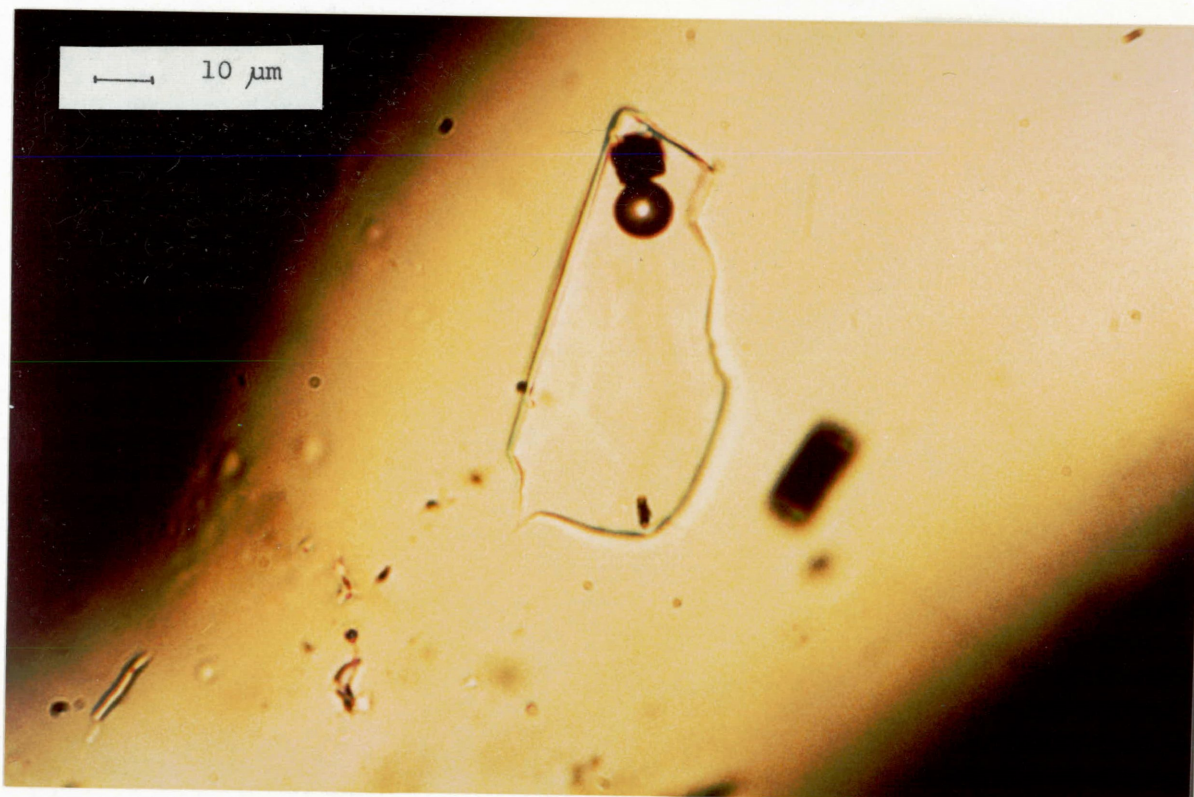


Figure 10: Primary three-phase (L+V+S) fluid inclusion. The cubic opaque mineral is pyrite. Note stretching indicated by inclusion form. (Silver Harbour Vein EA 99)

studies, showed changes in vapour volume indicating leakage had occurred. The shape of the inclusions had not, however, visibly changed.

The third type of inclusions observed were three-phase, liquid plus vapour plus solid. In the Silver Harbour vein, quartz was precipitated preceding and during pyrite deposition, and fluid inclusions contain 1-2 $\mu$ m euhedral pyrite crystals (Figure 10). Opaque daughter minerals were also observed in inclusions from the Keystone and Little Pig veins.

Non-opaque daughter minerals were also found, although they were often difficult to distinguish. In samples from the Little Pig and Silver Mountain veins these three-phase inclusions were hosted by fluorite and quartz, and the highly birefringent daughter crystals were easily observed. Inclusions in calcite from Jarvis Island occasionally contained a 1-2 $\mu$ m bright orange, transparent, anhedral daughter mineral tentatively identified as sphalerite.

Daughter minerals were less easily distinguished in calcite due to its high birefringence and double refraction, which tended to obscure the fluid inclusion walls. Artifacts thought to be daughter phases were observed, which upon examination from a different angle were found to be irregularities in the inclusion surface.

None of the daughter phases dissolved during microthermometric runs, even after the samples were heated substantially ( $100^{\circ}$ – $200^{\circ}$ C) above the liquid–vapour homogenization temperature. This indicates some disequilibrium within the system. However, it is possible that a prolonged run near the homogenization temperature would allow dissolution.

The fourth, rarest type of inclusion observed appeared to have a second meniscus around the vapour bubble, suggesting the presence of carbon dioxide. This observation was not confirmed by inclusion behaviour during heating or freezing; however, other inclusions in which no double meniscus was observed exhibited anomalous behaviour during freezing, suggesting carbon dioxide was present.

Both primary and secondary inclusions (Figure 11) are abundant in most vein material. Pseudosecondary inclusion planes are less common and difficult to identify. As far as possible microthermometric measurements were restricted to primary inclusions. In a few instances, particularly with sphalerite, pseudosecondary inclusions were used due to the lack of availability of primary inclusions. Pseudosecondary inclusions were only used if healed planes terminated within a single crystal, and inclusions had a constant vapour phase ratio.

All observations made were accompanied by notes on their

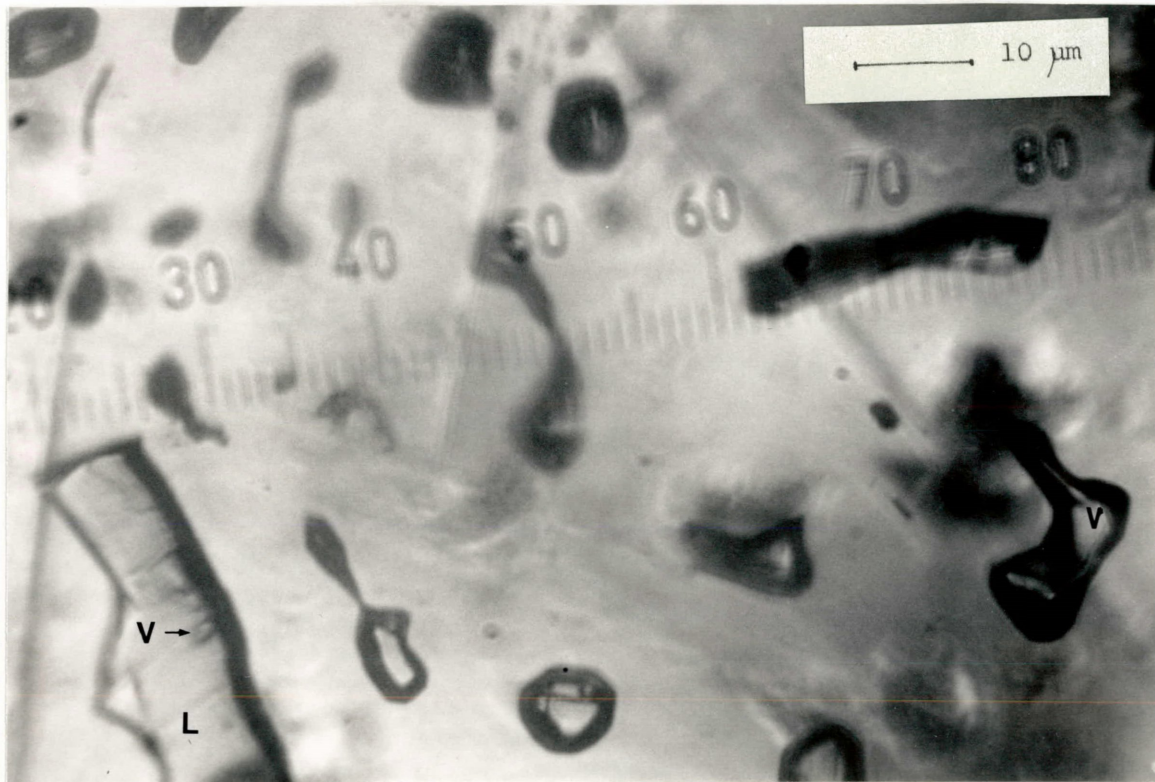


Figure 11: Plane of secondary inclusions in sphalerite.  
(Silver Islet SI 17)

quality, allowing anomalous temperatures obtained to be evaluated when data were analyzed.

### EXPERIMENTAL TECHNIQUE

Doubly polished thin sections were prepared at Lakehead University using a low-temperature preparation technique. The samples were not heated directly at any stage except by friction during grinding, which was minimized by the use of coolant. Lepage's Miracle Mender glue was used to attach thin sections to slides, as it is soluble at room temperature in acetone. Polished sections averaged 100 $\mu$ m in thickness but varied from 30 $\mu$ m to 2mm depending on the clarity of the mineral grains.

The fluid inclusion work was conducted on a Chaixmeca heating/freezing stage at Queen's University, Kingston. The Chaixmeca stage had a temperature range of  $<-150^{\circ}\text{C}$  to  $600^{\circ}\text{C}$ . The stage is directly heated by a thermal resistor placed under the sample area and subzero temperatures are achieved by the passage of liquid nitrogen cooled air through the sample chamber. The rate of temperature change is manually controlled, varying from 1-3 $^{\circ}$ /minute during freezing runs to 1/2 $^{\circ}$ /minute during heating runs.

Condensation during freezing runs caused optical problems, and generally inclusions  $\leq 10\mu$ m in diameter could not be used for

freezing. In contrast, during heating runs inclusions as small as  $5\mu\text{m}$  could be resolved.

The microthermometric stage was calibrated in the heating range twice during the experimental work (Table 2). A regression line was established by which all homogenization temperatures were corrected. This indicated a standard error of expectation of  $\pm 2.85^\circ\text{C}$  for these temperatures. A slight thermal gradient ( $\sim 0.5^\circ\text{C}$ ) was noted across the stage itself.

No calibrations below  $0^\circ\text{C}$  were performed during this time because previous calibration runs have shown minimal wandering. Calibration data obtained by A. Anderson (personal communication) was used to correct microthermometric data in the freezing range (Table 2). The standard error expectation in eutectic and melting temperatures is  $\pm 0.39^\circ\text{C}$ .

## RESULTS - FREEZING

As suggested by Bodnar and Bethke (1984), all freezing determinations were conducted prior to heating samples to prevent stretching of the inclusion.

Two important temperatures can be observed during freezing runs: the eutectic temperature ( $t_{\text{E}}$ ), from which an idea of solution composition can be gained; and the final melting

temperature ( $t_m$ ), from which an estimate of the salinity of the solution, in equivalent weight percent NaCl, can be made. Underlying assumptions are made that the inclusions are:

- 1) representative of the bulk hydrothermal solution compositions from which the minerals were precipitated,
- 2) unchanged by volume change or fluid leakage during geological history, and
- 3) at equilibrium during microthermometric determination.

The first assumption has been questioned by Barton et al. (1967) but has been generally accepted as valid. The second assumption can only be determined by careful examination of inclusions.

The question of equilibrium is of great importance, and many of the inclusions studied showed questionable behaviour. In the majority of instances the vapour phase either completely disappeared, or decreased in volume during freezing. In some cases it reappeared and regained its former volume before  $t_m$  was reached, while in other cases the vapour bubble reappeared only after two to three hours had passed at or near room temperature.

**TABLE 2: CALIBRATION OF CHAIXMECA STAGE**

Standard	Correct $T_m$ (°C)	Observed $T_m$ (°C)		
		Sept.	Jan.	Apr.
Napthalene	80.25	80.9 84.9 84.7 83.9	84.8	
Adipic Acid	151.4	160.0 159.2 161.0	160.0	
Merck 9800	200.0		215.7 214.5 214.8	
Merck 9847	247.0	259.4 258.6 254.7	258.9	
Sodium Nitrate	306.8	319.7 321.3 327.6 325.0	326.8	
Potassium Dichromate	398.0	423.5 419.7 418.3	439.4 437.4 447.4	
Chlorobenzene**	-45.6			-46.6 -46.4 -46.4
Carbon Tetrachloride**	-22.9			-23.1 -23.3 -23.8 -23.3
Water**	+0.01			0.2 0.3 0.3

\* calibration data obtained from A. Anderson (personal communication)

The disappearance of the vapour phase, as discussed by Lawler and Crawford (1983), could be due to:

- 1) metastability in the inclusion, which is a common problem in inclusions due to the small size of the system and is often demonstrated by pseudo-Brownian motion of the vapour phase at room temperature,
- 2) stretching of the fluid inclusion due to the pressure of crystallization of ice during freezing, or
- 3) leakage of fluid from inclusion via submicroscopic paths.

A decrease in vapour volume will change the melting behaviour of the ice, as internal pressure of the inclusion is affected. Therefore, the accuracy of some freezing data is questionable. Because of the possible volume change, heating experiments were not conducted on these inclusions.

Table 3 and Figure 12 present the results of the freezing determinations, indicating a range in  $t_m$  from  $-31.7^\circ$  to  $-1.1^\circ\text{C}$ .

Using the equation developed by Potter et al. (1978)

$$W_m = 0.00 + 1.76958\theta - 4.2384 \times 10^{-2}\theta^2 + 5.2778 \times 10^{-4}\theta^3 [+0.684]$$

where  $W_{\text{NaCl}}$  is the weight percent NaCl in solution and  $\theta$  the freezing point depression in °C. The salinities of inclusions were determined to be from 30.3 to 1.9 equivalent weight percent NaCl.

Eutectic temperatures were generally very difficult to observe, and often the procedure adopted was to note the "maximum eutectic temperature", the temperature when the presence of liquid was clear. Although this procedure provides poor quantitative data, it allows the differentiation qualitatively of the major salts in solution. The  $t_{\text{e}}$  of a number of salt solutions have been determined and are listed by Roedder (1984). By comparison, the low  $t_{\text{e}}$  determined indicates the composition of solutions is dominated by  $\text{CaCl}_2$  generally. A number of higher  $t_{\text{e}}$  determinations  $\sim -30^\circ\text{C}$  (e.g. RM1, EA12, EA3, SM22, EA99), are likely indicative of fluids dominated by other salts such as  $\text{MgCl}_2$ , NaCl or KCl.

Two inclusions, from Silver Harbour and the Keystone Mine, exhibited anomalous behaviour during freezing. Two ice phases appeared to form, accompanied by a decrease in volume of the vapour phase (Figure 13). The ice rimming the vapour phase could be clathrate crystals, although at and above room temperature, the presence of  $\text{CO}_2$  was not distinguishable. The icy rim was only visible when the inclusion was first frozen, supercooled to  $-120^\circ\text{C}$ , and disappeared upon warming to  $-59^\circ\text{C}$ .

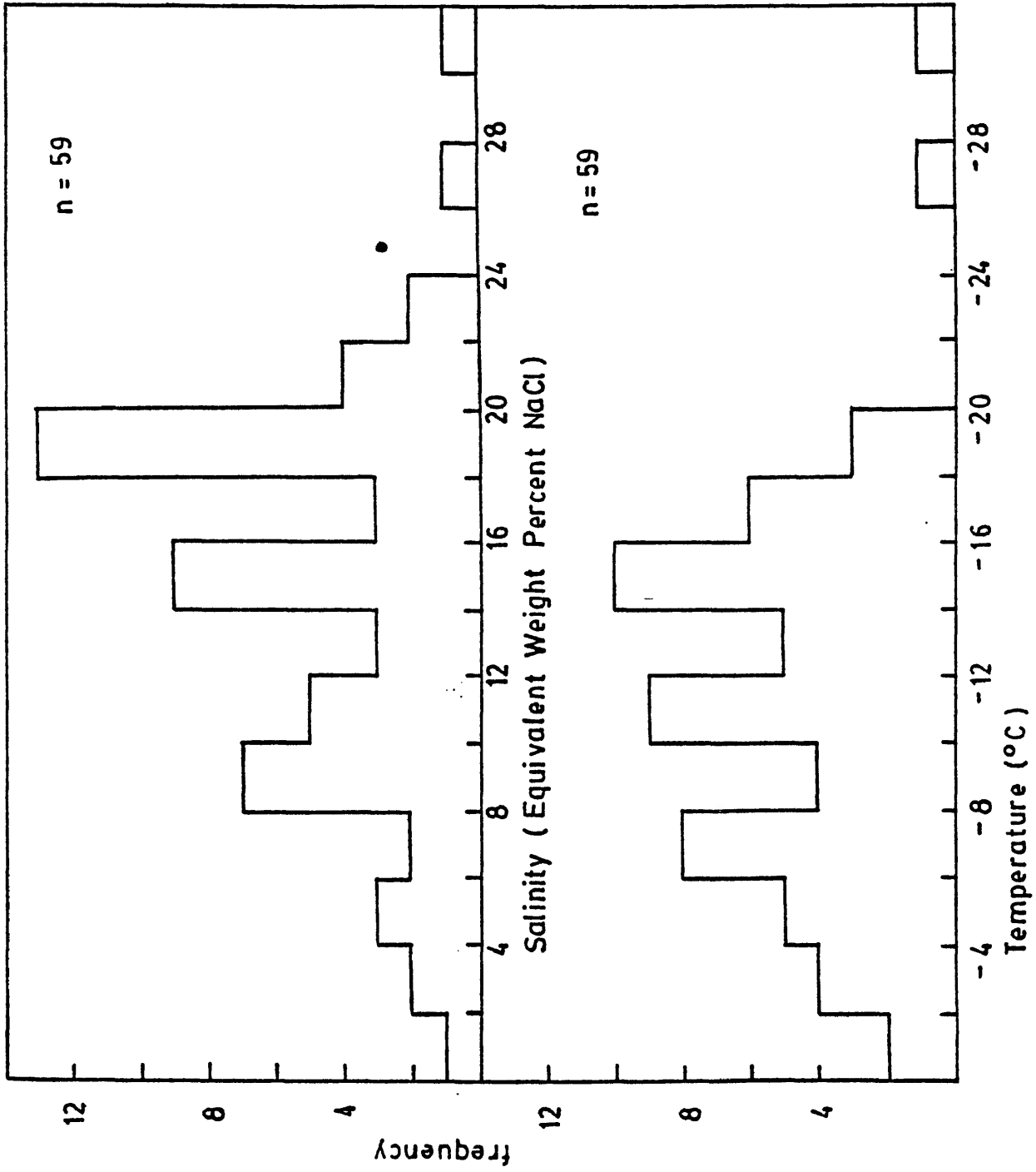
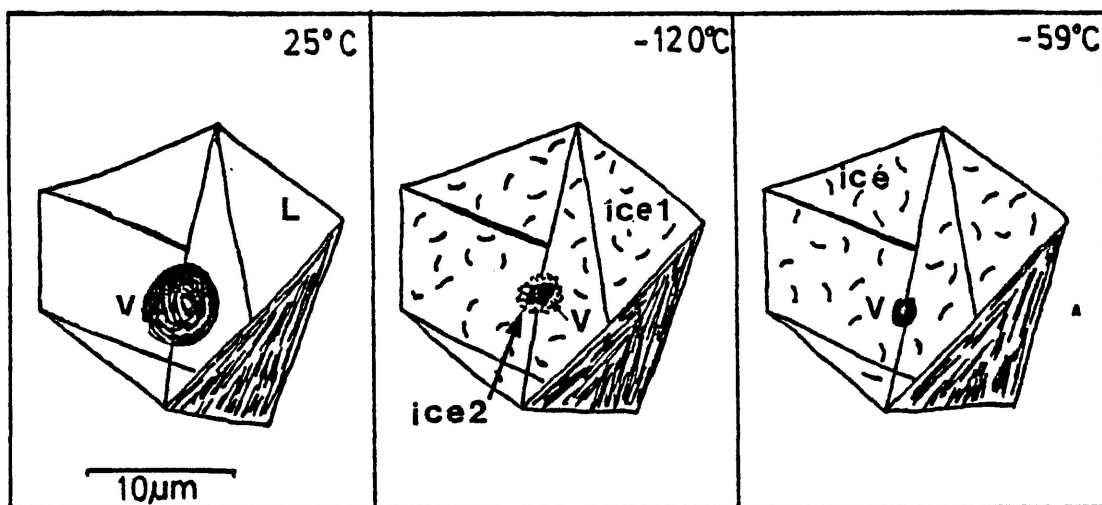


Figure 12: Histograms of microthermometric freezing determinations and salinity of fluid inclusions in calcite, quartz, fluorite, and sphalerite from all mines.

Figure 13: Behaviour of fluid inclusions from the Keystone and Silver Mountain Mines during freezing microthermometry. The two ice phases which appear at low temperatures may be  $H_2O$  + a clathrate, suggesting the presence of  $CO_2$  fluid.



**TABLE 3 : MICROTHERMOMETRIC FREEZING DATA****RABBIT MOUNTAIN GROUP**

<u>Sample</u>	<u>t<sub>m</sub>(°C)</u>	<u>t<sub>m</sub>(°C)</u>	<u>sal<sup>1</sup></u>	<u>host<sup>2</sup></u>
<b>Little Pig Vein</b>				
LP 22	~-50.0	-18.7	21.7	fl(p)
LP 23		-15.5	19.2	sph
LP 24	~-50.0	-12.2	16.2	sph
LP 26	-48.8	-10.7	14.7	fl(g)
<b>Big Harry Vein</b>				
BLC 009		-11.8	15.8	cc
BLC 019	~-55.0	-14.3	18.2	qtz
BLC 050	-51.9	-11.1	15.1	qtz
<b>Rabbit Mountain</b>				
RM 1	-35.6	-15.7	19.4	sph
RM 1	-50.6	-15.0	18.8	sph
<b>Badger</b>				
EA 69	≤ -37.5	-11.4	15.4	cc
EA 75	-41.8	- 9.2	13.1	cc
<b>West Beaver</b>				
WBe 1		- 4.3	6.9	qtz
EA 51	≤ -46.5	-11.9	15.9	cc
EA 51	≤ -43.0	-17.1	20.5	qtz
EA 52	-51.0	-11.9	15.9	sph
EA 53		- 3.3	4.3	sph
EA 53	-54.0	-12.7	16.7	sph
EA 54		- 6.1	9.3	cc

<sup>1</sup> sal - salinity (equivalent weight percent NaCl)

$$W_{\text{Na}} = 1.76958\theta - 4.2384 \times 10^{-2}\theta^2 + 5.2778 \times 10^{-4}\theta^3 [+0.684]$$

(Potter et al., 1978).

<sup>2</sup> host mineral: cc:calcite; fl(g):green fluorite;  
fl(p):purple fluorite; sph:sphalerite; qtz:quartz

Sample	$t_m$	$t_m$	Sal	Host
<b>Silver Creek</b>				
EA 10	~-50.0	- 5.2	8.1	sph
EA 12	-33.8	- 1.2	2.1	cc
<b>Porcupine</b>				
EA 14	-44.5	- 6.2	9.5	fl (g)
EA 61	≤ -40.0	-26.8	27.2	cc
<b>Keystone</b>				
EA 3	~-29.0	- 1.1	1.9	fl (g)
EA 5	-49.1	-15.8	19.5	fl (g)
EA 6		- 3.6	5.8	sph
EA 56	~-48.0	- 6.5	9.9	sph
EA 57	-46.8	-16.3	19.8	fl (p)
EA 57	-55.0	-17.5	20.8	cc
EA 59	-45.8	- 7.3	10.9	sph
<b><u>SILVER MOUNTAIN</u></b>				
SM 2A	-44.7	-19.3	22.2	fl (g)
SM 2B	~-50.0	- 7.7	11.4	sph
SM 2C	-38.4	- 2.1	3.5	sph
SM 3C	-38.6	-15.7	19.4	cc
SM 3C	-51.7	-13.1	17.1	fl (p)
SM 3D	-42.9	-19.7	22.4	cc
SM 3E	≤ -36.7	- 6.8	10.2	cc
SM 4C		-12.8	16.8	cc
SM 4D		-14.5	18.4	cc
SM 22	-31.7	- 4.6	7.3	fl (g)
SM 23	~-50.0	- 6.7	10.1	fl (g)
SM 24	-54.8	- 5.7	8.8	fl (g)
SM 51	~-40.0	- 8.2	12.0	sph
SM 71	~-48.0	-10.5	14.5	sph
SM Wend	~-50.0	-31.7	30.3	qtz
<b><u>PORT ARTHUR GROUP</u></b>				
<b>3 A</b>				
EA 101	-50.8	- 5.5	8.5	cc
EA 101		- 6.2	9.5	cc
EA 101		-11.2	15.2	cc
Ea 100	~-50.0	-14.2	18.1	cc

<u>Sample</u>	<u>t<sub>a</sub></u>	<u>t<sub>m</sub></u>	<u>sal</u>	<u>host</u>
<b>Shuniah</b>				
Sh 3	~-50.0	-15.8	19.5	cc
<b>Silver Harbour</b>				
EA 99	-34.5	-11.1	15.1	qtz
EA 99		- 8.1	11.8	qtz
<b>Thunder Bay</b>				
EA 82		- 3.3	4.3	cc
<b><u>ISLAND GROUP</u></b>				
<b>Spar</b>				
EA 39	-49.8	-16.2	19.8	cc
EA 40	-43.3	-16.0	19.6	cc
EA 41	-34.2	-14.9	18.7	cc
<b>Jarvis</b>				
EA 24	-49.8	-12.5	16.5	cc
EA 27		-17.8	21.0	cc
<b>Silver Islet</b>				
SI 17	-37.8	- 9.6	13.6	sph

## RESULTS - HEATING

Filling temperatures indicate that, with the exception of sphalerite, mineral phases were precipitated over a broad range of temperatures. Table 4 and Figures 14 to 16 present the homogenization and decrepitation temperatures determined.

The majority of inclusions homogenized to a liquid phase; however, in a few cases homogenization to both liquid and vapour phases within a single sample was observed, indicating solutions were boiling while the minerals were deposited. Approximately five percent of the inclusions examined decrepitated.

Filling temperature was commonly highly variable, for example over a length of 1.5cm, a 5mm band of green fluorite from Silver Mountain, contained six fluid inclusions which, when analyzed, ranged from 143.4° to 404.0°C.

The only mineral phase which was deposited at a consistent temperature in all deposits is sphalerite. Filling temperatures from primary and pseudosecondary inclusions filled in the 80° to 120°C range.

In contrast calcite, quartz, and fluorite all showed a broad range in homogenization temperature, weakly trimodal as can be seen from Figures 14 to 16. Calcite shows a peak at 100°C, and

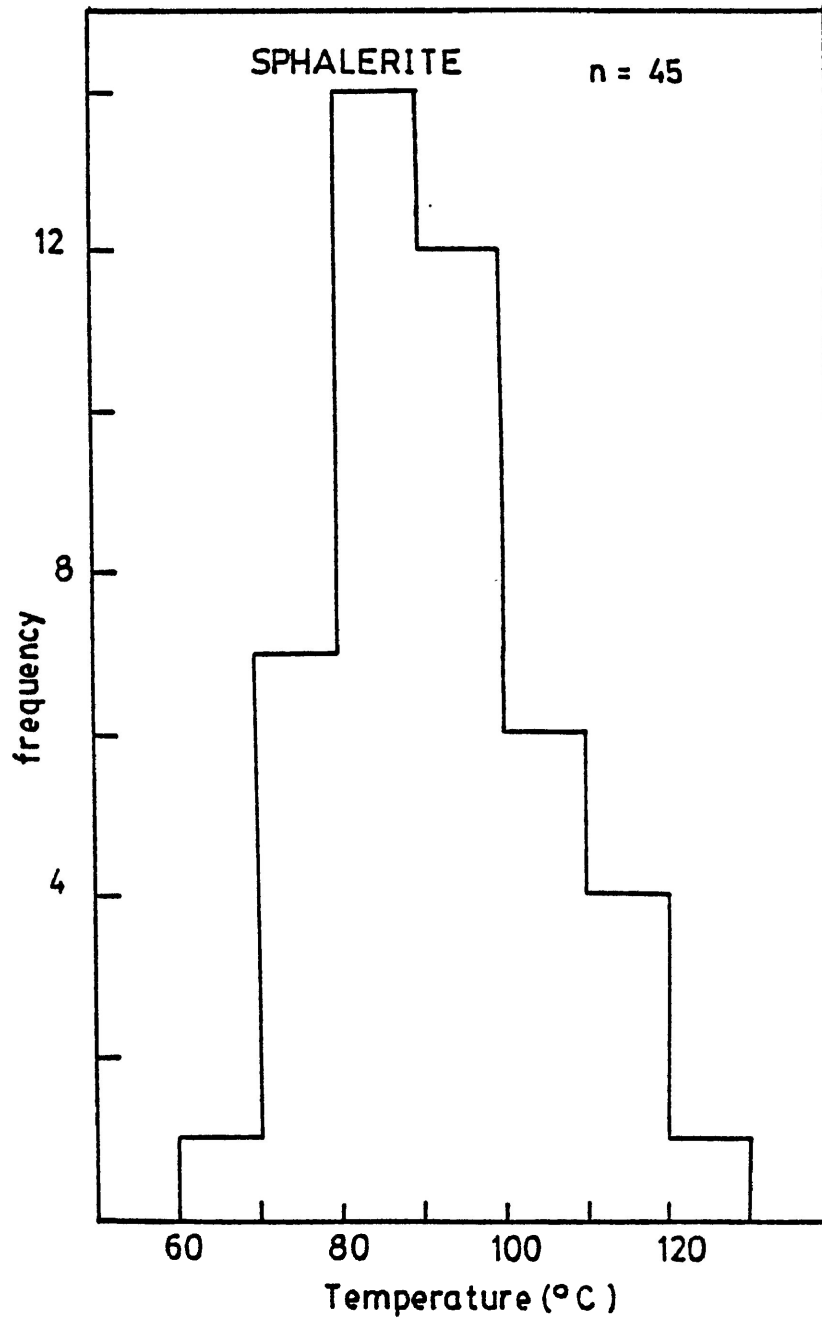


Figure 14: Histogram of microthermometric homogenization temperatures in sphalerite from all mines.

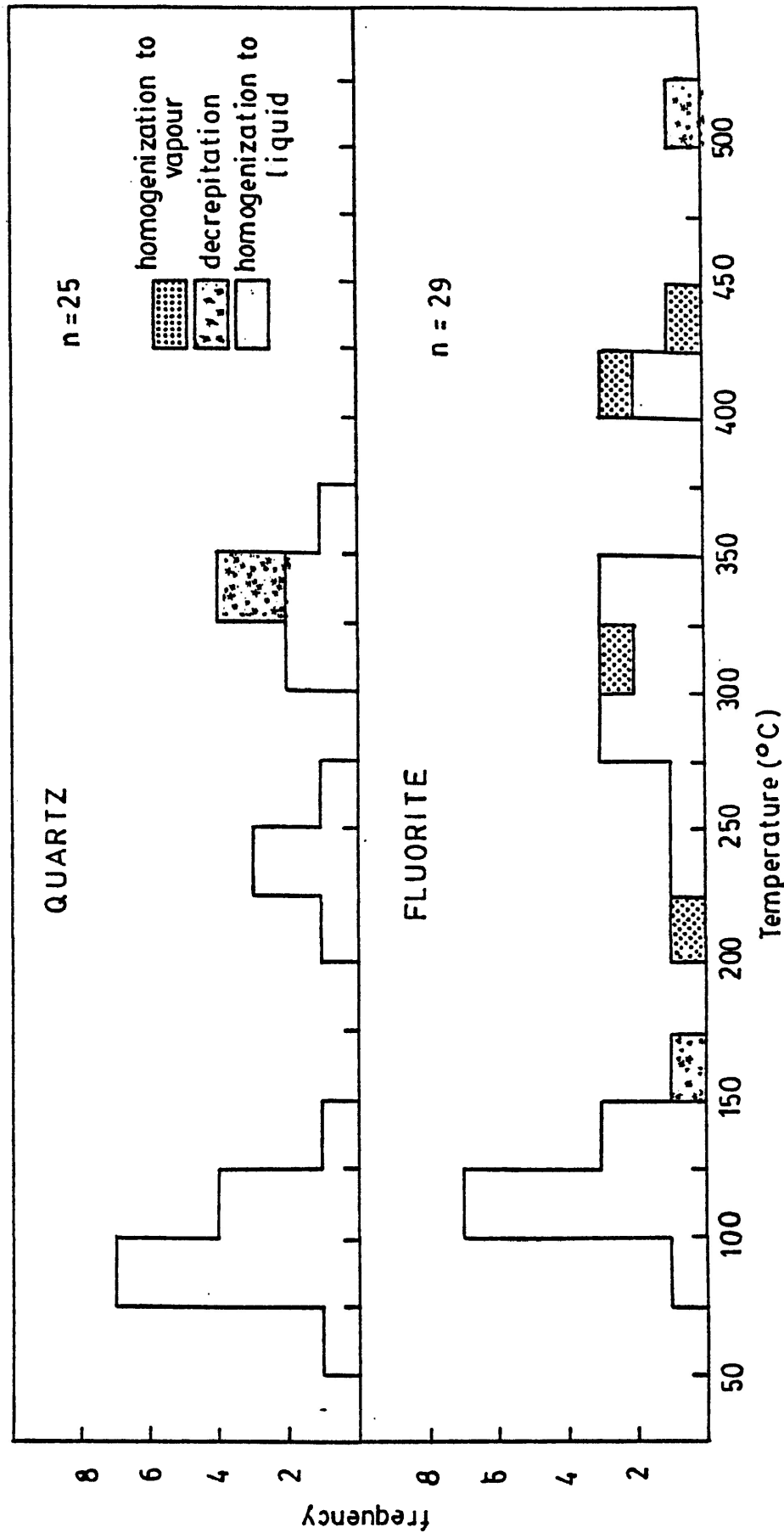


Figure 15: Histogram of microthermometric homogenization and decrepitation temperatures of inclusions in quartz and fluorite from all mines.

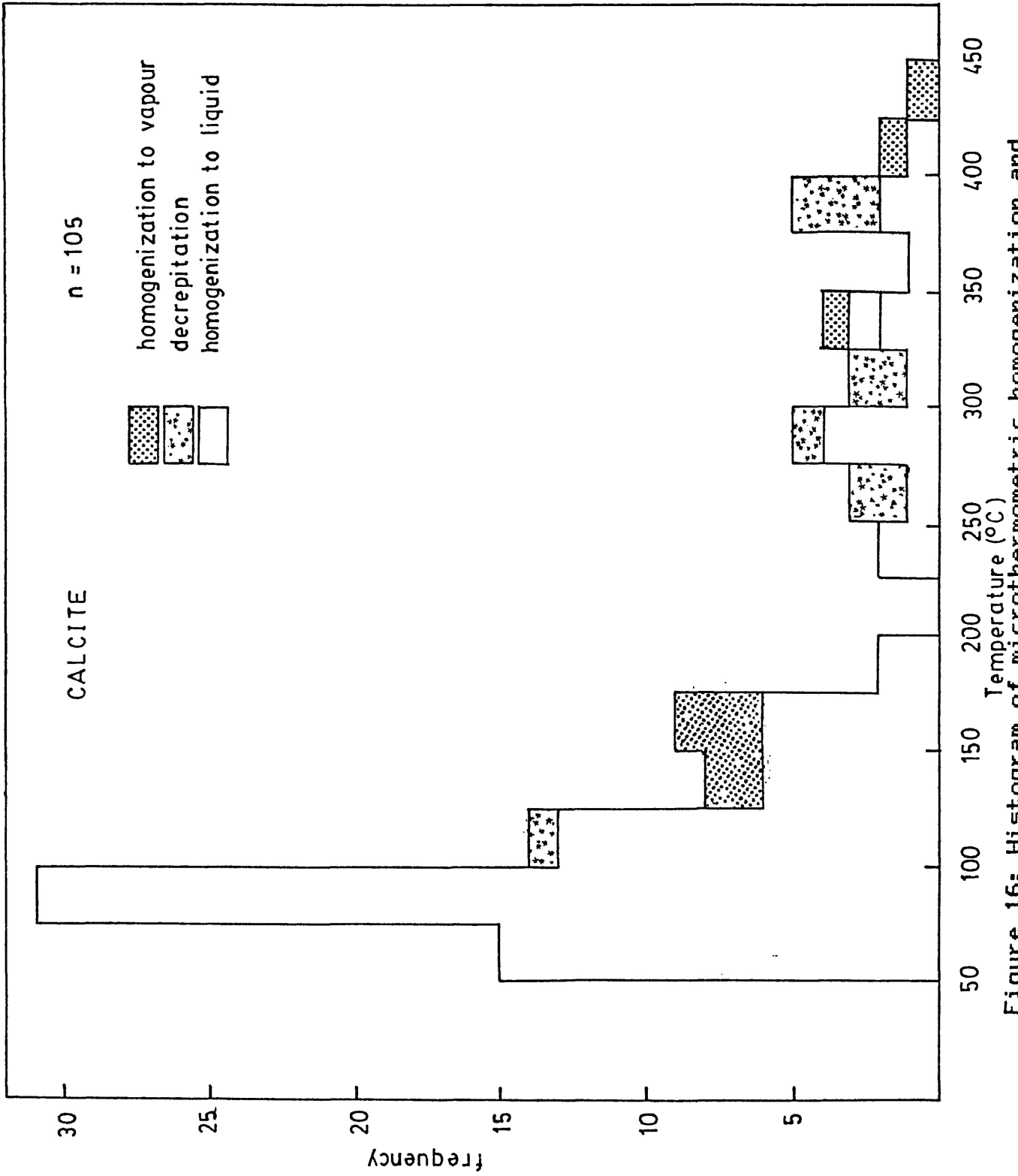


Figure 16: Histogram of microthermometric homogenization and precipitation temperatures of inclusions in calcite from all mines.

smaller peaks at 300° and 400°C. Quartz peaks occur at 100°, 250°, and 350°C. Fluorite peaks are similar at 125°, 325°, and 425°C. These peaks are poorly defined, however, and homogenization occurs throughout the 70°- 480°C range.

Figure 17 present the relationship between filling temperature and the paragenesis of each vein examined. In the following discussions temperatures and temperature ranges have been rounded off to simplify comparison.

The depositional temperatures of minerals in the two veins of the West Beaver mine vary, although the paragenesis of the veins is fairly similar (Figures 17A, 17B). In the Number 2 (silver-bearing) Vein, inclusions in early (pre-fracture) quartz and calcite suggest two periods of deposition at 150-200°C and 350°C. Green fluorite was deposited at 240°C. Some inclusions homogenized to vapour indicating the presence of boiling at 200°C in some parts of the system. The only inclusions analyzed from post-fracturing material were hosted in sphalerite, and these homogenized between 85° and 110°C.

In contrast, inclusions in quartz and calcite in the pre-fracture Little Pig (barren) vein material homogenized between 80° and 100°C, much lower temperatures. Green fluorite was deposited around 225°C, from boiling fluids. Post-fracture minerals tested include sphalerite, which was deposited between 90° and 115°C and calcite, from which inclusions homogenized at 135° and 425°C.

**TABLE 4: MICROTHERMOMETRIC HEATING OBSERVATIONS****RABBIT MOUNTAIN GROUP**

Sample	Class P/S/PS <sup>1</sup>	O.Q. <sup>2</sup>	t <sub>m</sub> (°C)	Phase <sup>3</sup>	t <sub>d</sub> (°C)	Vapour <sup>4</sup> Vol. %	Host <sup>5</sup> Mineral
<b>Little Pig Vein</b>							
LP 20	P	1	94.1	L		1	cc
LP 20	P	2	94.1	L		1	fl(g)
LP 20	P	1	83.9	L		3	fl(g)
LP 22	P	3	222.7	V		3	fl(p)
LP 22	P	2	225.0	L		2	fl(p)
LP 23	PS	2	114.4	L		1	sph
LP 24	PS	2	107.6	L		1	sph
LP 24	P	2	91.5	L		1	fl(g)
LP 25	P	3	87.9	L		1	fl(g)
LP 25	P	3	133.4	L		2	cc
LP 26	P	3	427.7	L		1	fl(g)
<b>Big Harry Vein</b>							
BLC 004	P	2	101.1	L		2	sph
BLC 005	P	1	73.5	L		1	sph
BLC 005	P	1	76.7	L		1	sph
BLC 005	P	2	91.8	L		2	cc
BLC 009	P	2	401.5	V		10 (V)	cc
BLC 013	P	2	105.1	L		3	cc
BLC 019	S	2	89.0	L		5	qtz
BLC 019	P	3	307.9	L		2	qtz
BLC 050	P	1	245.4	L		7	qtz
BLC 060	PS	3	92.5	L		1	qtz
BLC 060	PS	3	85.7	L		1	qtz

<sup>1</sup> P:Primary; PS:Pseudosecondary; S:Secondary

<sup>2</sup> O.Q.: Observational Quality - 1=poor; 3=excellent

<sup>3</sup> Homogenization phase - V:vapour; L:liquid

<sup>4</sup> (V):variable

<sup>5</sup> cc:calcite; fl(g):green fluorite; fl(p):purple fluorite;  
sph:sphalerite; qtz:quartz; am:amethyst

Sample	Class	O.Q.	$t_n$	Phase	$t_d$	V%	Host
<b>Rabbit Mountain</b>							
RM	1	P	2	80.9	L	1	sph
RM	1	P	1	82.4	L	1	sph
RM	1	S	3	113.7	L	2	sph
RM	2	P	3	99.7	L	3 (V)	fl (p)
RM	2	P	2	308.5	L	40 (V)	fl (p)
RM	3	PS	3	85.8	L	2	cc
RM	3	PS	3	79.2	L	2	cc
RM	3	PS	3	125.4	L	2	cc
RM	3	P	2	90.3	L	1	cc
RM	8	P	3	95.9	L	5 (V)	cc
RM	8	P	3	98.0	L	15 (V)	cc
RM	8	P	3	100.2	V	35 (V)	cc
RM	4	S	2	63.8	L	2	cc
RM	4	P	3	88.5	L	3	cc
<b>Badger</b>							
EA	68	P	3	108.3	L	1	sph
EA	69	P	3	284.7	L	1 (V)	cc
EA	69	P	3	284.7	L	3 (V)	cc
EA	69	P	3	284.7	L	25 (V)	cc
EA	69	P	3	101.3	L	2	fl (g)
EA	69	P	2		97.8	5	fl (g)
EA	70	P	3	105.6	L	3	fl (p)
EA	70	P	1	235.3	L	3	cc
EA	73	P	1	143.7	L	2	am
EA	75	P	3	110.3	L	3	cc
EA	75	P	3	107.6	L	5	cc
EA	76	P	3	104.9	L	2	qtz
<b>West Beaver</b>							
BE	2	P	3	173.0	V	35 (V)	cc
WBE	1	P	1	216.7	L	2 (V)	qtz
WBE	1	P	2	210.0	V	5 (V)	qtz
EA	51	P	1	337.4	L	5	cc
EA	51	P	3	240.9	L	10 (V)	fl (g)
EA	51	P	3		>550.0	30 (V)	qtz
EA	51	P	3	347.3	L	10 (V)	qtz
EA	52	PS	2	96.5	L	1	sph
EA	52	PS	2	88.9	L	1	sph
EA	53	P	3	111.3	L	2	sph
EA	53	P	3	90.3	L	1	sph
EA	54	P	3	142.1	L	2	cc
EA	54	P	3	198.6	L	2	cc

Sample	Class	O.Q.	t <sub>n</sub>	Phase	t <sub>a</sub>	V%	Host
<b>Silver Creek</b>							
EA	9	P	2	360.6	L	30 (V)	cc
EA	9	P	3	360.0	L	1	qtz
EA	10	P	3	102.4	L	1 (V)	cc
EA	10	P	1	106.0	V	20 (V)	cc
EA	10	P	2	87.8	L	1	sph
EA	11	P	1	53.7	L	1	cc
EA	11	P	2	71.7	L	1	cc
EA	12	P	3	140.2	L	2	cc
<b>Porcupine</b>							
PORC	1	PS	2	95.0	L	2	sph
PORC	1	P	2	91.8	L	1	cc
PORC	4	P	1	118.2	L	5	cc
EA	14	PS	2	103.4	L	2	cc
EA	14	P	3	312.5	L	2	cc
EA	14	P	3	262.4	L	20 (V)	fl(g)
EA	61	P	2	145.6	L	5	cc
EA	65	P	1	80.9	L	5	sph
EA	65	PS	3		326.3	3	cc
EA	66	P	2	98.8	L	5	cc
EA	67	P	3		270.1	30 (V)	cc
EA	67	P	2	73.9	L	5 (V)	cc
EA	67	P	3	174.0	L	3 (V)	cc
<b>Keystone</b>							
EA	1	P	3		415.1	3	sph
EA	1	P	2	93.0	L	2	sph
EA	1	P	3	77.5	L	1	sph
EA	1	P	1	69.8	L	3	sph
EA	1	P	2	99.9	L	2	cc
EA	2	P	2		188.5	1	sph
EA	2	P	3	478.0	L	1	cc in sph
EA	3	P	3	285.8	L	15 (V)	fl(g)
EA	3	P	3	119.6	L	3 (V)	fl(g)
EA	5	P	3	144.8	L	25 (V)	fl(g)
EA	5	P	2	134.1	L	3 (V)	fl(g)
EA	5	P	2	102.5	L	3	fl(g)
EA	5	P	2	102.1	L	3	fl(g)
EA	6	P	3	94.1	L	1	sph
EA	6	P	1		120.5	2	sph
EA	6	P	2	81.4	L	3	sph
EA	56	P	3	95.8	L	3	sph
EA	56	P	3	88.4	L	5	sph
EA	56	PS	2	98.2	L	1	sph
EA	56	PS	2	101.3	L	1	sph
EA	57	P	2	301.3	L	40 (V)	fl(p)
EA	57	P	2	102.4	L	3	cc
EA	59	P	2	106.8	L	2	sph

Sample	Class	O.Q.	$t_n$	Phase	$t_d$	VZ	Host
<b>Keystone (cont'd)</b>							
EA 59	P	3	94.5	L		2	sph
EA 59	P	2	86.8	L		2	sph
<b>SILVER MOUNTAIN</b>							
SM 2A	P	3	347.1	L		60 (V)	fl(g)
SM 2A	P	2	331.7	L		20 (V)	fl(g)
SM 2A	P	2	404.0	L		2 (V)	fl(g)
SM 2A	P	1	285.0	L		40 (V)	fl(g)
SM 2A	P	2	143.4	L		2 (V)	fl(g)
SM 2A	P	3			502.0	30 (V)	fl(g)
SM 2B	P	1	115.3			2	sph
SM 2B	P	2	310.6	L		10	fl(g)
SM 2B	P	2			174.7	20	fl(g)
SM 2C	PS	2	76.4	L		2	sph
SM 3A	P	2	152.1	L		5	cc
SM 3A	P	1	96.3	L		1	sph
SM 3C	P	3	78.1	L		2	cc
SM 3C	P	2	81.0	L		2 (V)	fl(p)
SM 3D	P	2			391.5	1	cc
SM 4A	PS	2	106.6	L			sph
SM 4C	P	2	134.5	L		15 (V)	cc
SM 4C	P	2	143.0	V		5 (V)	cc
SM 4C	P	1			264.1	1	cc
SM 4D	P	2			396.2	2	cc
SM 4E	P	2	87.0	L		1	sph
SM 4E	P	2			88.9	1	sph
SM 4E	P	1	83.6	L		1	sph
SM 13	P	3	432.4	V		30 (V)	cc
SM 13	P	3	340.0	L		3 (V)	cc
SM 21	P	1	298.2	L		25 (V)	fl(g)
SM 22	P	2	112.3	L		2	cc
SM 22	P	2	336.3	L		35 (V)	fl(g)
SM 23	P	2	420.3	V		15 (V)	fl(g)
SM 23	P	2	423.0	L		10 (V)	fl(g)
SM 24	P	3	468.0	V		35 (V)	fl(g)
SM 24	P	1	86.5	L		2	fl(g)
SM 51	P	3	87.7	L		1	sph
SM 70	P	2	145.6	L		10 (V)	cc
SM 70	P	2	153.6	L		3 (V)	cc
SM 70	P	2	393.6	V		20 (V)	cc
SM 70	P	2	398.0	L		10 (V)	cc
SM 71	P	3	90.7	L		2	sph
WEND-SM	P	2	231.3	L		8	qtz

Sample	Class	O.Q.	$t_n$	Phase	$t_d$	V%	Host
<b>PORT ARTHUR GROUP</b>							
<b>3A</b>							
EA 100	P	2	154.3	L		10	cc
EA 101	P	3	116.5	L		5	cc
<b>Shuniah</b>							
SH 1	P	2	100.5	L		1	cc
SH 3	P	3	111.2	L		1	cc
SH 3	PS	2	81.8	L		2	qtz
SH 3	PS	2	72.2	L		2	qtz
SH 3	PS	2	25.1	L		2	qtz
SH 3	PS	2	80.9	L		2	qtz
<b>Silver Harbour</b>							
EA 95	P	2	83.9	L		2	cc
EA 95	P	2	97.4	L		2	cc
EA 96	P	3	290.2	L		1 (V)	cc
EA 96	P	3			256.5	15 (V)	cc
EA 96	PS	3	176.8	L		20 (V)	cc
EA 96	PS	3	176.8	L		15 (V)	cc
EA 97	P	1	307.5	L		5 (V)	cc
EA 97	P	2	251.0	L		10 (V)	cc
EA 98	PS	2	86.7	L		2	qtz
EA 99	P	2	102.8	L		2	qtz
EA 99	P	3	230.7	L		5	qtz
EA 99	P	2	68.3	L		5	qtz
EA 99	P	3	101.5	L		10	qtz
EA 99	P	2	100.5	L		2	qtz
EA 99	P	2	96.9	L		5	qtz
EA 99	P	2	89.9	L		10	qtz
<b>Thunder Bay Vein</b>							
EA 85	P	3	97.6	L		2 (V)	cc
EA 85	P	2	275.2	L		10 (V)	cc
EA 85	P	2	245.0	V		3 (V)	cc
EA 86	P	2	246.3	L		10	cc
EA 87	PS	2	155.1	L		5	cc

Sample	Class	O.Q.	$t_n$	Phase	$t_a$	VZ	Host
<b>ISLAND GROUP</b>							
<b>Spar Island</b>							
EA 35	P	3	112.1	L		1	cc
EA 39	P	2	84.1	L		2	cc
EA 39	P	2	146.7	L		2	cc
EA 39	P	2	356.0	L		25 (V)	cc
EA 40	P	2			321.7	10 (V)	cc
EA 40	P	2	54.3	L		2	cc
EA 40	P	1	60.9	L		4	cc
EA 40	P	3	66.7	L		1	cc
EA 41	P	2	68.7	L		2	cc
EA 42	P	2	89.2	L		2	cc
EA 43	P	1	56.7	L		1	cc
EA 43	P	1	76.4	L		1	cc
EA 43	P	2	325.0	L		2 (V)	cc
EA 43	P	2	344.8	V		10 (V)	cc
EA 44	P	3	249.7	L		30 (V)	cc
EA 44	P	3			328.1	10 (V)	cc
<b>Jarvis Island</b>							
EA 24	P	2	106.8	L		1	cc
EA 24	P	1	51.4	L		1	cc
EA 24	P	3	168.5	L		10	cc
EA 27	P	2	114.0	L		3	cc
EA 27	P	2	107.0	L		2	cc
EA 27	P	2	149.0	V		2	cc
EA 27	P	2	86.5	L		1	cc
EA 27	P	2	73.6	L		1	cc
EA 28	P	2			380.7	15	cc
EA 31	P	3	325.7	L		35 (V)	cc
EA 33	P	2	423.7			20 (V)	cc
<b>Victoria Island</b>							
EA 19	P	2	62.6	L		2 (V)	cc
EA 22	P	2	112.5	L		1	cc
EA 22	P	1	60.9	L		1	cc
EA 20	P	2			324.5		cc
EA 20	P	3	55.3	L		1	cc
EA 20	P	2	56.3	L		1	cc
EA 20	P	2	48.3	L		3	cc

<u>Sample</u>	<u>Class</u>	<u>O.Q.</u>	<u>t<sub>n</sub></u>	<u>Phase</u>	<u>t<sub>d</sub></u>	<u>v%</u>	<u>Host</u>
<b>Silver Islet</b>							
SI	A	P	1	77.8	L	2	sph
SI	A	P	1	77.7	L	2	sph
SI	B	P	3	117.3	L	3	fl (p)
SI	B	P	2	87.5	L	3	fl (p)
SI	5	P	2	68.7	L	1	cc
SI	7	P	3	326.6	L	15	qtz
SI	7	P	2	89.9	L	2	qtz
SI	7	P	2	86.0	L	5	qtz
SI	8	P	2	306.3	V	35 (V)	qtz
SI	8	P	2	161.6	L	5	cc
SI	17	P	1	84.1	L	2	sph
SI	17	P	2	80.0	L	2	sph
SI	17	P	1	77.7	L	2	sph
SI	17	P	1	91.5	L	1	sph
SI	20	P	2	253.3	L	10	cc

At the Badger mine (Figure 17C), early calcite deposition occurred at two temperatures: 235°–285°C and 100°–110°C. Early quartz, purple fluorite and sphalerite was deposited near 105°C. The only post-fracture mineral analyzed was vug-filling amethyst, which was deposited at 145°C.

Green fluorite from the Porcupine mine (Figure 17D) was deposited at 260°C, the other pre-fracture mineral tested, calcite, was deposited at lower temperatures from 90°–120°C. Post-fracture calcite showed a broad range of homogenization temperature, from 75° to 310°C. Sphalerite was precipitated at 80°–95°C.

Both pre- and post-fracture quartz from the Big Harry vein (Figure 17E) were tested, the former deposited between 250° and 310°C, the latter at 85°–90°C. Early calcite showed two depositional temperatures, at 90°–105°C and from boiling fluids around 400°C. Post-fracture sphalerite precipitated between 75° and 100°C.

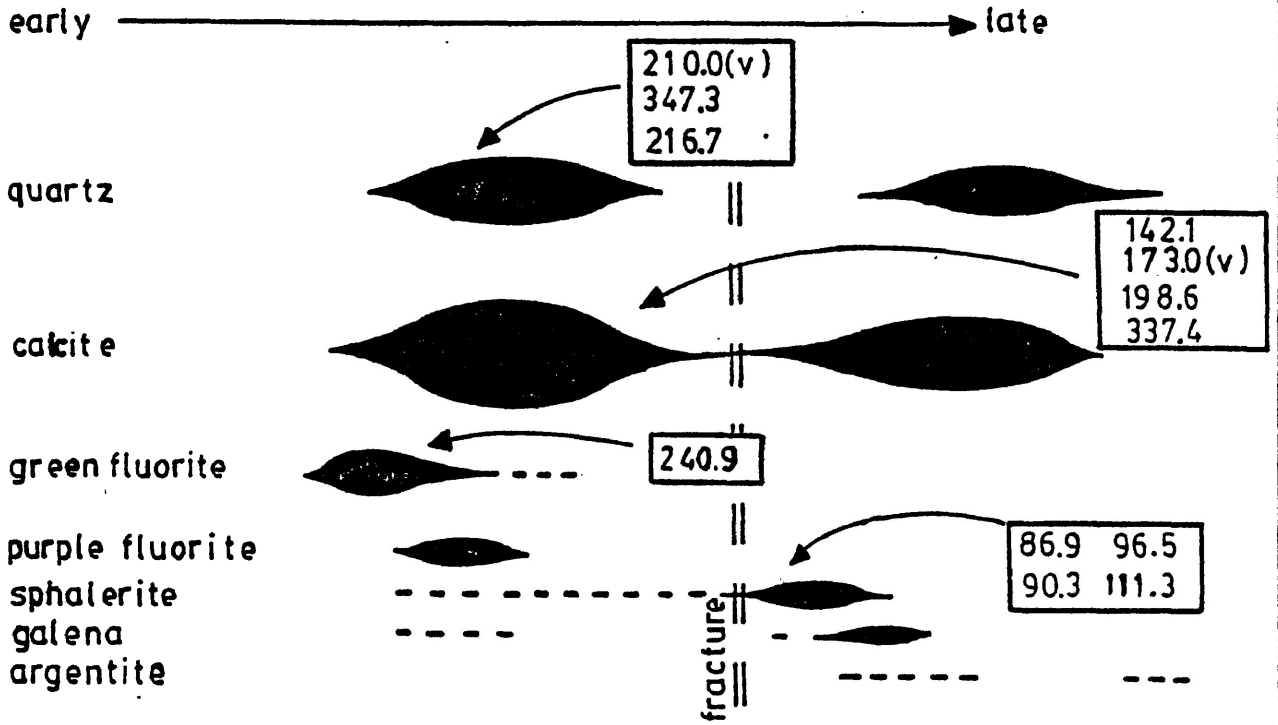
At Silver Creek (Figure 17F) early calcite was deposited at 100°, 140°, and 360°C, post-fracture quartz at 360°C and sphalerite at 70°–90°C.

**Figure 17: The relationship between paragenetic sequence and homogenization temperature from Mainland and Island Belt Mines.**

- A. West Beaver No. 2 Vein
- B. West Beaver Little Pig Vein
- C. Badger
- D. Porcupine
- E. Big Harry
- F. Silver Creek
- G. Rabbit Mountain
- H. Keystone (Climax)
- I. Silver Mountain
- J. Shuniah
- K. Silver Harbour (Beck)
- L. Thunder Bay
- M. 3A
- N. Victoria Island
- O. Jarvis Island
- P. Spar Island
- Q. Silver Islet

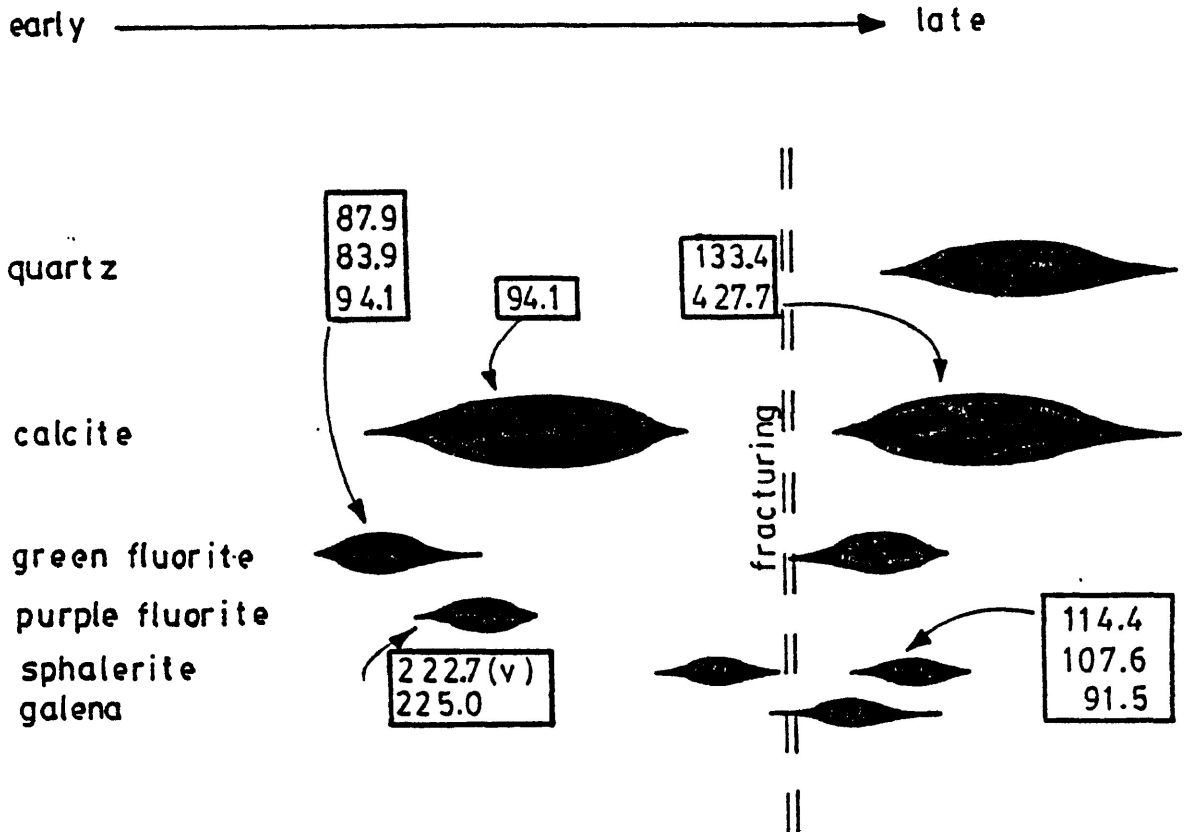
**A**

WEST BEAVER no.2 VEIN

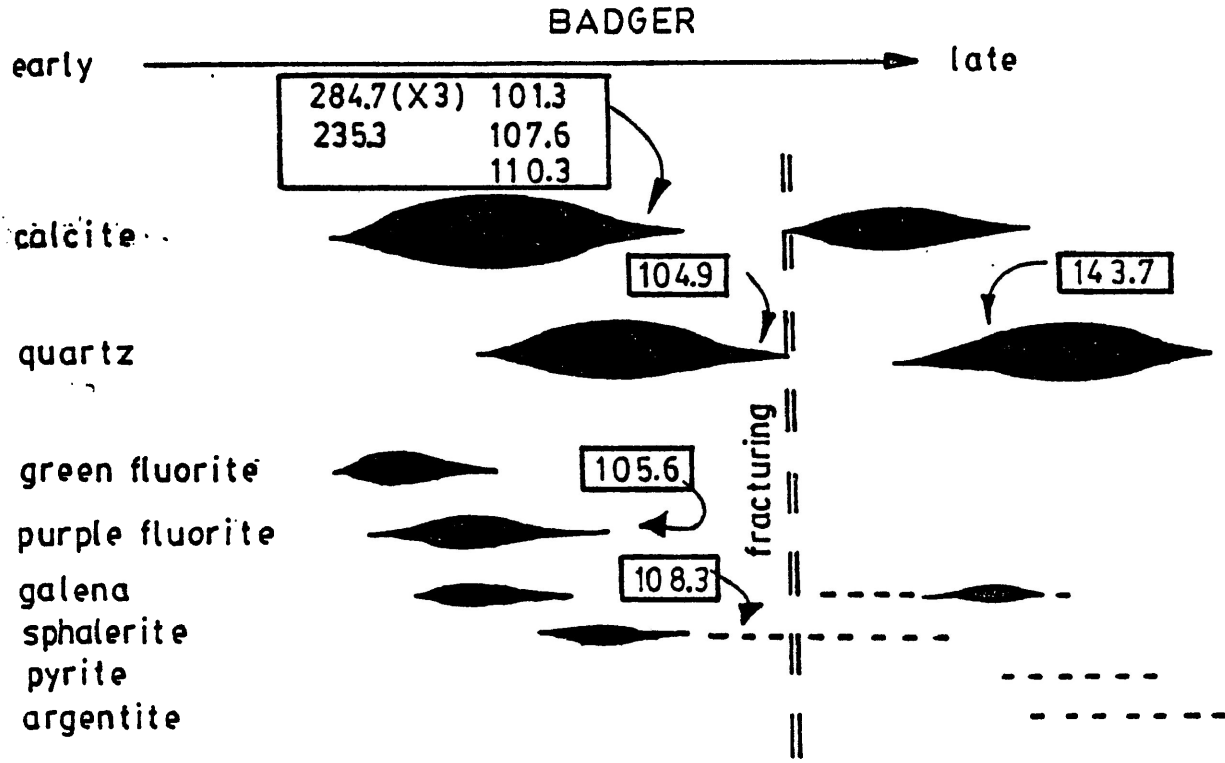


**B**

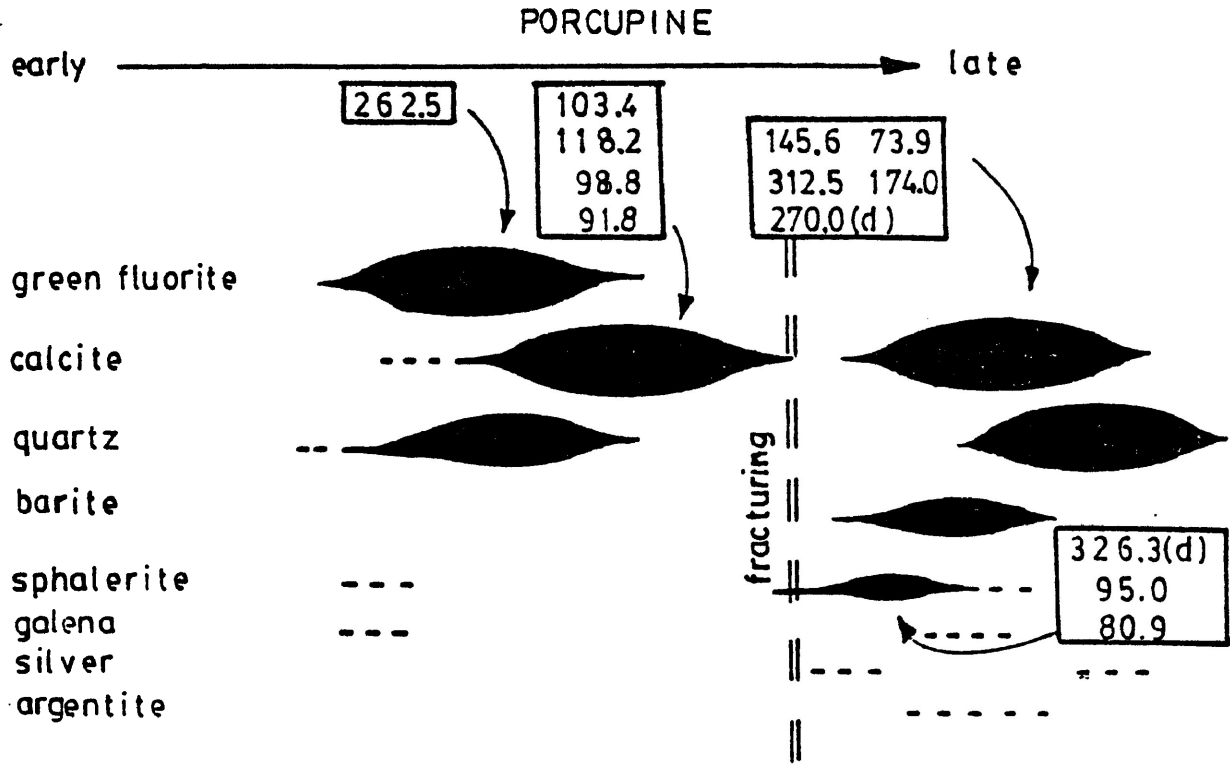
WEST BEAVER LITTLE PIG VEIN



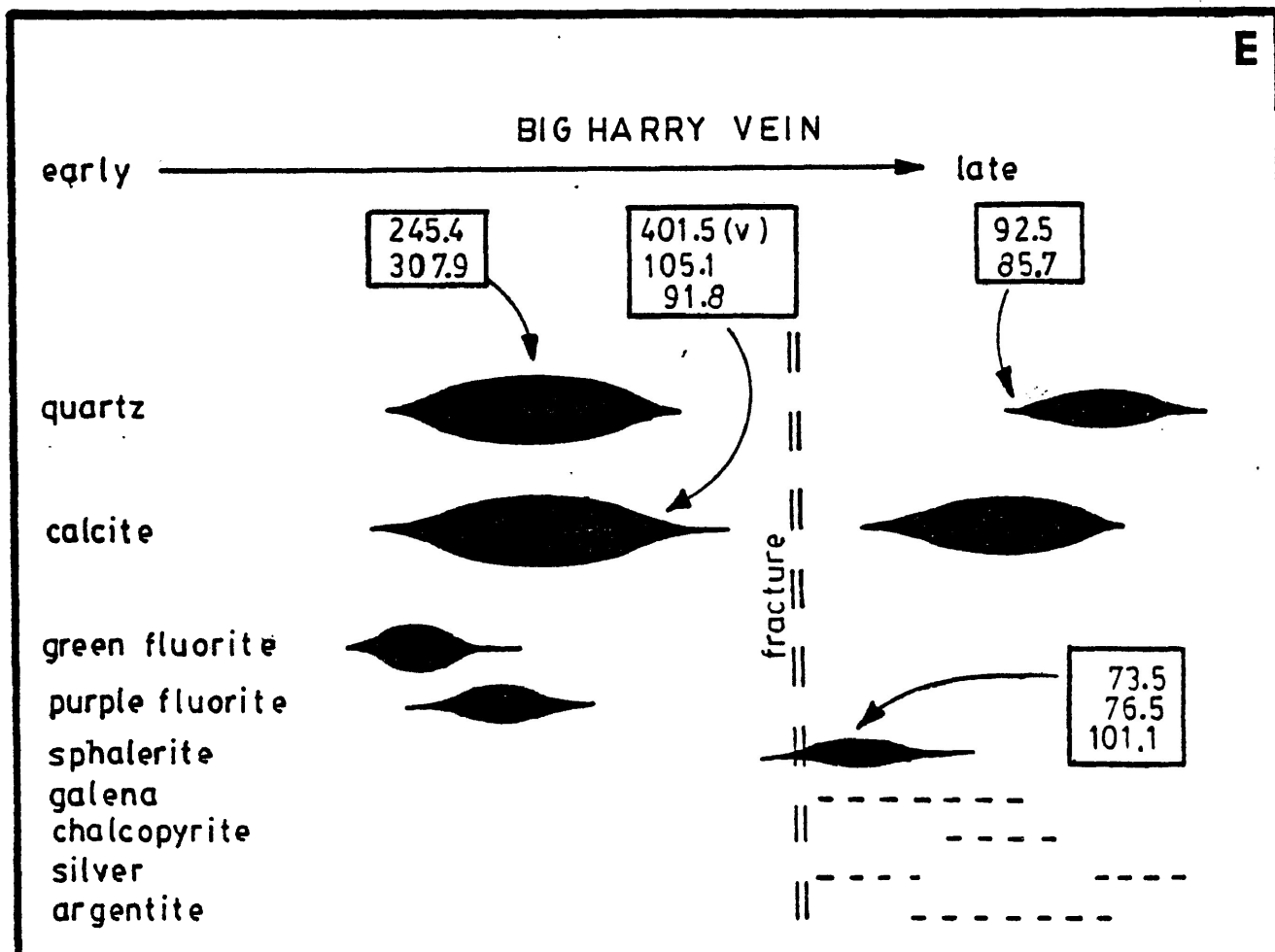
C



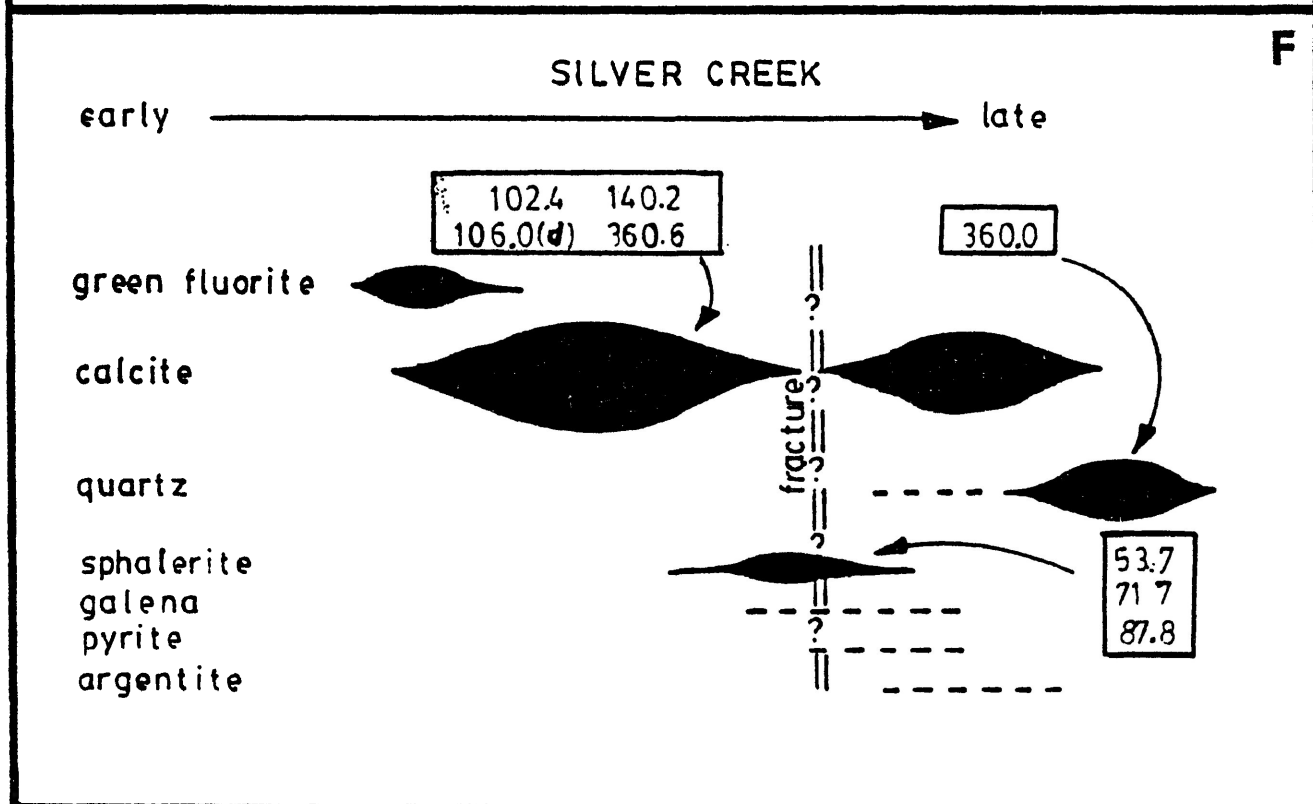
D



E

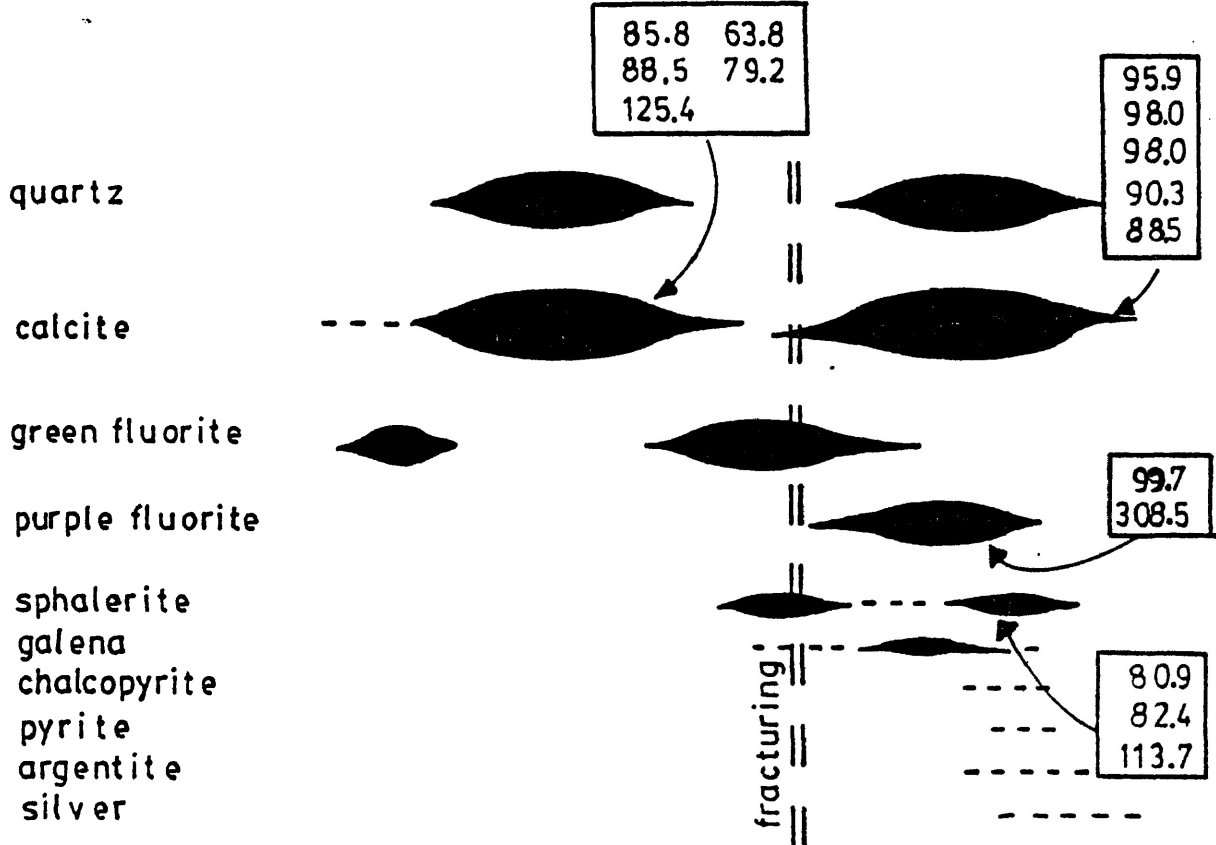


F



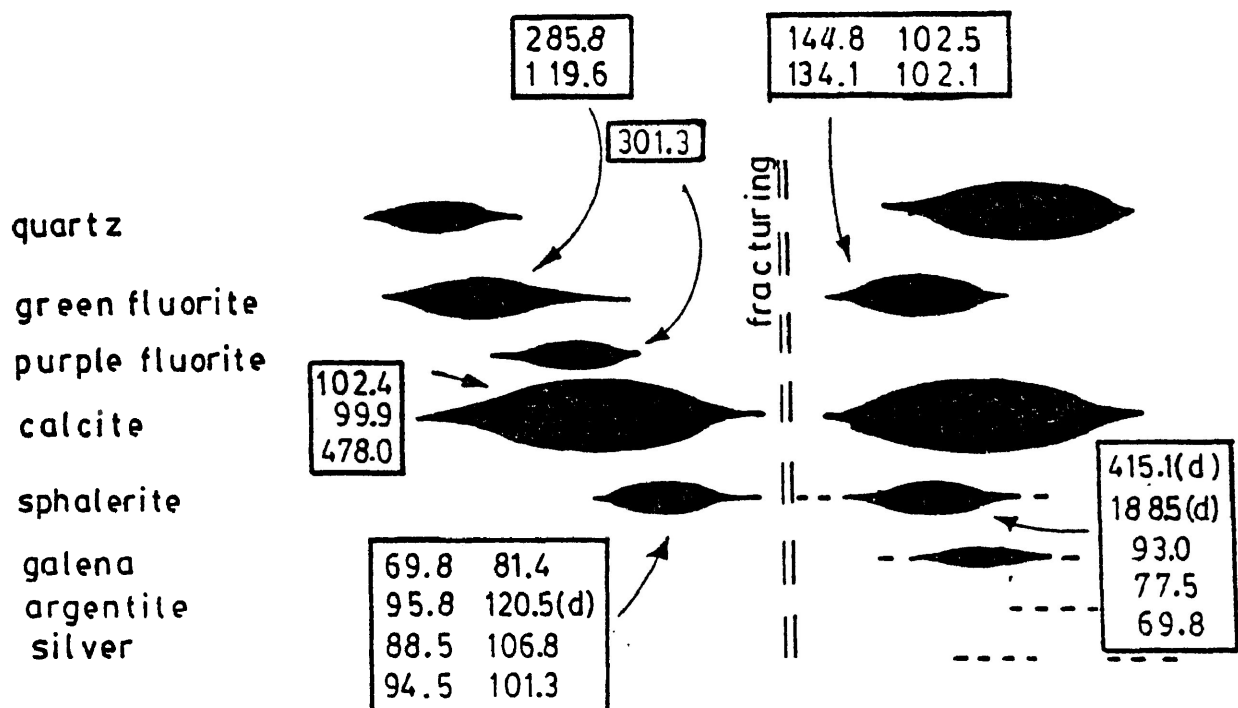
RABBIT MOUNTAIN

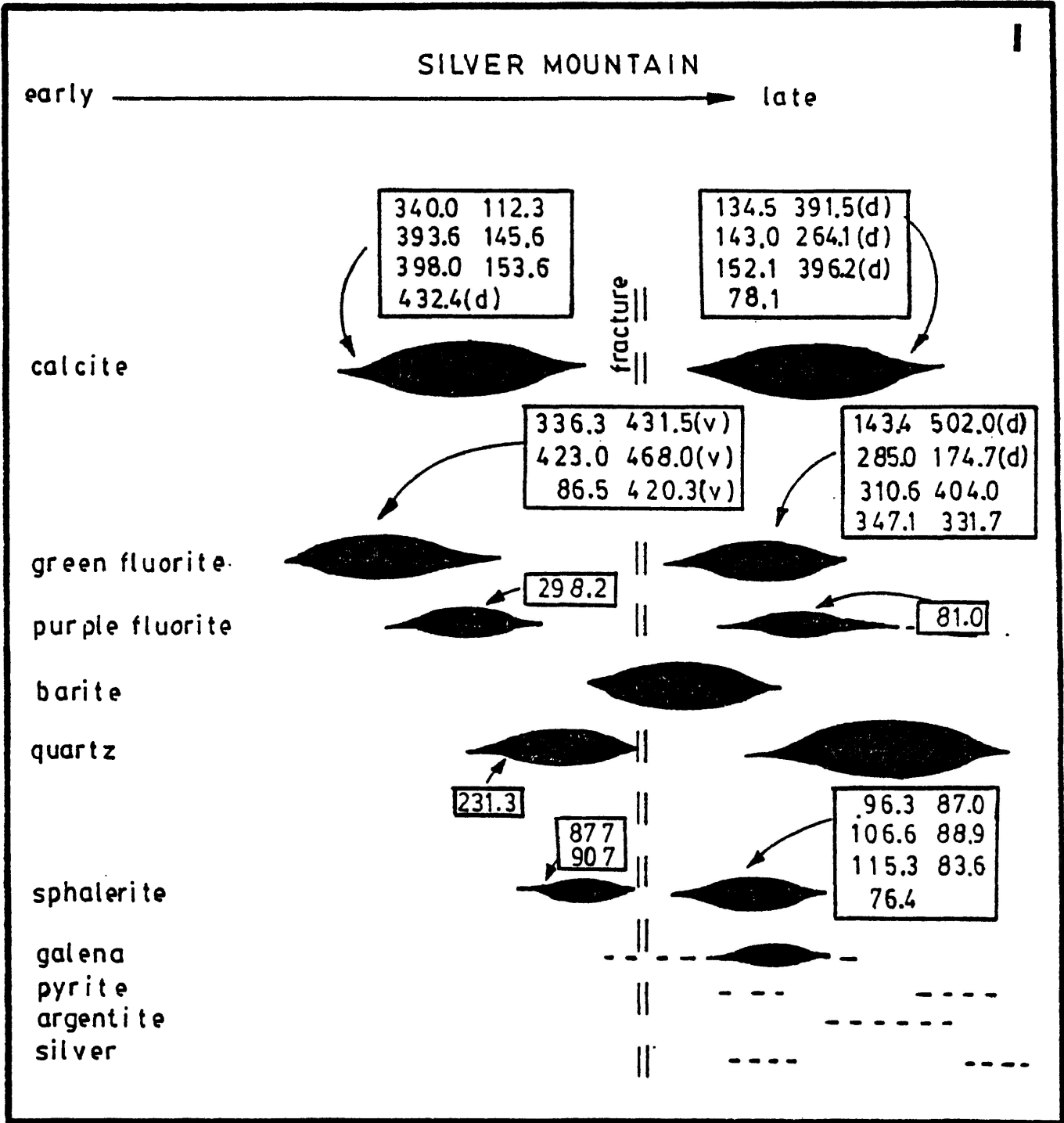
early → late

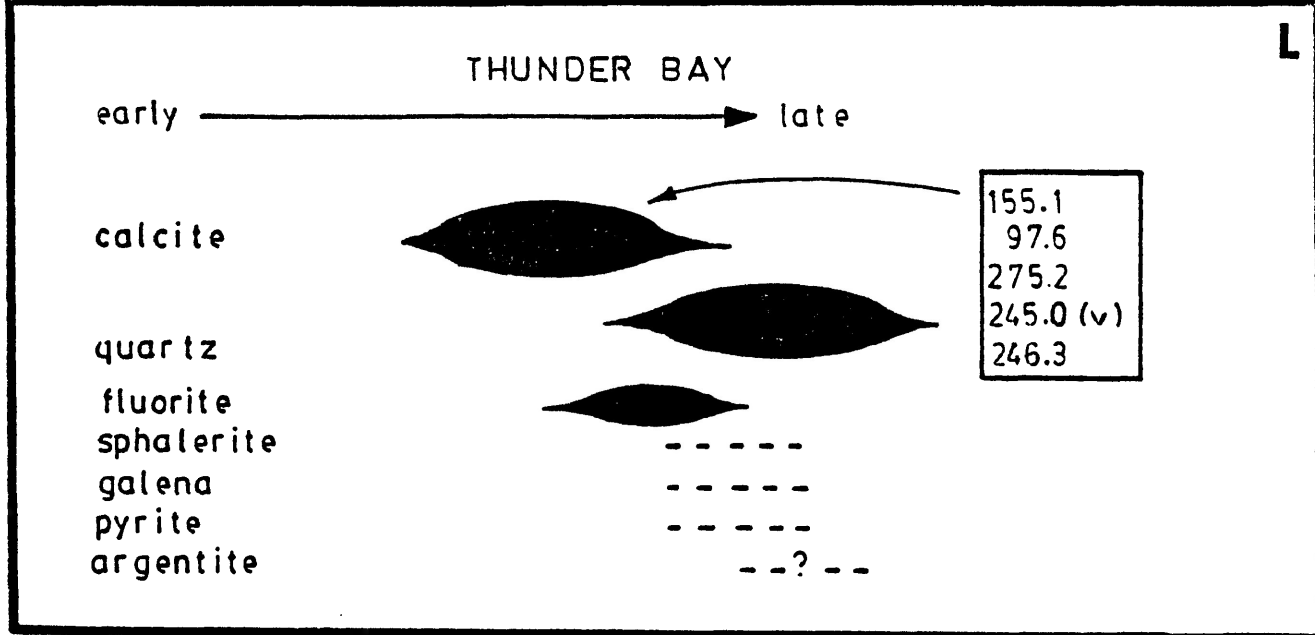
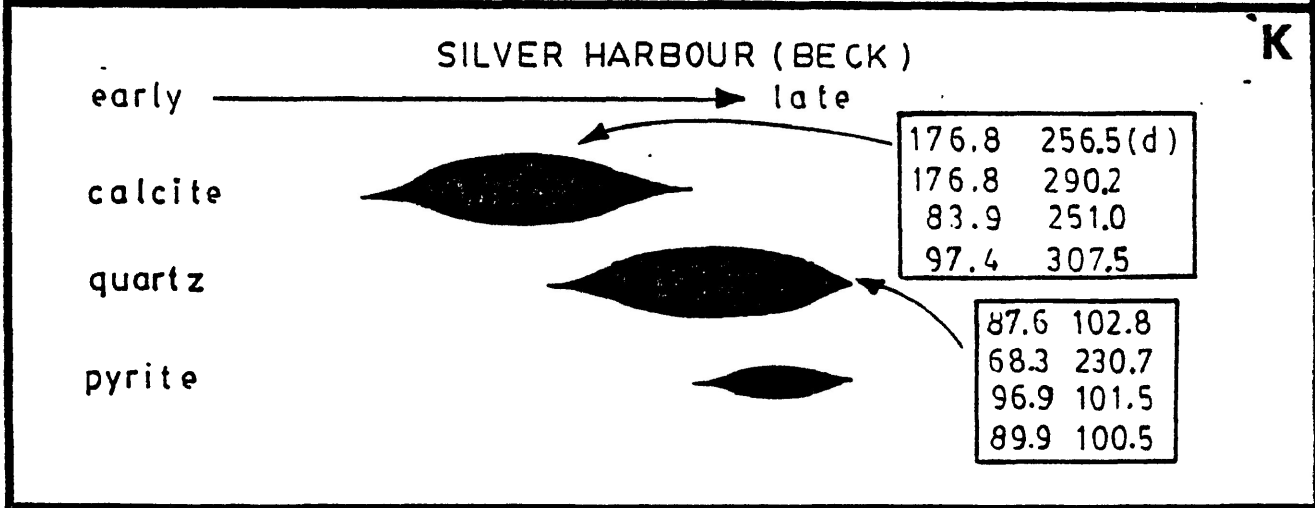
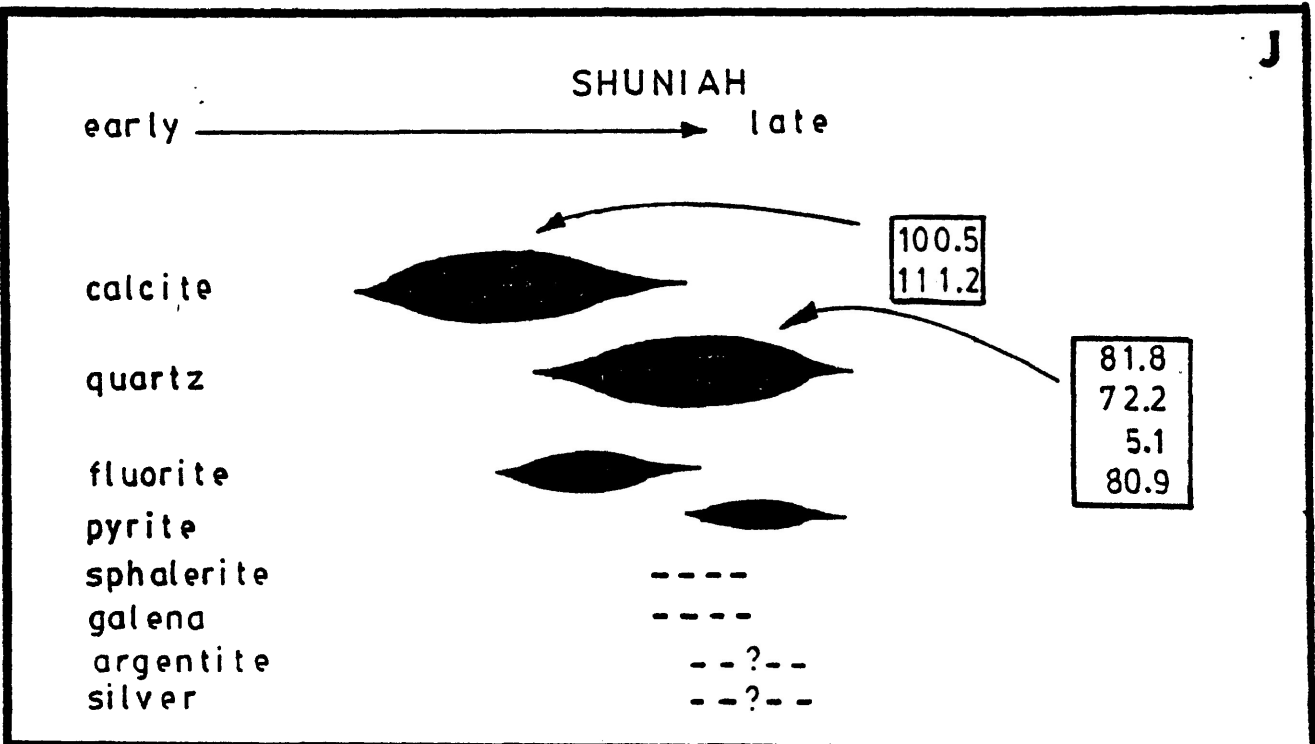


KEYSTONE (CLIMAX)

early → late



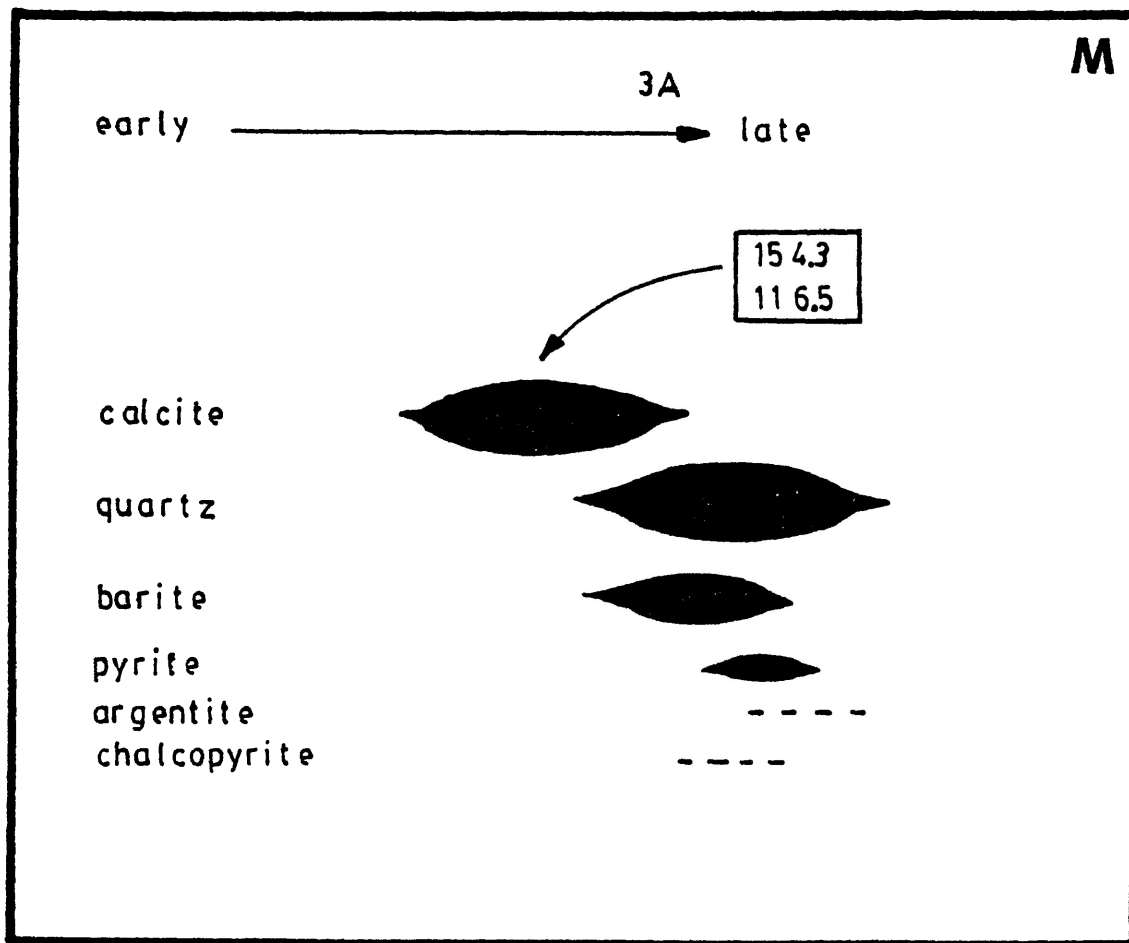


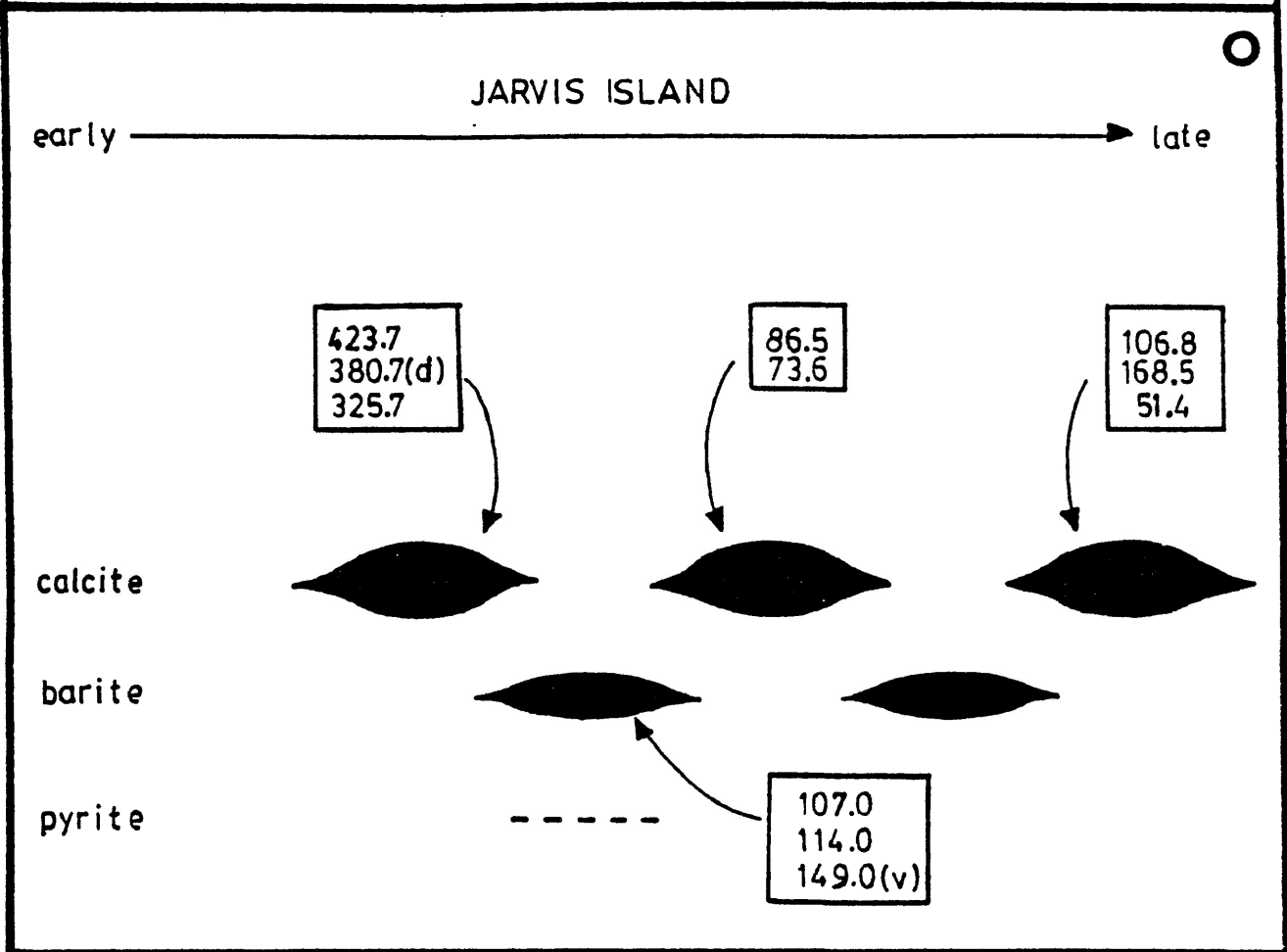
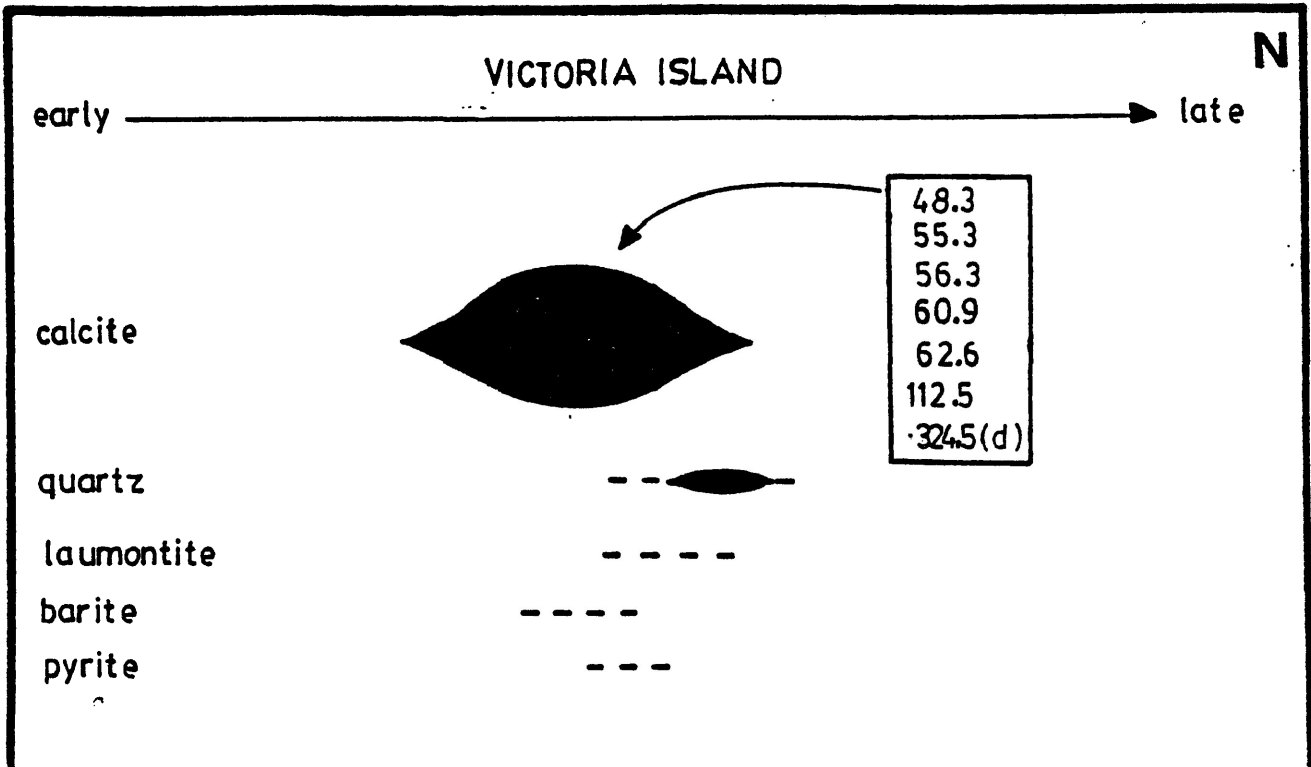


J

K

L



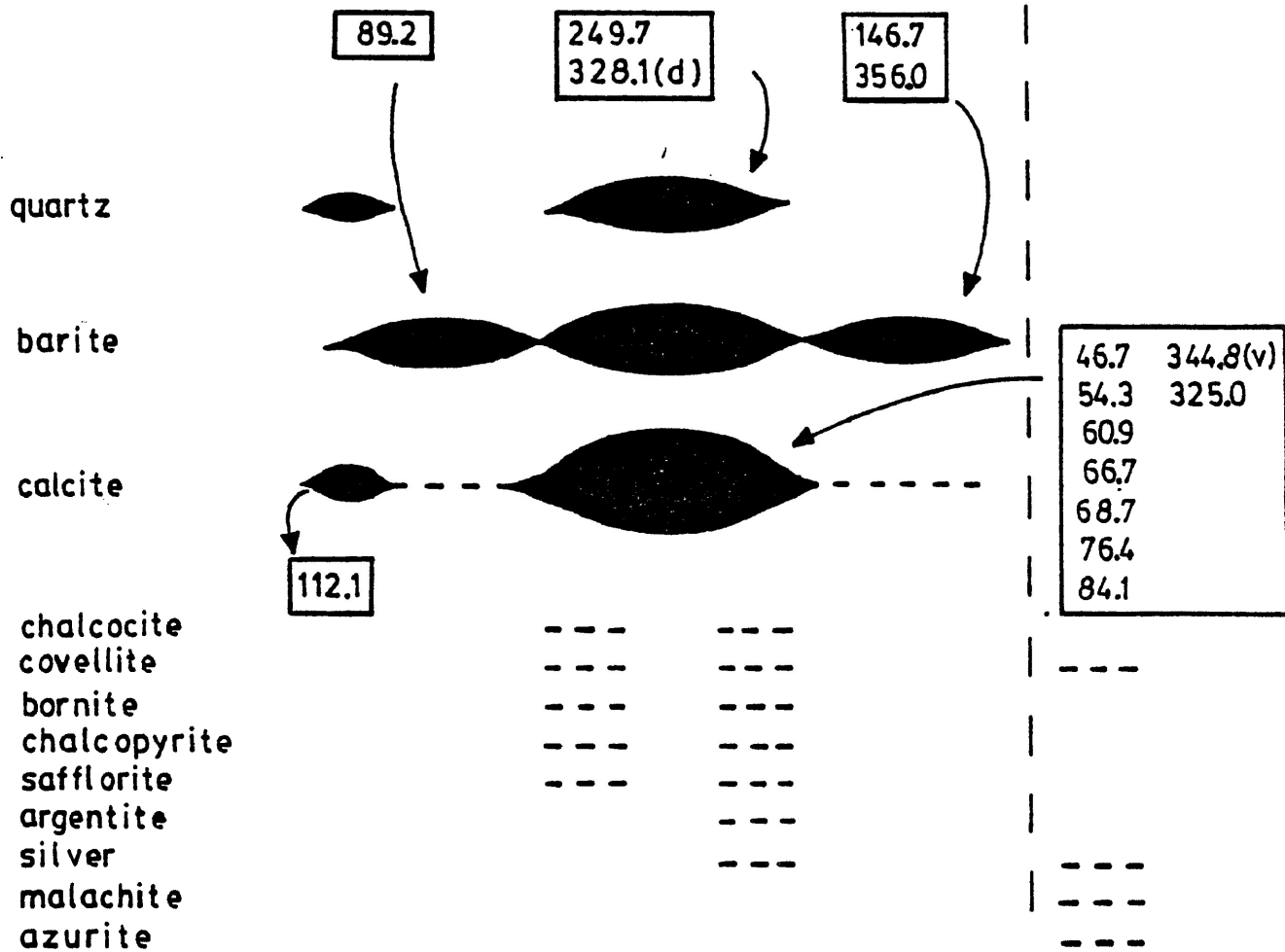


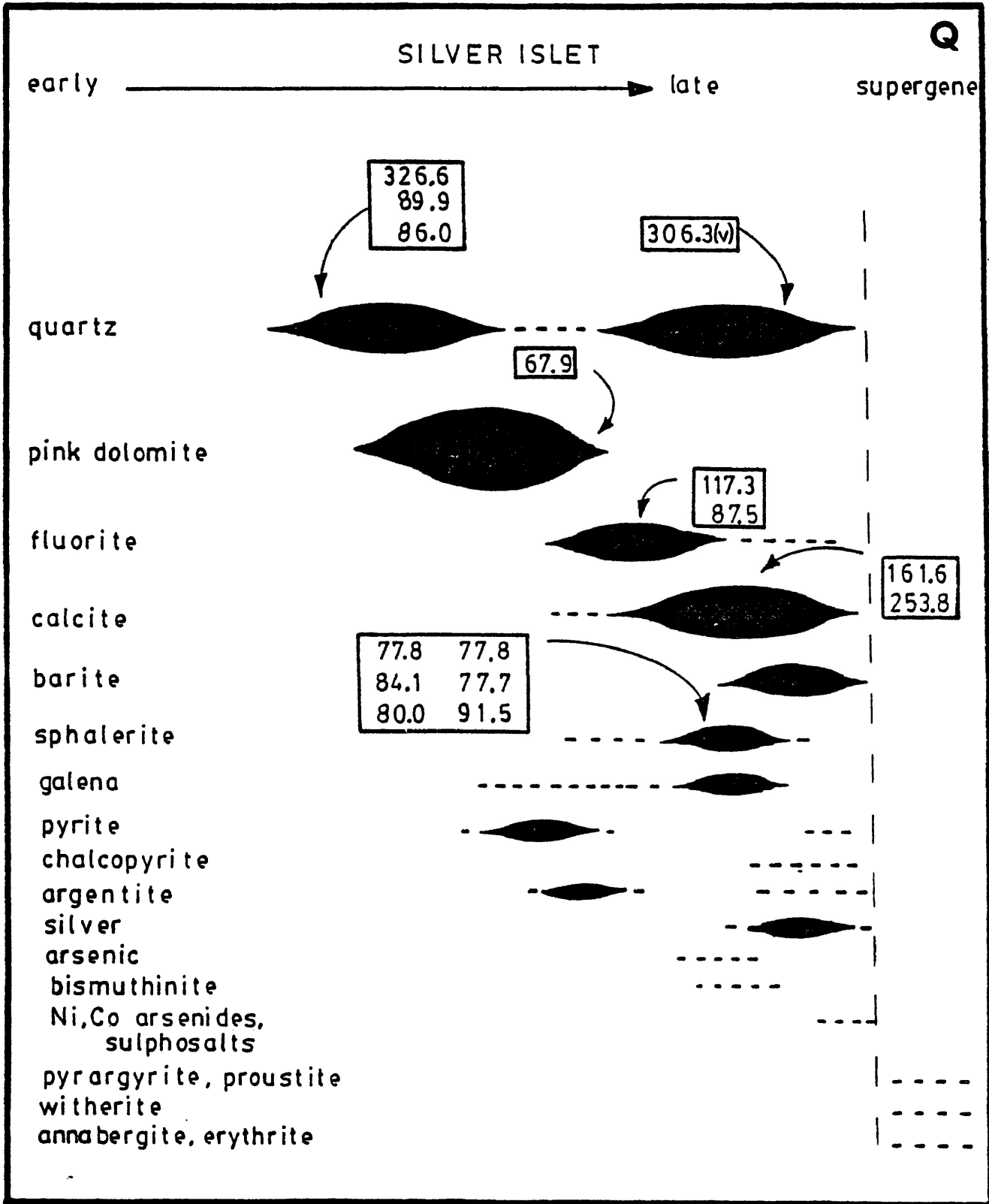
P

SPAR ISLAND

early → late

supergene





Homogenization of inclusions from early Rabbit Mountain (Figure G) calcite ranged from 65° to 125°C, while post-fracture calcite the numbers were tightly clustered between 90° and 100°C. Post-fracture purple fluorite had inclusions homogenize at 100° and 310°C. Sphalerite temperatures ranged from 80°-115°C.

At the Keystone mine (Figure 17H), pre-fracture fluorite was precipitated at 120° and 285°-300°C, while post-fracture fluorite ranged from 100°-145°C. Early calcite was precipitated at 100°C. Both pre- and post-fracture sphalerite showed a temperature range of 70°-100°C. A calcite inclusion in sphalerite, presumably formed in the hydrothermal fluids before they reached the open fracture system in which the vein was deposited, indicated a formation temperature of 480°C.

At Silver Mountain (Figure 17I), early calcite inclusions homogenized at 340°-400° and 150°C, while post-fracture calcite inclusions homogenized at 135°-150°C. Many of the latter decrepitated near 400°C, perhaps indicative of a second, higher temperature depositional period. Almost all inclusions in early green fluorite showed homogenization between 335° and 470°C, and many indicated the presence of boiling by their homogenization vapour. The one lower temperature inclusion (85°C) may have been stretched, or had fluid leak from it. Purple fluorite associated with this stage was precipitated at 300°C. Post-fracture green fluorite had inclusions that homogenized over a broad temperature

range, from 140° to 405°C. This temperature range was observed over an interval of 1.5cm of fluorite encrustation. Purple fluorite from the vug-lining stage showed low temperature homogenization at 80°C. Early quartz was precipitated at 230°C, sphalerite (early and late) between 85° and 115°C.

In the Port Arthur Group (Figure 17J-M) the parageneses are simpler. Quartz and calcite at the Shuniah were deposited between 75° and 110°C. At the Silver Harbour mine two stages of quartz and calcite deposition occurred, at 80°-95°C and 175°-310°C. Because samples were from dump material it was not possible to establish the relationship between these two stages with respect to time. At the 3A mine calcite homogenization temperatures of 155° and 115°C were observed. Finally, calcite from the Thunder Bay vein showed deposition occurred at 100°, 155°, and 250°-275°C. The latter was accompanied by boiling of the hydrothermal fluids.

Calcite from the Victoria Island veins (Figure 17N) had inclusions homogenized at very low temperatures, 50°-65°C, except one at 110°C. Many of the inclusions were not of good quality, and they were very small (~5µm); however, the same criteria were used to classify them as for the other deposits.

At Jarvis Island (Figure 17O) the initial phase of vein deposition, calcite, occurred at high temperatures of 325°-425°C.

This was followed by a pulse of barite deposition between 110° and 150°C. There appears to have been some boiling or effervescence associated with the latter. The ensuing period of calcite deposition occurred at even lower temperatures of 75°–85°C. A following pulse of barite deposition occurred at unknown temperatures. The final period of deposition was dominated by calcite deposition over a wide range of temperatures, 50°–170°C.

At Spar Island (Figure 17P) a slightly different pattern of temperature change is observed. Initial deposition of calcite and barite at low temperatures (50°–110°C) was followed by pulses of deposition of the barite with minor quartz at much higher temperatures (250°–350°C). During the high temperature deposition of barite hydrothermal fluids were boiling. Sulfide deposition preceded and post-dated the high temperature episode. The final stage of vein deposition was dominated by calcite precipitation with minor barite over a wide range of temperatures from 75° to 355°C.

At Silver Islet (Figure 17Q) early vein deposition was dominated by quartz and dolomite precipitation. Initial quartz was deposited from hot temperatures (325°), but the bulk of this period occurred at temperatures of 65° to 90°C. Towards the end of this stage, fluorite first appears; it was deposited between 90°–120°C. As the gangue mineralogy becomes dominated by the presence of quartz and calcite, a general increase in

temperatures to 160°–305°C is observed, accompanied by boiling at the higher temperatures. This increased temperature was not universal, or perhaps not constant, as indicated by the lower homogenization temperature of sphalerite associated with stage, which indicate depositional temperatures of 75°–90°C.

It should be noted that these temperatures and temperature ranges are not drawn from a large enough body of data to test them statistically. In general only 2 or 3 inclusions from a single paragenetic stage could be closely observed, although by racking and shifting the stage, it was usually observable whether or not the inclusion's behaviour appeared typical of others.

#### TEMPERATURE CORRECTION DUE TO PRESSURE

Homogenization temperatures of fluid inclusions do not represent trapping temperature, but can be modified to do so, if an estimate of lithostatic and hydrostatic pressures and fluid salinity can be formed.

Potter (1977) has constructed graphs which have been used to estimate temperature correction factors for all inclusions for which salinity was determined. The pressure was estimated by assuming a burial by 1km of overlying shale, based on the present maximum Rove thickness of 960m (Morey, 1969). By assuming an average density of 2.5 g/cm<sup>3</sup>, a lithostatic pressure of 25 MPa was applied in this estimation.

In the low temperature inclusions ( $\sim 100^{\circ}\text{C}$  homogenization) the correction applied is on the order of  $35^{\circ}\text{--}45^{\circ}\text{C}$ , significantly raising the trapping temperature to  $\sim 150^{\circ}\text{C}$ . In the higher temperature range, the average correction applied is  $10^{\circ}\text{C}$ , which affects the filling temperature to a much lesser extent (Figure 18).

The variability of lithostatic and hydrostatic pressure is difficult to evaluate from the limited fluid inclusion data obtained from each mine, but some variability is suggested by the evidence of sporadic boiling. Hence, application of these correction factors in discussing results has been avoided because of their questionable validity. The presence of boiling during mineral precipitation, as indicated by some samples, implies a communication with the surface uninhibited by the load of a column of rock. The minerals exhibiting this evidence of low pressure therefore have a trapping temperature equal to their filling temperature. Samples containing inclusions which exhibited behaviour characteristic of boiling were generally found in restricted zones in close proximity, physically and paragenetically, to inclusions formed in non-boiling sections of the vein. Analyses of sphalerite crystals with respect to their temperature - ~~and~~ conditions of formation, as will be discussed, indicate that temperatures uncorrected for pressure effects are more compatible with observed mineral stability fields, such as that of native silver, than those for which a correction factor

is applied. It is therefore suggested that some change in pressure, varying from lithostatic to hydrostatic probably occurred, but further work is required to clarify the proper correction factor to apply to homogenization temperature.

All temperatures referred to in discussions of the environment of deposition are therefore homogenization temperatures.

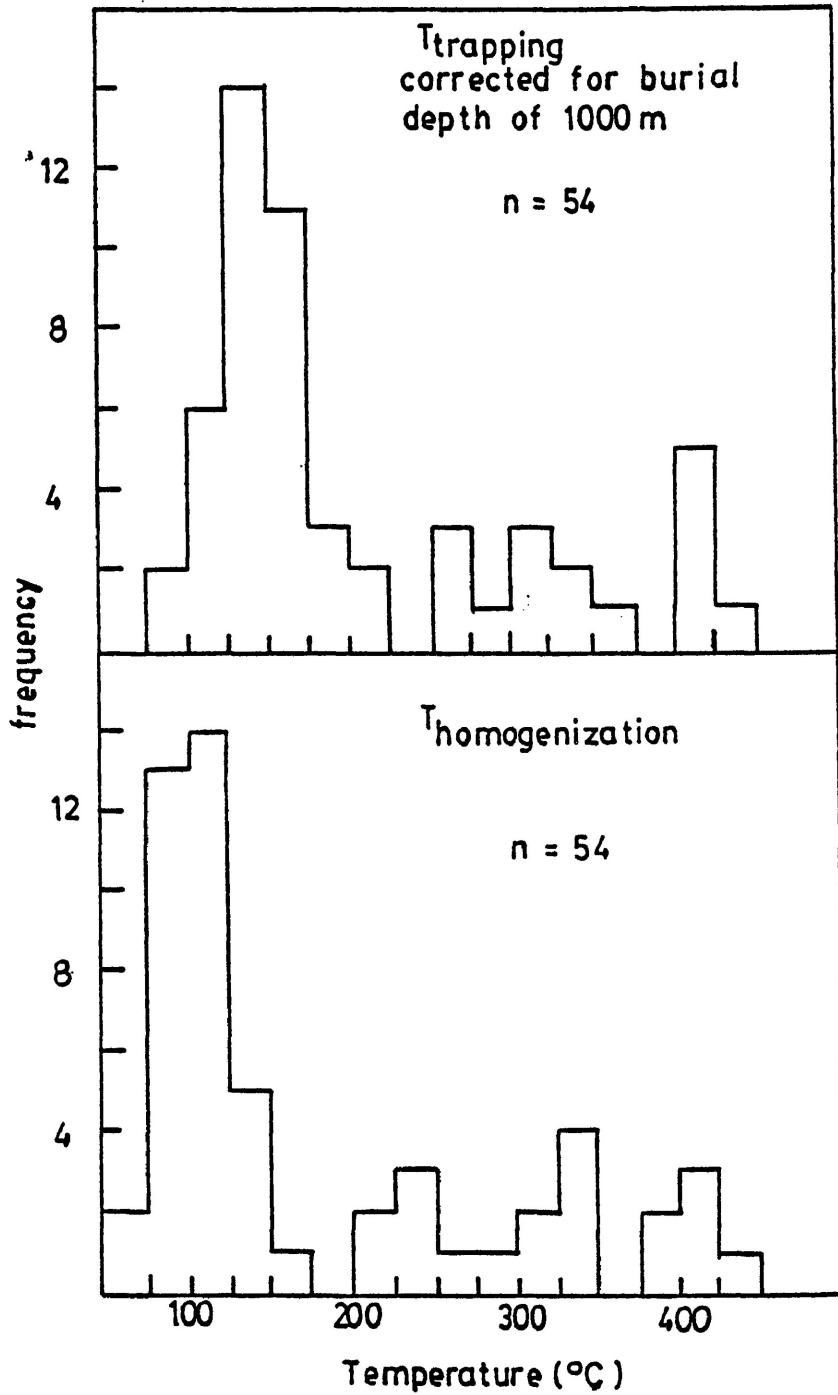


**Figure 18: Comparison of homogenization temperatures to trapping temperatures of fluid inclusions assuming 1000m burial.**

## MINERALOGICAL INVESTIGATIONS

### INTRODUCTION

Three techniques were employed to investigate the mineralogy of the silver veins: microprobe analyses of major and minor elements in sphalerite and unknown phases from Silver Islet, Spar Island, and Edward Island; Gandolfi camera X-ray diffraction identification of nickeline; and X-ray powder diffraction powder patterns of hydrothermal clay minerals.

### EXPERIMENTAL TECHNIQUE

Microprobe analyses were conducted on the ETEC microprobe with energy dispersive analytic package at the University of Toronto. A 105 nA current, with a beam potential of 20 kV, was employed. Data was reduced by the computer program PESTRIP, a University of Toronto modification of Stratham's (1976) procedure.

Synthetic standards of sphalerite containing 5 and 25 mol% Fe, natural chalcopyrite, and synthetic  $Ag_2S$ ,  $MnS$  and  $CdS$  were used for calibrations during sphalerite analyses. Detectability limits were calculated using Birk's (1969) formula:

$$CDL = C_{std} \times \frac{3 \sqrt{I_{std}}}{I_p}$$

where CDL = calculated detection limit in wt %  
C = composition of the standard in wt %  
 $I_b$  = background intensity during calibration  
 $I_p$  = peak intensity during calibration

The calculated detectability limits of the minor elements analyzed were as follows: Fe = 0.01 wt %, Cd = 0.02 wt %, Ag = 0.03 wt %, Cu = 0.02 wt %, and Mn = 0.01 wt %.

### MICROPROBE RESULTS

Thirty samples of sphalerite were analyzed to determine iron content and detect the presence of trace elements.

Weak zoning and patchy anomalous anisotropy is seen in many sphalerite crystals, and representative analyses were made to document any compositional causes for these phenomena.

Most sphalerite contains 0.25 - 0.50 wt % Fe (Table 5), the extreme ranges from 0.0 to 2.47 wt %. Cd occurred in trace quantities in several veins. In the Mainland Belt, 0.25-1.5 wt % Cd was found in sphalerite in the Keystone, Silver Mountain, West Beaver, Rabbit Mountain and Big Harry veins, but was absent at the Little Pig, Silver Creek, and Porcupine veins. In the Island Belt, only Edward Island sphalerite contained trace cadmium, but in considerably higher quantities than the Mainland Belt sphalerite, from 0.73 to 4.37 wt %. At Edward Island minor iron

(0.38 wt %) was incorporated in the sphalerite when it was initially precipitated, after the termination of native arsenic deposition. As deposition continued, the sphalerite became iron-free but cadmium rich, and was co-precipitated with native silver and minor chalcopyrite.

Other trace elements found in sphalerite are copper (0.36-0.42 wt %) and silver (0.33 wt %), both of which were only detected in sphalerite from Silver Islet. No manganese was detected in any of the sphalerite analysed.

Microprobe analyses of native silver from Silver Islet indicated the presence of trace quantities of mercury (Table 6), but no other elements were observed superimposed on the silver spectrum. Most silver contained 2-4 wt % Hg; however, in one sample the mercury content was as high as 11.56 wt %. The relatively Hg-poor silver occurred in veinlets, some of which clearly were the product of remobilization of silver initially deposited at the cores of nickeline-gersdorffite rosettes. The Hg-rich silver appears to be late stage, often occurring along fracture and cleavage planes, but did not appear to have been remobilized from a previous depositional event. This suggests the mercury content of silver may have been low relatively early in paragenesis and increased over time; however, with only three silver-bearing samples to work with, such an hypothesis is insufficiently tested.

**TABLE 5: MICROPROBE ANALYSES OF SPHALERITE COMPOSITION**

<u>Sample</u>	<u>Zn</u>	<u>Fe</u>	<u>Cd</u>	<u>Cu</u>	<u>Ag</u>	<u>S</u>	<u>Total</u>	<u>FeS<sup>1</sup></u>
<b><u>MAINLAND BELT</u></b>								
<b>Little Pig Vein</b>								
LP25	66.70	0.33	---	---	---	32.23	99.26	0.57
LP25	66.64	0.44	---	---	---	31.83	98.91	0.77
<b>Big Harry Vein</b>								
BLC4	66.84	0.40	---	---	---	31.62	98.86	0.69
BLC4	67.05	0.26	---	---	---	31.88	99.21	0.46
BLC5	67.94	0.25	0.35	---	---	33.16	101.72	0.43
BLC5	68.15	0.37	---	---	---	32.96	101.48	0.63
BLC5	67.47	0.97	---	---	---	33.17	101.60	1.66
<b>Rabbit Mountain</b>								
RM 1	66.38	0.53	---	---	---	31.95	98.86	0.92
RM 1	67.44	0.18	0.51	---	---	31.84	99.97	0.31
<b>Badger</b>								
BAD1	64.95	0.48	---	---	---	30.41	95.84	0.86
BAD1	66.22	1.12	0.31	---	---	32.01	99.66	1.94
BAD1	67.03	0.34	0.36	---	---	31.88	99.61	0.56
BAD4	63.60	2.09	---	---	---	31.60	97.29	3.70
BAD4	64.57	2.26	---	---	---	32.22	99.05	3.94
EA68	66.51	0.28	---	---	---	32.20	98.99	0.49
EA68	64.69	0.68	---	---	---	32.62	97.99	1.22
<b>West Beaver</b>								
EA52	66.19	0.90	---	---	---	33.30	100.39	1.57
EA52	65.72	0.21	---	---	---	33.38	99.31	0.38
EA52	65.52	0.37	---	---	---	33.38	100.27	0.65
EA52	67.07	0.23	---	---	---	33.63	100.93	0.40
EA52	66.61	0.27	---	---	---	33.90	100.78	0.47
EA53	63.25	0.31	---	---	---	32.10	95.66	0.58
EA53	63.49	0.14	---	---	---	32.31	95.94	0.26
EA53	64.36	0.27	---	---	---	32.18	96.81	0.49
EA53	65.55	0.60	0.25	---	---	32.65	99.05	1.05
EA53	64.79	1.10	---	---	---	32.60	98.49	1.95

<sup>1</sup> mol % FeS in sphalerite

<sup>2</sup> detectability limits - Fe:0.01 wt.%; Cd:0.02 wt.%;  
Ag:0.03 wt.%; Cu:0.02 wt.%;  
Mn:0.01 wt.%.

<u>Sample</u>	<u>Zn</u>	<u>Fe</u>	<u>Cd</u>	<u>Cu</u>	<u>Ag</u>	<u>S</u>	<u>Total</u>	<u>FeS</u>
<b>Silver Creek</b>								
EA10	65.79	0.34	--	--	--	32.37	98.50	0.60
EA10	65.60	0.27	--	--	--	32.49	98.36	0.48
<b>Porcupine</b>								
EA67	63.73	2.16	--	--	--	32.04	97.93	3.82
EA67	65.12	1.57	--	--	--	32.71	99.40	2.74
<b>Keystone</b>								
EA 1	63.00	0.39	--	--	--	32.74	96.13	0.72
EA 1	66.62	0.42	--	--	--	33.48	100.52	0.73
EA 1	66.32	0.39	--	--	--	33.66	100.37	0.65
EA 1	66.31	0.28	--	--	--	33.78	100.37	0.49
EA 1	66.78	0.22	--	--	--	33.59	100.59	0.38
EA 1	65.27	0.32	0.59	--	--	31.55	97.73	0.56
EA 1	66.77	0.37	--	--	--	32.44	99.58	0.64
EA 2	64.35	0.32	--	--	--	31.81	96.48	0.58
EA 2	63.82	0.23	--	--	--	31.13	95.18	0.42
EA 2	67.68	0.25	--	--	--	31.86	99.79	0.43
EA 6	65.76	0.47	--	--	--	32.44	98.67	0.83
EA 6	65.33	0.59	--	--	--	32.50	98.42	1.04
EA 6	65.55	0.12	0.33	--	--	31.60	97.60	0.21
EA 6	64.28	0.35	--	--	--	31.75	96.38	0.64
EA56	65.64	0.13	1.50	--	--	32.37	99.64	0.23
EA56	66.76	0.13	0.79	--	--	32.70	100.38	0.22
EA56	67.14	0.24	0.62	--	--	28.15	96.15	0.41
EA57	67.03	0.28	--	--	--	32.31	99.62	0.48
EA57	66.63	--	0.34	--	--	32.39	99.36	0.00
EA57	67.94	0.19	--	--	--	28.09	96.22	0.33
<b>Silver Mountain</b>								
SM51	65.95	0.13	0.32	--	--	32.19	98.59	0.21
SM51	67.06	0.26	--	--	--	32.20	99.52	0.46
SM51	66.79	0.40	--	--	--	32.22	99.41	0.70
<b><u>ISLAND BELT</u></b>								
<b>Silver Islet</b>								
SI17	66.21	0.47	--	--	--	32.82	99.50	0.82
SI17	64.03	2.33	--	--	--	32.98	99.34	4.08
SI17	65.57	0.45	--	--	--	32.95	98.97	0.78
SI17	64.90	0.39	--	--	--	33.01	98.30	0.70
SI17B	64.36	1.77	--	--	--	31.94	98.07	3.12
SI-B	64.81	0.36	--	--	--	31.87	97.04	0.64

Sample	Zn	Fe	Cd	Cu	Ag	S	Total	FeS
<b>Silver Islet (cont'd)</b>								
SI-B	63.81	0.52	--	--	--	32.45	96.78	0.94
SI-A	66.52	0.48	--	--	--	33.07	100.07	0.83
SI-A	63.44	0.86	--	--	--	32.27	96.57	1.56
SI-A	64.84	0.41	--	--	--	31.97	97.22	0.73
SI-A	66.03	0.73	--	--	--	33.37	100.13	1.26
SI-A	66.67	1.18	--	--	--	31.35	99.20	1.88
SI-A	63.90	0.33	--	--	--	31.94	96.17	0.60
SI19	61.38	1.65	--	--	--	31.74	94.77	3.05
SI19	60.63	1.99	--	0.36	--	31.99	94.97	3.68
SI19	63.90	1.76	--	0.42	--	32.43	98.51	3.10
SI22	64.75	0.27	--	--	--	31.93	96.95	0.48
SI22	65.80	--	--	--	--	32.08	97.88	0.00
SI22	66.56	0.29	--	--	--	32.52	99.37	0.51
M12460	66.93	1.82	--	--	--	32.37	101.51	3.09
M12460	64.61	1.85	--	--	--	31.91	98.37	3.24
M12460	65.55	2.47	--	--	--	33.10	101.12	4.22
<b>Prince Location</b>								
PR10	66.45	0.33	--	--	--	32.19	98.97	0.58
PR10	66.43	0.29	--	--	0.33	31.99	99.04	0.51
PR10	67.04	0.50	--	--	--	32.56	100.10	0.87
PR 2	63.58	1.17	--	--	--	31.80	96.55	2.10
PR 2	65.48	0.63	--	--	--	31.82	97.93	1.15
PR 3	64.14	0.22	--	--	--	31.30	95.66	0.40
PR 3	65.82	1.43	--	--	--	32.20	99.45	2.48
<b>Edward Island</b>								
9170A3	62.03	--	2.09	--	--	31.92	96.04	0.00
9170A3	65.91	0.38	0.87	--	--	32.32	99.49	0.66
9170A3	65.66	--	3.44	--	--	32.19	101.29	0.00
9170A3	64.03	--	4.37	--	--	32.12	100.52	0.00
9170B	67.42	0.16	0.52	--	--	32.81	100.91	0.26
9170B	66.98	0.18	0.56	--	--	32.74	100.46	0.31
9170B	66.73	0.30	0.73	--	--	32.97	100.73	0.52

**TABLE 6: MICROPROBE ANALYSES OF NATIVE SILVER**  
**AND NATIVE ARSENIC**

	As	Sb	Ag	Hg	Total
<b><u>Native Arsenic - Edward Island</u></b>					
M9170A3	98.81	2.99			101.81
M9170A3	92.26	3.32			95.58
M9170	99.67	3.08			102.76
<b><u>Native Silver - Silver Islet</u></b>					
SI-17			97.73	3.94	101.67
M12460			91.28	9.31	100.58
M12460			88.62	11.56	100.18
M9412			99.75	2.17	101.92
M9412			98.07	2.09	100.16
S1A			94.28	2.30	96.59

Qualitative analyses of a traverse across rhythmically encrusted native arsenic from Edward Island showed the consistent presence of trace quantities of antimony; however, no enrichment or depletion trends in this element was observed. Quantitative analyses (Table 6) show the native arsenic averages 3 wt % Sb.

Several mineral phases from Silver Islet, Spar Island, and Edward Island were identified by a combination of qualitative and quantitative microprobe analyses.

From Edward Island sphalerite co-precipitated with native arsenic contains fractures lined by fine drusy crystals of loellingite less than 1 $\mu$ m in diameter. These crystals were too small to obtain a quantitative analysis.

One to two micron-sized inclusions in a digenite-chalcocite intergrowth from Spar Island were analysed, and determined to be safflorite, a mineral previously unreported in this vein (Table 7). Cu and S in the analysis are a result of interference of the digenite-chalcocite host, caused by the small size of the inclusions. The safflorite also occurs as fine veinlets within chalcocite, averaging 50 to 10 $\mu$ m in length.

Four samples of silver-arsenide-sulfosalt ore material from Silver Islet were obtained during this study (see Appendix 3 for mineral formulae). The bulk of this ore was hosted by

manganiferous dolomite, and was of dendritic form, generally showing a zonation of nickel-cobalt arsenides surrounding native silver cores.

Nickeline and gersdorffite are the most common dendrites (Table 7). In samples M12460, SI-17, and SI-A, native silver is commonly at the core of rosettes with an inner rim of nickeline, or nickeline with fine intergrowths of gersdorffite, and an outer rim of gersdorffite (Figure 19). In SI-A, the nickeline is also associated with a complex intergrowth which is tentatively identified by semi-quantitative analysis as galena, bravoite, and argentite. Bismuthinite also occurs in SI-A, forming anhedral masses to 0.5mm in diameter.

Sample 9412 from Silver Islet is composed of massive native silver and native arsenic, with bornite and safflorite. Euhedral bornite is rimmed by a complex mineral (Table 7) tentatively identified as tetrahedrite. Minute inclusions within bornite were qualitatively analysed, and appear to be a Ag-rich tetrahedrite. The latter does not contain the Fe or Bi found in the main tetrahedrite phase which rims bornite.

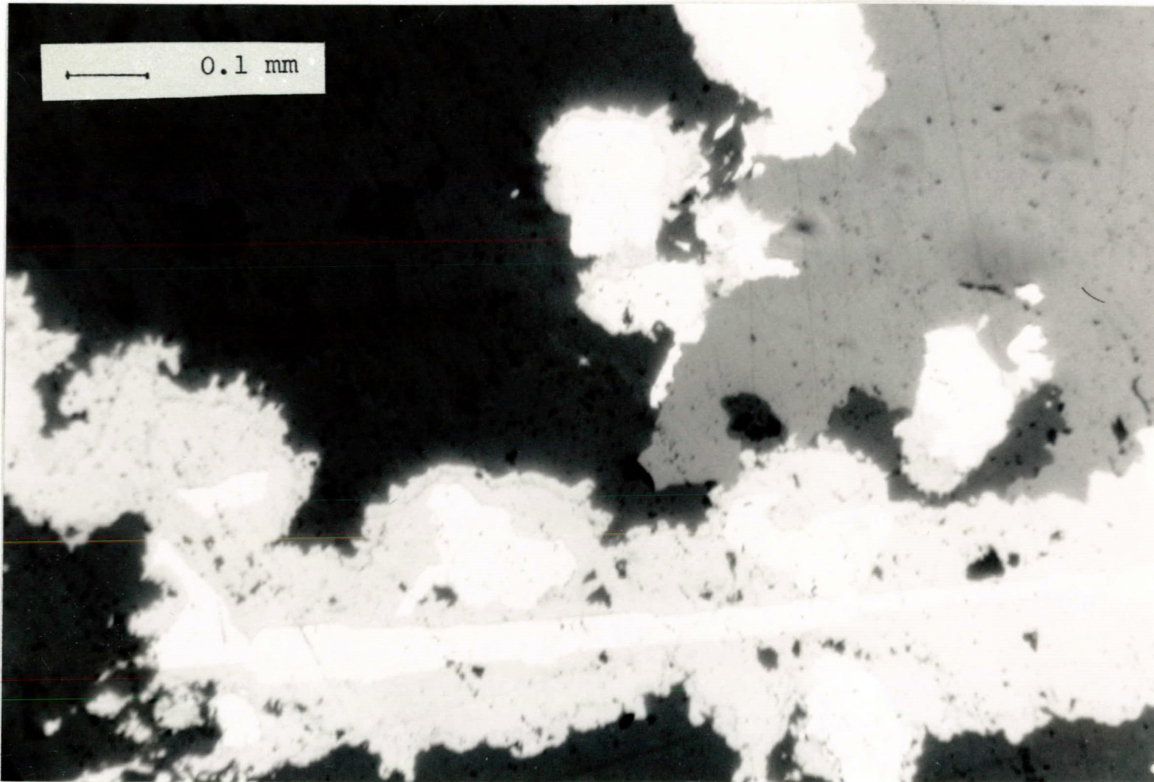


Figure 19: Typical textures observed in Silver Islet ore. Native silver (white) occurs in the cores of rosettes surrounded by nickeline and complex arsenide intergrowths (light grey) and as cross-cutting, remobilized veinlets. Silver ore is hosted by sphalerite (medium grey) and calcite (dark grey). (SI 17)

**TABLE 7: MICROPROBE ANALYSES OF ARSENIDES**  
**AND SULFARSENIDES FROM THE ISLAND BELT**

	SAMPLES							
	WEIGHT PERCENT				NUMBER OF IONS			
	1	2	3	4	1*	2*	3*	4*
Ni	36.27	---	15.66	15.81	0.77	---	0.57	0.53
Co	1.87	---	6.80	6.62	0.04	---	0.25	0.22
Fe	---	2.99	---	---	---	0.91	---	---
Ag	---	0.99	---	---	---	0.16	---	---
Cu	---	38.08	8.94	7.82	---	10.3	0.30	0.24
As	55.17	---	65.95	68.39	0.91	---	1.88	1.88
Sb	2.99	26.89	0.72	0.71	0.03	3.7	0.02	0.01
Bi	---	9.69	---	---	---	0.79	---	---
S	1.40	24.38	1.57	1.81	0.06	13	0.10	0.11
Total	97.70	103.02	99.63	101.17				

1. SI-A - nickeline
2. M9412 - tetrahedrite (?)
3. Sp1 - safflorite inclusion in chalcocite
4. Sp1 - safflorite veinlet in chalcocite

1\* based on 1 (As, Sb, S)

2\* based on 13 S

3\* based on 2 (As, Sb, S)

4\* based on 2 (As, Sb, S)

## DISCUSSION

Scott (1983) has used experimental data on the Fe content of sphalerite precipitated at various temperatures to estimate the activity of  $S_2$  in hydrothermal fluids. Experimentation proved difficult except at high temperature ( $\geq 250^\circ\text{C}$ ), but a linear relationship between  $\log a_{S_2}$  and  $T$  can be extended to lower temperatures (Scott, personal communication).

In applying the experimental data to the vein systems an assumption is made that local equilibrium among sulfides, at the examined stages of deposition and at the low temperatures observed, was obtained. Using temperatures obtained from fluid inclusion homogenization, sphalerite data has been plotted on Figure 20 to indicate a range of  $S_2$  activity from  $10^{-18}$  to  $10^{-25}$ . If trapping temperatures are used, assuming a  $45^\circ\text{C}$  correction due to increased pressure, the sulfur activity range increase to  $10^{-14}$  to  $10^{-21}$ . Because of the presence of primary native silver with several of these samples and the relative position of the argentite-silver stability field (Figure 20), it is likely that this correction is too large, and, therefore, the first  $a_{S_2}$  range discussed is thought to be correct. The presence of native arsenic at Silver Islet and Edward Island also confirm this activity range.

In general sphalerite growth was initially relatively iron rich, but iron content decreased towards the perimeter of sphalerite crystals. This indicates a slight increase in sulfur fugacity during sphalerite deposition. Sphalerite exhibiting this behaviour includes crystals from the Rabbit Mountain, Badger,

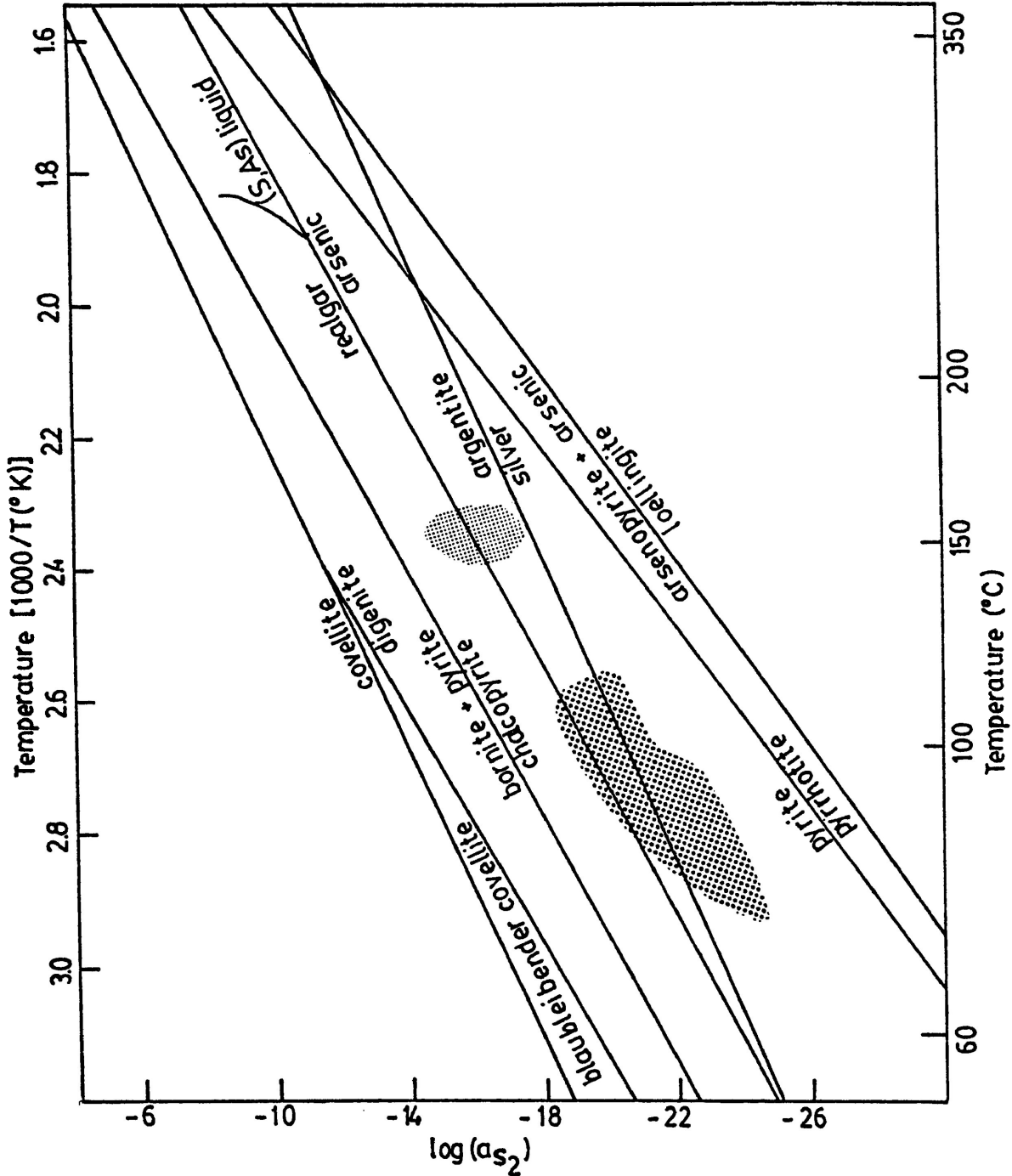


Figure 20: Sulfur activity during sulfide deposition as indicated by Fe content of sphalerite and observed mineral assemblages. Heavy stippling shows region defined by homogenization temperatures, light stippling shows region defined if pressure correction for 1000m burial is applied. Mineral stability field after Barton and Skinner (1979), sphalerite composition plotted by

Silver Creek, Silver Mountain, Silver Islet, Prince, and West Beaver mines. Post-fracture sphalerite from the Porcupine and sphalerite from the Little Pig mines showed the opposite trend, indicating a decrease in sulfur fugacity during sphalerite deposition. At the Keystone mine pre-fracture and post-fracture sphalerite indicate an increasing  $a_{S_2}$ , but late stage vug-filling sphalerite indicate a decreasing  $a_{S_2}$ .

No obvious pattern was established between composition and anisotropy of the crystals; however, in two cases (e.g. Bad 1, EA6) where anisotropy was patchy within a single crystal, the isotropic zones contained Cd, which was absent from the anisotropic zones.

The  $a_{S_2}$  range can be estimated in the Spar Island vein on the basis of the copper minerals present. The coexistence of primary blaublichbender covellite and a digenite-chalcocite intergrowth indicate a much higher  $a_{S_2}$  ( $10^{-14}$  -  $10^{-16}$ ) than was present for any of the sphalerite growth at other mines. The sequential deposition of blaublichbender covellite rimmed by bornite rimmed and veined by chalcopyrite suggests a decrease in sulfur activity during deposition. No native silver was observed at Spar Island during this study, but it is suggested that its deposition occurred fairly late in the paragenesis, in accord with the sulfur activity trend.

If the presence of pyrrhotite noted by Tanton (1931) referred to mineralization in the vein systems, rather sulfides in

metamorphosed Rove shale, then several veins may have had periods of higher temperature and/or lower  $a_{S_2}$  during sulfide deposition than indicated by the sphalerite composition. No pyrrhotite has been observed in vein material during the present study.

### X-RAY DIFFRACTION

A Gandolfi camera X-ray photograph was made of an intergrowth from Silver Islet. The negative was exposed to  $\text{CuK}\alpha$  radiation ( $\lambda = 1.54178 \text{ \AA}$ ) for 8 hours in a small (28.65mm diameter) camera. A nickel filter was used to minimize exposure to undesirable wavelengths in the Cu spectrum. A fine diameter (0.4mm) collimator was used to minimize background radiation. After irradiation the film was developed and the reflections measured using a Vernier scale.

A programmable Texas Instrument calculator, using a program developed by Kissin (unpublished), was employed to calculate d-spacings,  $2\theta$  values, and standard deviations for the measured diffraction pattern (Appendix 2). Comparison of the spectra with the X-ray powder diffraction file allowed identification of the minerals nickeline, galena, and annabergite.

An X-ray powder diffraction pattern was obtained of hydrothermal clay minerals from the Keystone Mine. The sample was pulverized with mortar and pestle, and then spread thinly on a

glass slide. The sample was rotated from 4 to 80°, at a rate of 1° per minute. The sample was exposed to CuK $\alpha$  radiation ( $\lambda = 1.54178\text{\AA}$ ), using a nickel filter. The pattern obtained shows the presence of a mixture of tri-octahedral illite, montmorillonite, and quartz. A complete identification, using such techniques as dehydration of the clay, was not completed.

## SULFUR ISOTOPIC COMPOSITION

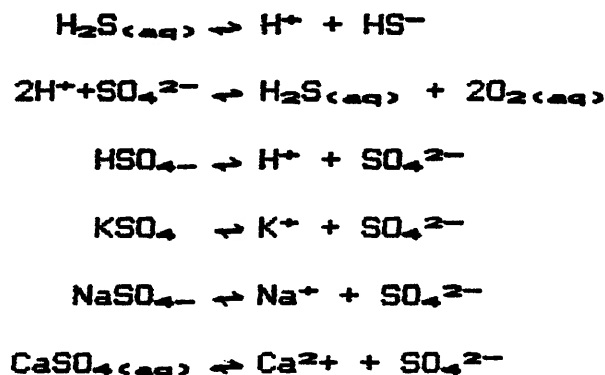
### INTRODUCTION

Sulfur isotopic composition has been used as a straightforward indicator of sulfur origin in the past, until Sakai (1968) and Ohmoto (1972) demonstrated a large variation in isotopic value can be caused by environmental factors. Although some information regarding the sulfur source can still be obtained, one must first understand the processes and conditions (e.g. T, pH,  $f_{O_2}$ ,  $m\{S\}$ ) which affected the sulfur during its transportation and deposition, causing isotopic fractionation.

The recognition that  $^{34}S$  enrichment occurs preferentially in some compounds relative to others dominantly as a function of temperature has allowed the use of sulfide pairs as geothermometers. Assuming the mineral phases were precipitated in equilibrium, and that no isotopic exchange occurred after precipitation, the difference in the  $^{34}S/^{32}S$  ratio is inversely proportional to  $T^2$ , by a factor of an experimentally determinable equilibrium fractionation constant (Sakai, 1968).

Sulfur isotopic variation can also occur as a function of pH,  $f_{O_2}$  and  $m\{S\}$ , so that knowledge of the isotopic composition of an homogeneous sulfur source can be used, along with geological information such as mineral assemblages, to delineate environmental conditions of ore formation.

In most hydrothermal systems the controlling reactions are (Ohmoto, 1972):



### EXPERIMENTAL TECHNIQUE

Sulfides and sulfates were carefully separated from vein material by hand after coarsely crushing the rock host. Mineral separates were then examined under a binocular microscope to assure purity of the material. Finally the separates were bathed in dilute (15%) hydrochloric acid to remove the traces of calcite commonly coating the crystals.

The sulfur isotope analyses were completed by Kreuger Enterprises Inc., Geochron Laboratories Division, located in Cambridge, Massachusetts.

### RESULTS

The  $\delta^{34}\text{S}$  obtained are presented in Table 8. A duplicate of one sulfide sample was sent and a difference in  $\delta^{34}\text{S}$  of 0.2% was obtained.

Barite from the Island Belt was found to have  $\delta^{34}\text{S}$  values between +8.3 and +6.5%. . Barite from Silver Mountain and Silver Harbour has similar  $\delta^{34}\text{S}$  except sample SM30 (=+30.9%). Calcite in SM30 shows textural evidence of supergene dissolution. Fluids responsible for this may also have affected the barite causing isotopic re-equilibration, as supergene sulfates typically show a distinct isotopic signature (Ohmoto and Rye, 1979).

Sulfur isotopic composition of galena from the Island Belt was fairly consistent, varying from +3.6 to + 4.1%. . With the exception of one sample, the sphalerite from the Island Belt also had fairly consistent sulfur isotope values, from +4.2 to +10.9%.. The sphalerite sample SI-05 was examined in polished section, and observed to contain very fine late stage alteration to marcasite, and therefore the anomalous isotopic value is not regarded as representing primary sulfur values. The bulk of the Island Belt data is based on Silver Islet material, as sulfides are very uncommon at other Island Belt veins.

Sulfur isotopic composition of sulfides in Mainland veins is more variable, sphalerite ranging from -1.2 to +9.9%. within the Rabbit Mountain vein; these values also represent the range found through the entire belt. Sulfur in galena ranges from -9.3%. at Rabbit Mountain to +3.6%. at the Keystone Mine. Two analyses of pyrite gave a value of +4.3%. at Silver Mountain, and +0.7%. at the Shuniah Mine.

TABLE 8: SULFUR ISOTOPE RATIO ANALYSES

SAMPLE	LOCATION	MINERAL			
		Sphalerite	Galena	Pyrite	Barite
EA 15	Victoria Island				+ 8.3
EA 32	Jarvis Island				+ 7.7
EA 39	Spar Island				+ 8.3
EA 41	Spar Island				+ 6.5
SI 4	Silver Islet	+10.0	+3.6		
SI 5	Silver Islet	+25.6			
SI 7	Silver Islet	+ 4.2	+4.1		
SI 17	Silver Islet	+ 9.8			
SI A	Silver Islet	+ 9.7	} duplicate		
SI A	Silver Islet	+ 9.9			
M 9170	Edward Island	+10.9	+3.8		
BLC 1	Big Harry	+ 4.7			
BLC 3	Big Harry	+ 6.3			
BLC 5	Big Harry	+ 7.1			
BLC 7	Big Harry	+ 6.3			
RM 1	Rabbit Mountain	- 1.2			
RM 3	Rabbit Mountain	+ 3.5	-9.3		
RM 6	Rabbit Mountain	+ 9.9			
RM 8	Rabbit Mountain	+ 9.3			
SM 30	Silver Mountain				+30.9
SM 51	Silver Mountain	+ 6.4			
SM 501	Silver Mountain				+ 7.0
SM 514	Silver Mountain				+ 8.7
SM 600	Silver Mountain	+ 9.2	+3.0	+4.3	
EA 1	Keystone	+ 5.7			
EA 6	Keystone	+ 6.8	+3.6		
EA 50	Keystone	+ 6.7			
EA 52	West Beaver	+12.2	-0.4		
EA 56	Keystone	+ 3.5			
EA 61	Porcupine	+ 6.7			
EA 95	Silver Harbour	+ 3.4			
EA 98	Silver Harbour		-0.7		+ 6.6
EA 101	3A	+ 2.2			
SH 11	Shuniah		-1.7	+0.7	
TB 3	Thunder Bay	+ 7.6	+2.2		

DISCUSSION

Sulfur isotopic analysis can be used to investigate geothermometry, sulfur source, and the chemical environment of mineral deposition.

With the exception of pyrite from SM600, samples from which multiple sulfide phases were extracted for analysis showed textural evidence suggesting equilibrium between the two phases. Usually the minerals were disseminated through a massive carbonate phase of the vein, and often the sulfides were in grain to grain contact. In some samples the sulfides formed a discrete horizon within the vein. The formulae, from Ohmoto and Rye (1979),

$$\text{pyrite - galena } T(^{\circ}\text{K}) = \frac{(1.0 \pm 0.04) \times 10^3}{\Delta^{1/2}}$$

$$\text{sphalerite - galena } T(^{\circ}\text{K}) = \frac{(0.85 \pm 0.03) \times 10^3}{\Delta^{1/2}}$$

were employed to estimate depositional temperatures of mineral pairs; however, the results proved instead that, with a few exceptions and regardless of textural evidence, the sulfide minerals were not precipitated in isotopic equilibrium. Sphalerite-galena pairs EA6, TB3, SM600, SI4, and M9170 provide temperatures in the 50°-200°C range, which is compatible with fluid inclusion data, but of questionable validity because of the problems with the other samples. Neither pyrite-galena pair

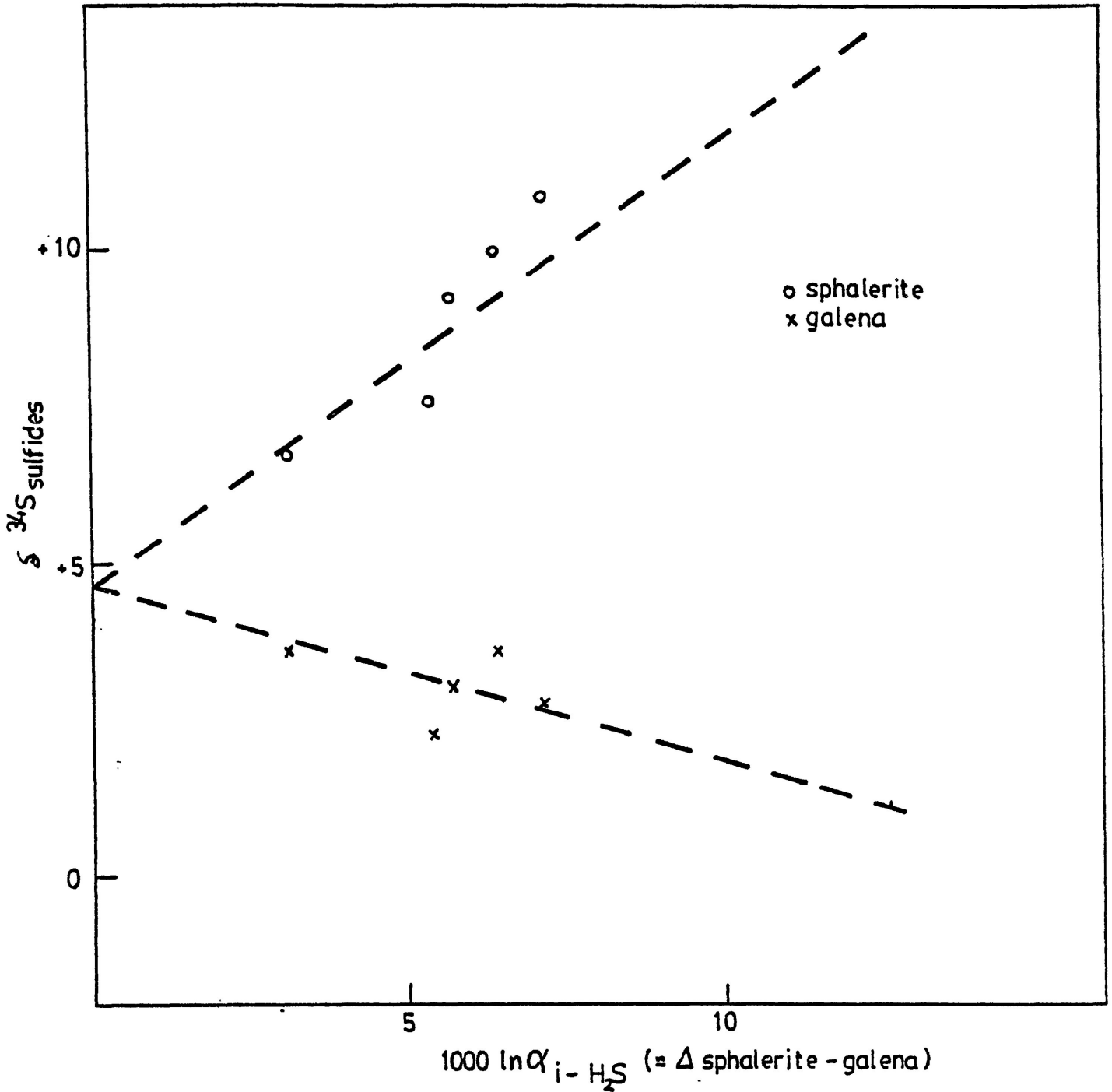


Figure 21: Sulfur isotopic composition of sphalerite-galena pairs. The merging of regression lines suggests  $\delta^{34}\text{S}$  of 5% for the sulfur source.

represented equilibrium conditions.

Samples from which barite was analyzed did not appear to contain co-precipitated sulfides, so that no geothermometry was possible using these samples.

A plot of  $(\delta^{34}\text{S}_{\text{sphalerite}} - \delta^{34}\text{S}_{\text{galena}})$  versus  $\delta^{34}\text{S}$  can be used to estimate the sulfur composition of the hydrothermal fluids if the following conditions are met (Pinckney and Rafter, 1972).

- (1) the minerals are coprecipitated at isotopic equilibrium
- (2) the relation  $\ln\alpha$  is proportional to  $1/T^2$  is applicable to the system, which implies a closed system.

From Figure 21, an estimate of the source sulfur isotopic composition is +4.7%. . The textural evidence and reasonable temperatures derived from geothermometric data suggest that for some of the mineral pairs the first condition is met. Most of the mineral pairs come from different vein systems, contradicting condition (2); however, it is suggested that the source sulfur composition was similar for all these veins because the pairs behave as predicted by a single closed system (Figure 21). It should be noted that the three sphalerite-galena pairs which were clearly not in isotopic equilibrium (as evidenced by impossible temperatures) have not been plotted on Figure 21 or used to determine the regression lines. The second condition also requires the systems remain closed to sulfur throughout the paragenesis, starting with the removal of sulfur from its source and remaining

closed until deposition of the sulfides and sulfates analyzed. Again there is no clear evidence that this condition was met, as there is fluid inclusion evidence of sporadic boiling occurring through most vein systems.

The effect of boiling sulfur bearing fluids is to preferentially enrich the fluids in  $\text{SO}_2$  and deplete them in  $\text{H}_2\text{S}$ . Partitioning of lighter sulfur in  $\text{SO}_2$  and heavier sulfur in  $\text{H}_2\text{S}$ , results in the sulfur isotopic composition of the fluid becoming heavier. The inhomogeneity of the fluids is also supported by Pb-isotope work done by Franklin et al. (in press).

The isotopic composition of pyrite in both the Rove Shale and argillaceous members of the Gunflint Formation is known. The pyrite did not occur in or near veins, and appeared to be sedimentary in origin, and so is assumed to represent the sulfur isotopic value of sulfides in the original sediments. Cameron (1983) analyzed 22 samples of the Upper Tuff Argillite Member, Gunflint Formation from Kakabeka Falls, which have  $\delta^{34}\text{S}$  of  $+3.5 \pm 1.3\%$ . Shegelski (personal communication) analyzed pyrite from several localities, including Current River, Kakabeka Falls and Whitefish Falls. The 26 samples have a mean  $\delta^{34}\text{S}$  of  $8.9 \pm 2.1\%$  ranging from  $-4.1$  to  $+15.7\%$ . He notes that marcasite in cross-cutting fracture sets at Boulevard Lake has an anomalous  $\delta^{34}\text{S}$  of  $+20.3\%$ . Fifteen samples of Rove Formation from four localities, the base of the Sibley Peninsula, the intersection of Hwy. 61 and

the Cloud River, the Silver Mountain area, and the International Border near Pigeon River, have a mean  $\delta^{34}\text{S}$  of  $17.7 \pm 4.4\%$ , ranging from +12.1 to + 25.3%. (Cameron, personal communication). No work has been done on the isotopic composition of sulfur in the Logan Sills.

## PHYSICAL AND CHEMICAL CONDITIONS OF ORE DEPOSITION

Although some suggestions have been previously made on the probable conditions of ore formation in the silver veins (e.g. Franklin et al. in press), this is the first data other than observed mineral assemblages that has been gathered to test these hypotheses.

The native silver and argentite observed during the present study were associated with two particular stages of the paragenesis:

- (1) hypogene deposition, generally post-dating a fracturing event in the Mainland Belt, associated with the deposition of sphalerite and galena.
- (2) late-stage, vug-filling deposition, usually associated with colourless, amethystine, or smokey quartz.

In the case of Silver Islet, an additional, earlier stage of argentite deposition was associated with precipitation of dolomite and pyrite. Spar Island is unique in that the silver and argentite deposition was associated with a period of barite deposition.

All temperatures from microthermometric measurements

discussed in this section are homogenization temperatures. As discussed previously, the presence of boiling in the systems and the  $a_{H_2O}-T$  relationships show vein formation occurred at low confining pressure, probably equivalent to a hydrostatic rather than lithostatic load.

The best documented environment determined is hypogene ore deposition in which case fluid inclusions from sphalerite indicate temperature and salinity at deposition, and determinations of mole percent FeS in sphalerite allows estimation of  $a_{H_2O}$ . In addition most sulfur isotope data from sphalerite and galena are also representative of this stage.

Temperature of deposition of sphalerite ranges from 73.5° to 115.3°C, as determined from both primary and pseudosecondary inclusions. These temperatures are consistent at all deposits, indicating a universally low temperature of sphalerite deposition at or near 100°C. This temperature range is thought to represent all sulfide deposition at or near this stage in the paragenesis, including native silver and argentite. Geothermometric results from paired sulfur isotopic data support this temperature, although they show a broader range from 50°-200°C. This may be a result of imperfect isotopic equilibrium between sulfides during deposition.

It should be emphasized that these temperatures represent depositional conditions only. A fluid inclusion in a calcite crystal which was trapped in sphalerite homogenized at 487°C. This

temperature is interpreted as representing the temperature of the solution at some point during its evolution, probably quite near the point of sphalerite deposition or one would have expected the calcite crystal to dissolve.

Salinity of the fluids from which the sulfides were derived displayed the same variability throughout vein formation. Salinity of sphalerite fluid inclusions ranges from 3.5 to 19.2 equivalent wt.% NaCl, the bulk of the data between 10 and 15 wt.%. The dominant salt in the ore forming solution was probably  $\text{CaCl}_2$  as indicated by  $t_m$ , although the relative amounts of KCl,  $\text{MgCl}_2$  and NaCl could not be determined microthermometrically. This is also consistent with salinity determined for gangue deposition.

The iron content of sphalerite indicates quite low sulfur activity during deposition, ranging from  $10^{-6}$  to  $10^{-20}$ . If one assumes a total molality of sulfur for the system of  $10^{-3}$ , it is possible to use this information, and acidity constraints to establish the oxygen activity (Giordano and Barnes, 1981).

It is difficult to establish the pH of the ore forming fluids. In some systems the stability of K-feldspar has been used to estimate pH; however, because of the lack of quantitative analysis of the composition of fluid inclusions (used to estimate  $a_{\text{K}^+}$ ), and the suggestion of K-feldspar was not always stable (by the presence of primary illite and montmorillonite at the Keystone Mine), it is not possible to use this limitation for the silver veins. Other pH

limiting reactions, such as the solubility of calcite and dolomite are equally equivocal because textures indicating dissolution of these minerals was observed in some specimens.

A pH range of 6.3 - 8.0 is comparable to that found in modern systems depositing silver, e.g. Broadlands, New Zealand (Weissberg et al) and has been used to constrain  $a_{O_2}$ . This range is also supported by the sulfur-isotopic composition. Because of the difficulty in establishing both isotopic equilibrium and closure of the vein systems, the effect of chemical environment on the sulfur isotopic composition of barite and sulfides has not been discussed in any quantitative manner. However, it can be used to estimate pH.

The fractionation patterns expected at variable pH - T -  $f_{O_2}$  are presented in Figure 22. The curve representing 150°C and an  $f_{O_2}$  of  $10^{-10}$  approximates ore forming conditions. A general consistency of isotopic composition in sulfides and sulfates such as is found in the veins could be produced if the pH of the fluids was assumed to have stayed fairly constant and was near neutral (pH 6-7).

From Figure 23 it can be seen that the oxygen activity during the first stage of ore deposition is in the order of  $10^{-10}$  to  $10^{-12}$ .

There were few good fluid inclusions in late vug-filling quartz, but those heated generally homogenized at fairly low

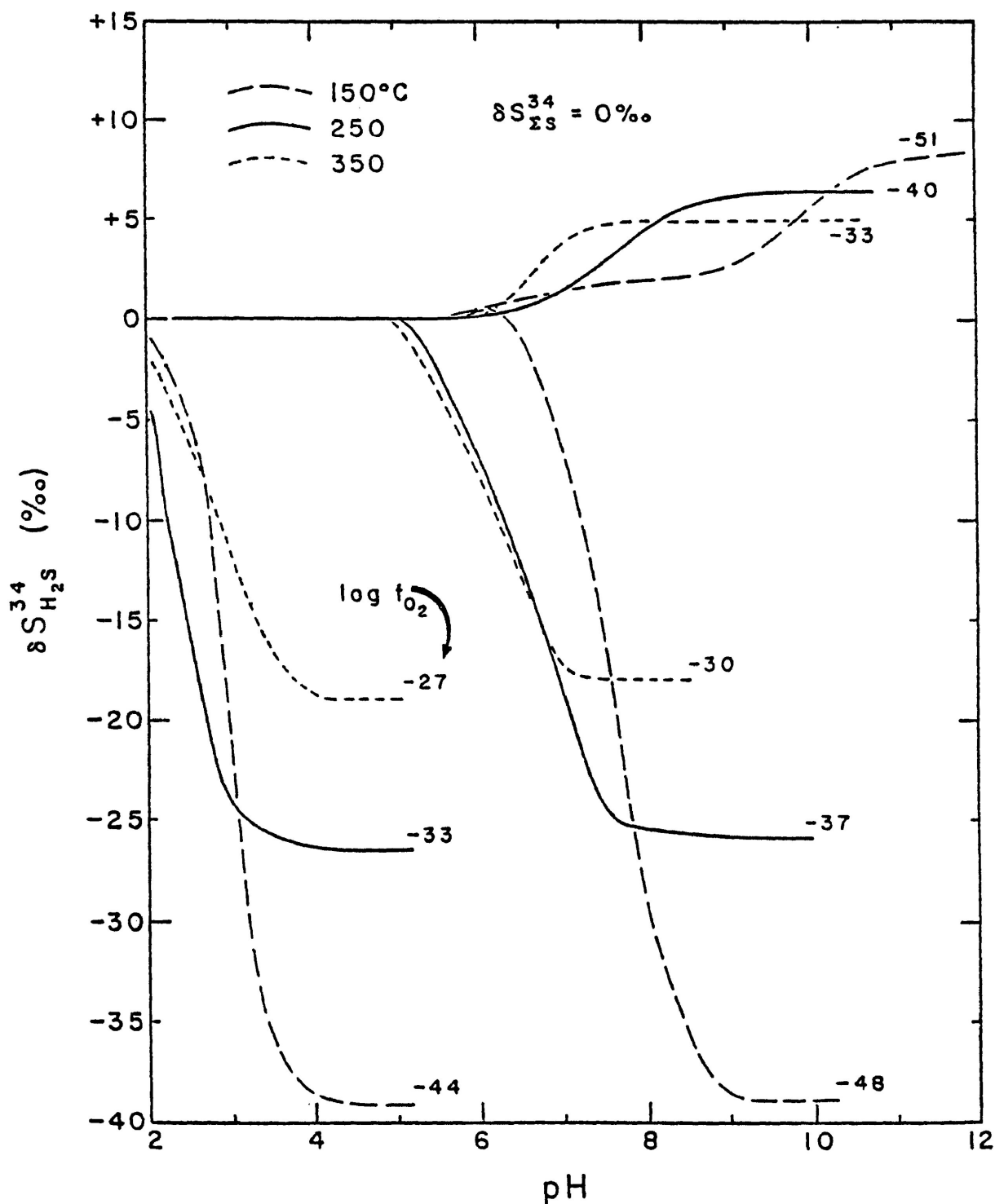


Figure 22: Fractionation of sulfur isotopes at varying temperature and oxygen activity conditions (from Ohmoto, 1971).

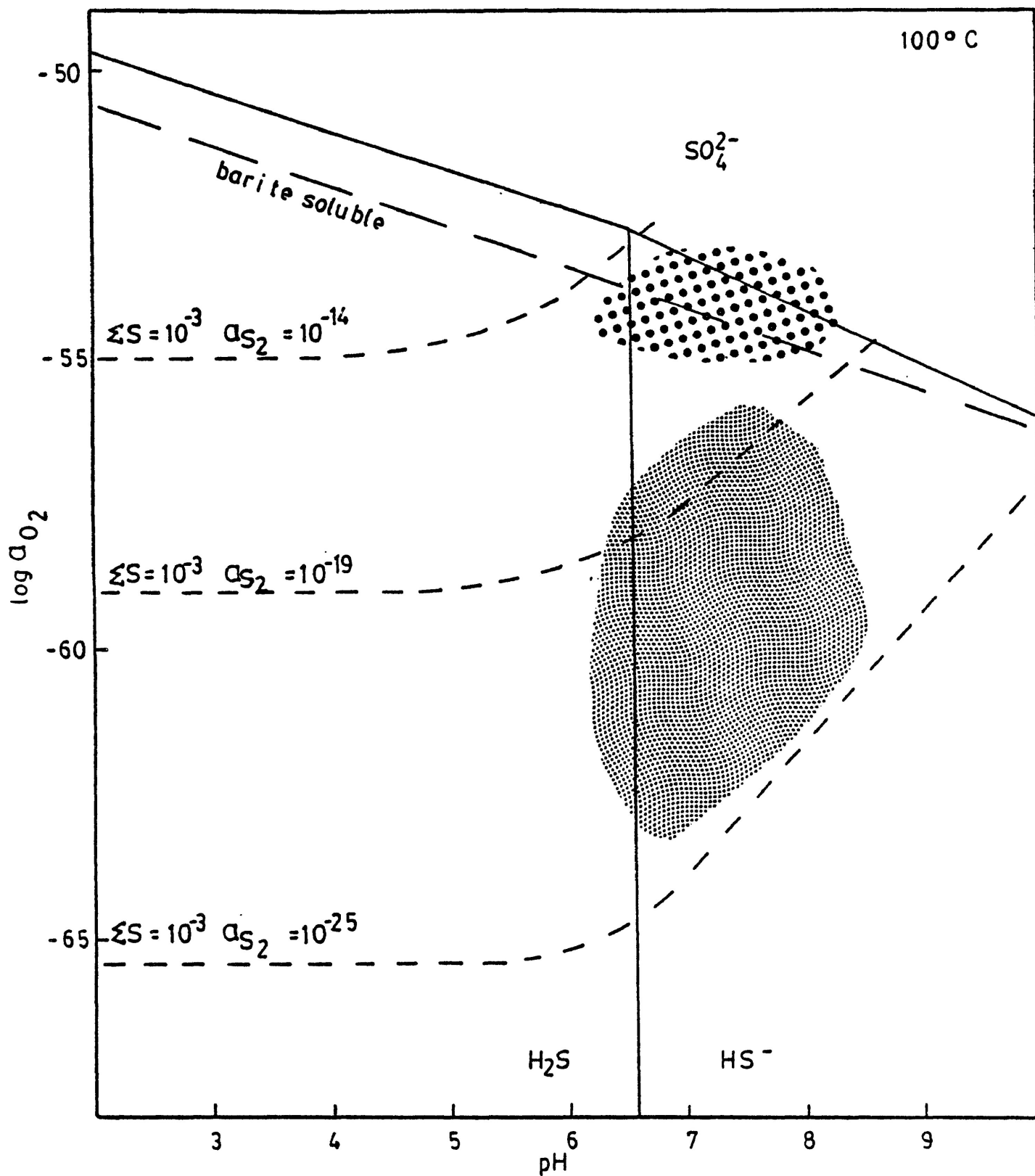


Figure 23: Probable fields of ore precipitation (100°C) at Spar Island (heavy stippling), Mainland Belt and Silver Islet (light stippling). Stability fields and sulfur activity contouring after Giordano and Barnes (1981).

temperatures, 80°-150°C. The character of the fluids is thought to be similar to that indicated by the previous period of silver deposition. The slightly higher temperatures would result in a slight shift towards higher oxygen activities.

Similarly the conditions of the first period of silver and argentite at Silver Islet can only be estimated as similar to that indicated by Figure 23.

At Spar Island the mineral assemblages found indicate a higher  $a_{\text{O}_2}$  was present. Because of the lack of sphalerite in the sulfide horizons it is again necessary to estimate depositional temperatures. Calcite was deposited with barite, postdating ore precipitation at 150°C. Figure 24 shows the  $a_{\text{O}_2}$  - temperature conditions suggested by the sequential deposition of covellite and blaubleibender covellite, chalcocite-digenite, rimmed by chalcopyrite. Replacement of chalcocite by blaubleibender covellite suggests a decrease in temperature and sulfur activity at some point.

Applying this  $a_{\text{O}_2}$  range to the  $a_{\text{O}_2}$  - pH diagram, and further constraining the area of deposition by the co-precipitation of barite it is shown on Figure 23 that oxygen activities of  $10^{-6.0}$  to  $10^{-6.5}$  were prevalent. This assumes that similar quantities of total dissolved sulfur were present as for other fluids ( $10^{-3}\text{m}$ ). It is interesting to note that the pH indicated using these conditions is similar to that found at Broadlands, New Zealand (Seward, 1976).

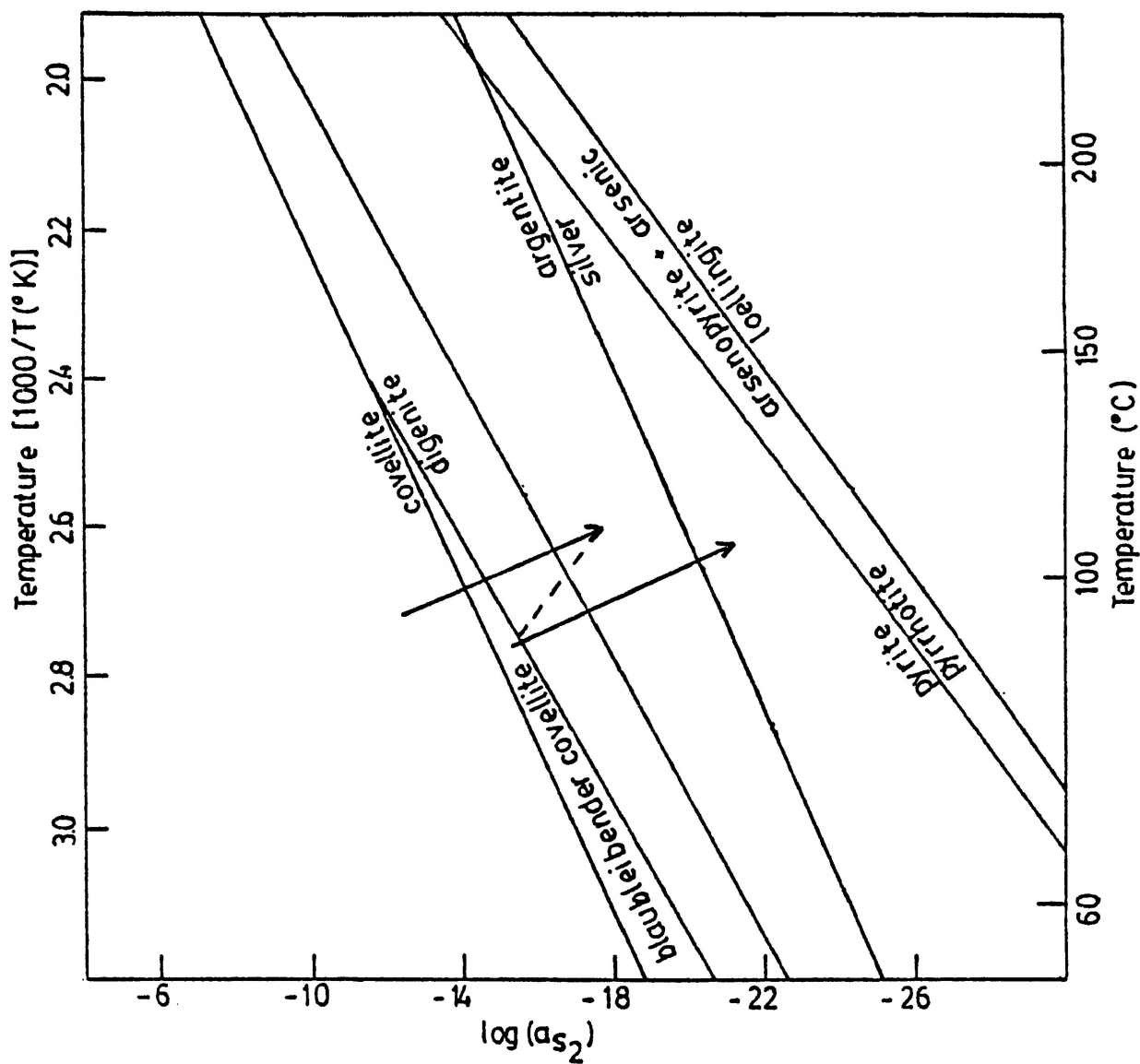


Figure 24: Sulfur activity during sulfide deposition at Spar Island. Mineral stability fields after Barton and Skinner (1979). Arrow shows relationship of sulfur activity with the paragenetic sequence.

## VEIN GENESIS

### GENESIS OF VEINS OF THE FIVE-ELEMENT ASSOCIATION

The formation of veins of the 5-element type, particularly with respect to the fluid source, has been a much disputed area of research. Classical examples of this vein type can be found in the Jachymov District, Czechoslovakia; Erzgebirge, Germany; Great Bear Lake, Northwest Territories, Canada; and Cobalt-Gowganda, Ontario, Canada.

Hall and Stumpfl (1972) summarized the models generally used to explain genesis of the 5-element vein type as:

- 1) direct hydrothermal evolution from felsic intrusions,
- 2) direct hydrothermal evolution from mafic intrusions,
- 3) metahydrothermal evolution, elements are leached from either organic-rich sediments (shales) or massive sulfide deposits, or
- 4) introduction of a 5-element solution which forms near the crust-mantle interface and escapes to surface along deep fracture systems.

In the model (3), connate and meteoric fluids trapped in rocks intruded by dykes or sills are set in motion, forming convection cells, by the cooling of the magma. As the fluids

pass through the rock they evolve, leaching the metals, sulfur, and other elements which are eventually precipitated at the depositional site.

Badham (1976) has suggested the majority of these veins occur at continent-ocean subduction margins, forming at a late to post orogenic stage, often postdating Sn-W mineralization. The actual fluid source is a mixture of fluids emanating from the felsic batholiths which host many of the deposits and from the basic magmas. The mixture of fluids from these two sources is then responsible for the mixed affinity of the elements in the assemblage. He notes that the Thunder Bay and Cobalt-Gowganda veins do not conform to this model.

Robinson and Ohmoto (1973) suggested the Echo Bay, NWT veins formed from connate waters trapped in a volcanic-sedimentary sequence, heated by intrusions of diabase. While passing through the volcanics, metal concentration was increased by a combination of boiling, reaction with alkali metals increasing K/Na and possibly lowering pH) and reaction with ferrous minerals such as hornblende, pyroxene, and magnetite (decreasing oxidation state). They support this theory with fluid inclusion and stable isotope data.

Changkakoti et al. (1986) found considerable fluctuation in temperature and salinity of hydrothermal fluids from Great Bear Lake, NWT, silver vein fluid inclusions. They interpreted these as

the result of hydrothermal fluid pulses. They suggest the presence of either two fluids of contrasting salinity, one of which may have been of meteoric or marine origin, the other a highly saline magmatic fluid or the presence of one fluid affected by shifting confining pressure, lithostatic to hydrostatic, to a two-phase field.

Scott (1972), and Petruk and Jambor (1971) have supported the theory that the Nipissing diabase is the source of mineralization fluids in the Cobalt-Gowganda district. Evidence cited includes zonation of the arsenide minerals symmetrically about diabase sills, and assemblages indicating temperature gradients in accordance with this zonation. They emphasize the inevitable presence of the diabase sills at all ore bodies, and the variation in lithologies hosting the veins and sills. Scott also suggests that at least one of the sills, Siscoe Metals Number 13 vein, was formed from more than one pulse of mafic magmatism, and that it is possible that a more differentiated magma elsewhere in the area was responsible for these pulses, and could be the source of hydrothermal fluids.

In contrast, Boyle and Dass (1971) support a lateral secretion (metahydrothermal) evolution of the Cobalt-Gowganda silver veins. The presence of veins cross-cutting the entire width of some sills is presented as evidence that vein emplacement post-dates sill cooling. In addition, the presence of mercury in silver and allargentum supports this theory, as the only rocks in the area

from which this would likely be derived are the Archean sediments.

### MODELS OF FORMATION OF THE THUNDER BAY DISTRICT VEINS

In contrast to the areas discussed in the previous section, the veins of the Thunder Bay area rarely contain elements of the 5-element association; the exceptions to this rule being Silver Islet (Island Belt), Spar Island (Island Belt), Big Harry (Rabbit Mountain Group), and the 3A (Port Arthur Group).

Of the theories of vein genesis outlined by Halls and Stumpfl (1972), both derivation of fluids from a mafic magmatic source (Tanton 1931, Franklin 1970) and from connate waters trapped in the Animikie sediments (Franklin 1970, Franklin et al in press) have been proposed for veins in this area.

The most compelling evidence from the involvement of fluids from mafic magmas is the ubiquitous presence of diabase or gabbro sills and dykes at all silver veins. This is true not only in the Thunder Bay District, but also at Cobalt-Gowganda, Ontario, Great Bear Lake, Northwest Territories. The most common arguments against the involvement of such fluids are:

- 1) the cross-cutting relationship between silver veins and the diabase dykes,
- 2) the lack of differentiation (Blackadar, 1956) in the Logan Sills, and

3) the almost inevitable presence of the Rove Shale.

It should be noted, however, that with few exceptions (e.g. Silver Islet), veins narrow as they enter diabase sills. This fact has been used to support a lateral secretion model (see below); however, it may be unrelated to fluid source. Depositional sites for veins are largely controlled by the presence of pre-existing open fractures or faults. The termination of veins as they enter the sills is probably a function of the closure of these features as they enter a hotter, more plastic material present at the center of the sills from a cooler, more brittle material at the margins of sills.

In addition, the presence of a more highly differentiated magma from which hydrothermal fluids were derived present in the subsurface, as suggested by Scott (1972) at the Siscoe Metals deposit, Cobalt, could also occur in the Thunder Bay area. Scott's suggestion was based on the theory a series of magmatic pulses from an underlying source. Textural and mineralogical evidence of such events in the Logan Sills have been discussed (Regional Geology), and could have such a source.

Evidence which has been cited to support a lateral secretion model includes:

- 1) the presence of Rove Formation shales at all veins except those in the Port Arthur Group, which are hosted

- by the Gunflint Formation,
- 2) the depletion of metals in the metamorphosed shales in contact with the Logan Sills,
  - 3) the general lack of silver mineralization in veins where they enter mafic intrusions and the general concomitant narrowing of the veins,
  - 4) the tenor of veins and their size is restricted to fairly shallow depths, usually veins extend <<100m below surface, and
  - 5) the inhomogeneity of lead isotopes in galena.

The importance of the presence of Rove Shales in the genesis of the veins can be examined by comparing the nature of veins in the Rabbit Mountain Groups with those in the Port Arthur Group. Veins from all three areas were important producers of silver, and all these veins are associated with Logan Sills. If fluids from a magmatic source are solely responsible for the formation of the veins, it is very difficult to explain the difference in vein character as one moves from a Rove Shale host to a Gunflint Formation host. In the former, calcite  $\pm$  fluorite are major and usually dominant gangue minerals, while in the latter the dominant gangue is quartz. There is also a change in the common sulfides found: in Rove hosted veins sphalerite and galena  $\pm$  chalcopyrite and pyrite are found; in contrast, it is rare to find any sulfide but pyrite in the Port Arthur Group. The chert and taconite found in the Gunflint Formation, however, would provide a silica and iron rich source. In contrast the plagioclase in the Rove Formation

could break down upon metamorphosed to albite + CaO (Morey 1969), providing a source for calcite and fluorite.

Metals can be found in the shales in the organic fraction, in carbonaceous material, as sulfides, in the detrital fraction, and independently. In the latter case the metals would generally be adsorped to clay minerals. Analysis of a large number of shales (Vine and Tourtelot 1970) indicates that Ag, Zn, Cu, and Ni are most abundant in the organic, and independent fractions, whereas Pb and Co are most abundant in the independent and detrital fractions.

Removal of metals from the independent fraction can be accomplished by metamorphism of 1M illite to 2M illite, which decreased the number of sorption sites (Franklin, 1970). In some veins (e.g. Silver Islet) the presence of graphite suggests the transportation of carbonaceous materials, which would also allow the release of metals from this fraction. Metamorphism of pyrite to pyrrhotite could provide a source of sulfur (Franklin, 1970).

Depletion of trace metals from the shales bordering veins and sills has been tested at two locations, at the Porcupine Mine (Franklin, 1970) and the Rabbit Mountain Mine (Harvey, 1985). The results are presented in Table 9, along with the quantities of these metals found in analyses of Rove and Gunflint Formations completely removed from veins from Cameron and Garrels (1980). They show zones of depletion of Cu, Pb, Zn, and Ag do occur in the shale as it nears the vein, although the area immediately adjacent

to veins is often enriched in those metals. This is in accordance with the lateral secretion model as outlined by Boyle (1968). All analysis of the shale in the vicinity of veins contained considerable more Zn (100-600 vs 17ppm) and Ag (1.3 - 10.6 vs .46ppm) than the background level indicated by the Cameron and Garrels data. The data from metamorphosed versus unmetamorphosed shale (Franklin, 1970) does show a clear trend of depletion in trace metals.

The restriction of veins to shallow levels (e.g. except in the Port Arthur Group above the Gunflint Formation) could be a result either of the limiting presence of shales or the lack of available depositional sites (open faults and fractures) in the deeper strata. The lack of veining at low levels is also evidence against a mafic magmatic fluid source, as the sills themselves are too narrow to have generated a fluid, but one would expect veins to be more continuous at depth if their source was a deep-seated magma.

Similarly, the general lack of high tenor material and the general narrowing of veins as they enter intrusions could suggest the metals are derived from shales.

The vein deposits of the Island Belt are dissimilar to those of the Mainland Belt in two significant respects:

- 1) The Mainland Belt veins are associated with Logan Sills, the Island Belt veins are associated with Logan

**TABLE 9: TRACE METALS IN THE ROVE SHALE (ppm)**

	<u>Cu</u>	<u>Zn</u>	<u>Ni</u>	<u>Pb</u>	<u>Co</u>	<u>Ag</u>	<u>As</u>	<u>Hg</u>
A1 <sup>1</sup>	52.5	359	57.3	30.3	20.4	4.3	1.8	<0.05
A2	14.5	440	47.6	41.7	33.5	0.9	3.2	<0.05
A3	74.0	298	68.7	33.4	19.3	1.4	4.2	<0.05
A4	51.3	228	23.9	5.5	16.0	2.2	7.0	<0.05
A5	12.8	348	28.9	56.1	24.5	3.5	3.3	<0.05
A6	83.4	197	40.1	8.8	12.5	2.3	5.6	<0.05
C1 <sup>2</sup>	81.8	644	32.9	41.9	50.9	6.8	4.5	0.55
C2	53.5	412	32.7	31.8	31.8	6.1	3.7	0.10
C3	21.9	93	14.0	7.0	20.7	4.6	10.6	<0.05
C4	14.7	107	13.5	3.0	18.0	1.3	4.8	<0.05
C5	42.0	362	21.0	12.5	13.0	2.5	6.2	<0.05
C6	70.8	211	21.5	15.0	12.7	2.8	6.3	<0.06
C7	73.6	181	21.5	13.0	13.3	2.4	6.1	<0.05
D1 <sup>2</sup>	91	109	75	25		1.5		
D2	54	75	58	21		1.3		
E1 <sup>3</sup>	70	17	69	22	19	.46	14	299 <sup>4</sup>
E2	34	36	22	12	14	.08	57	611 <sup>4</sup>

<sup>1</sup> From Harvey (1985); numbers indicate increasing distance from vein: 1 closest - 7 furthest

<sup>2</sup> From Franklin et al (in press); D1 unmetamorphosed - D2 metamorphosed

<sup>3</sup> From Cameron and Garrels (1980); E1 Rove Shale - E2 Gunflint

<sup>4</sup> in ppb

Sills, Pigeon River Dykes, and the Pine Point-Mount Mollie Gabbro.

- 2) The Mainland Belt veins, with the exception of those hosted by the Gunflint Formation, are fairly consistent in nature (e.g. mineralogy, morphology, and extent). In contrast the veins of the Island Belt display heterogeneity in all these respects, differing both from Mainland veins and from each other.

Smyk (1984) and Franklin et al. (in press) suggest these attributes can be reconciled by the involvement of some intrusions in the Island Belt (e.g. at Silver Islet) either as a direct source of some fluids or as a part of the system through which connate  $\pm$  meteoric fluids pass while scavenging metals. The source of the Ni, Co, and possibly As is ascribed to the intrusion in either role. The larger size of some intrusions would indicate slower cooling and the establishment of a larger convection cell, perhaps hotter and more effective at leaching.

The vein at Silver Islet is unique in setting in that it is almost entirely hosted by gabbro, pinching out rapidly as it enters the Rove Formation. It is also unique morphologically, rarely showing textural evidence of open space filling except in the late vug-filling stage.

The lateral secretion model is supported by Pb-isotope data from the Mainland and Island Belts (Franklin et al., in press).

From Figure 25 it can be seen in the  $Pb^{207}/Pb^{206}$  plot that most lead is not anomalous with the exception of a sample from Shuniah, but it does form secondary isochron(s). The Island Group data is from Silver Islet, and distinctly more radiogenic than the leads from the Mainland. This can be interpreted to suggest:

- 1) the secondary isochrons are a result of inhomogeneous fluids.
- 2) the Pb had a source with U/Pb close to the crustal average.
- 3) Pb was usually derived from minerals which were not enriched in U, Th.

Without direct comparison with the lead isotopic composition of the Rove Shale and mafic intrusions it is not possible to prove the lead's source; however, Franklin et al. suggest that variable and ineffective leaching of lead from both detrital minerals (zircon and monazite) and authigenic clay minerals in the Rove could be responsible for the pattern found. The more radiogenic lead found at Silver Islet could be a result either of a more efficient leaching system (caused by higher temperature) or a different source for lead than that of the Mainland Belt. The Shuniah lead was also very radiogenic compared to the other samples, and such a source as Archean pegmatites is suggested in this case.

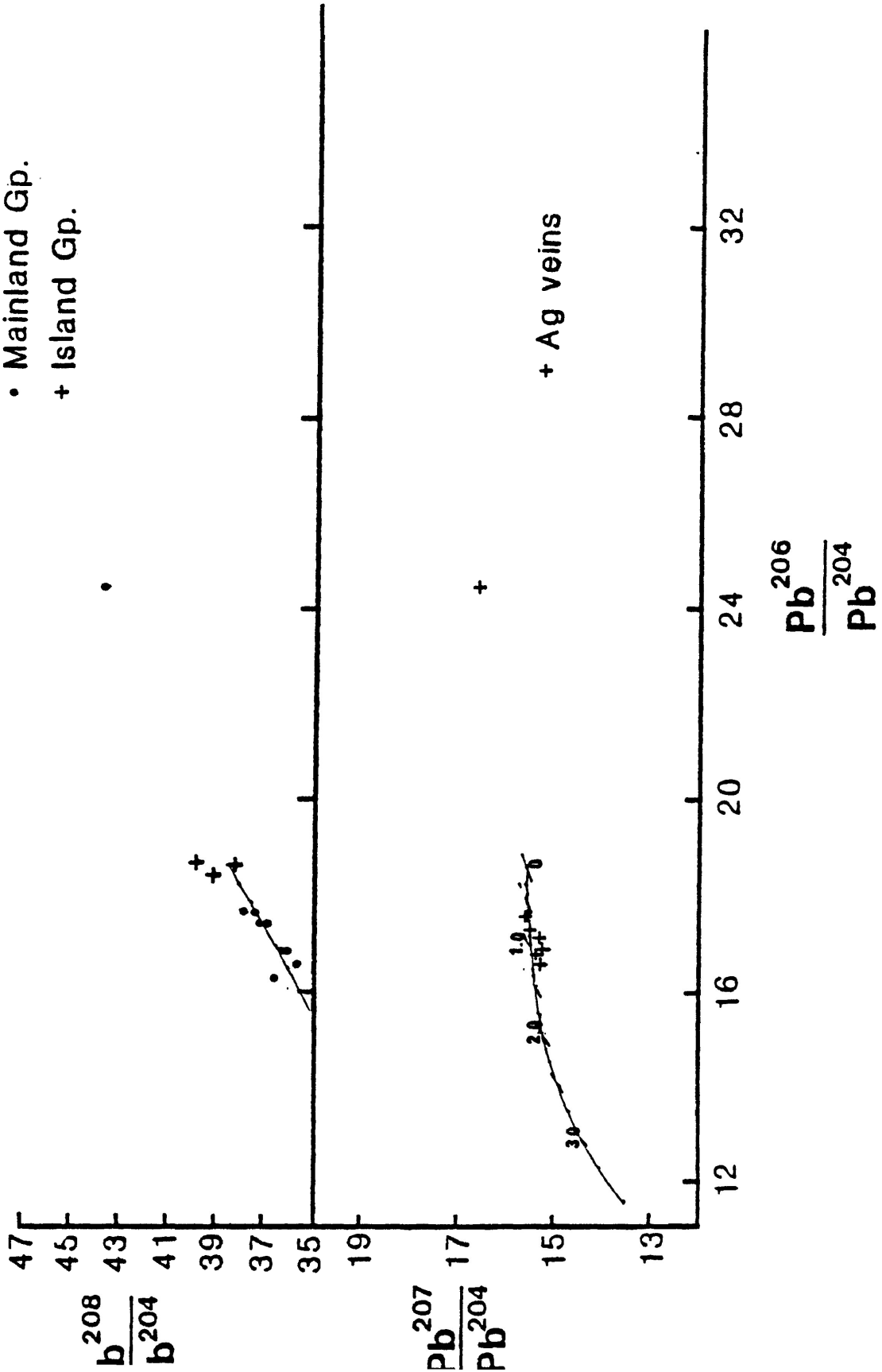


Figure 25: Summary plot of lead isotopic compositions of galena in the Thunder Bay District (Franklin et al., in press).

## APPLICATION OF FLUID INCLUSION AND SULFUR ISOTOPIC DATA TO GENETIC MODELS

Many characteristics of veins in the Thunder Bay District are quite diverse, varying in metal association (barren, silver-bearing, S-element) and to some extent morphologically (open space filling versus massive at Silver Islet). Fluid inclusion and sulfur isotopic information regarding this spectrum is remarkably consistent. It is suggested that this uniformity reflects a consistency in depositional environment and the nature of hydrothermal fluids as they reach these sites. The most important condition controlling vein depositions was the presence of an open fracture or fault system. These fractures occur in two linear belts, regional caused by the regional warping during the sinking of the Lake Superior Synclinorium. In the Island Belt, the fracture belt is occupied by mafic intrusions, while the veins occupy fractures generated during the cooling of these intrusions or cross-cutting the intrusions (Silver Islet).

Homogenization temperatures of Mainland Belt veins generally show deposition of minerals at high (250°–400°C), followed by low (80°–150°C) temperatures, repeating this cycle after a period of brittle deformation or continuing at low temperatures (Figure 26). A similar pattern (high–low–high–low temperature) is suggested by the limited data from Silver Islet, without any evidence of fracturing episode. At Spar Island there is no evidence of an initial high temperature episode (Figure 27), and again fracturing

is absent. Except at Silver Islet, evidence of boiling is restricted to the early high-temperature episode.

Two explanations of this behaviour are proposed:

- 1) The hydrothermal fluids are uniformly hot (300°–500°C) before entry into fracture system or opening of fracture system. They are then trapped in the system and vein material is precipitated. The period of brittle fracturing allows a new flux of fluid into the system, the cycle is repeated.
- 2) The hydrothermal fluids are free to the system at all times, but the source(s) of the fluids is of variable temperature.

Sphalerite was deposited only at low temperatures (~100°C), which is probably true also of the other sulfides and native silver. In the Mainland Belt the bulk of the base metals and the initial native silver mineralization postdated the fracturing event. The sulfide-rich material is often closely associated with high-temperature gangue minerals, indicating the fracture was a highly variable system at that time and suggesting a period of mixture between residual fluids from the initial phase of deposition and a fresh influx of hot fluids. The low activities of sulfur indicated in the systems by both the common presence of native silver as well as acanthite and the iron content of

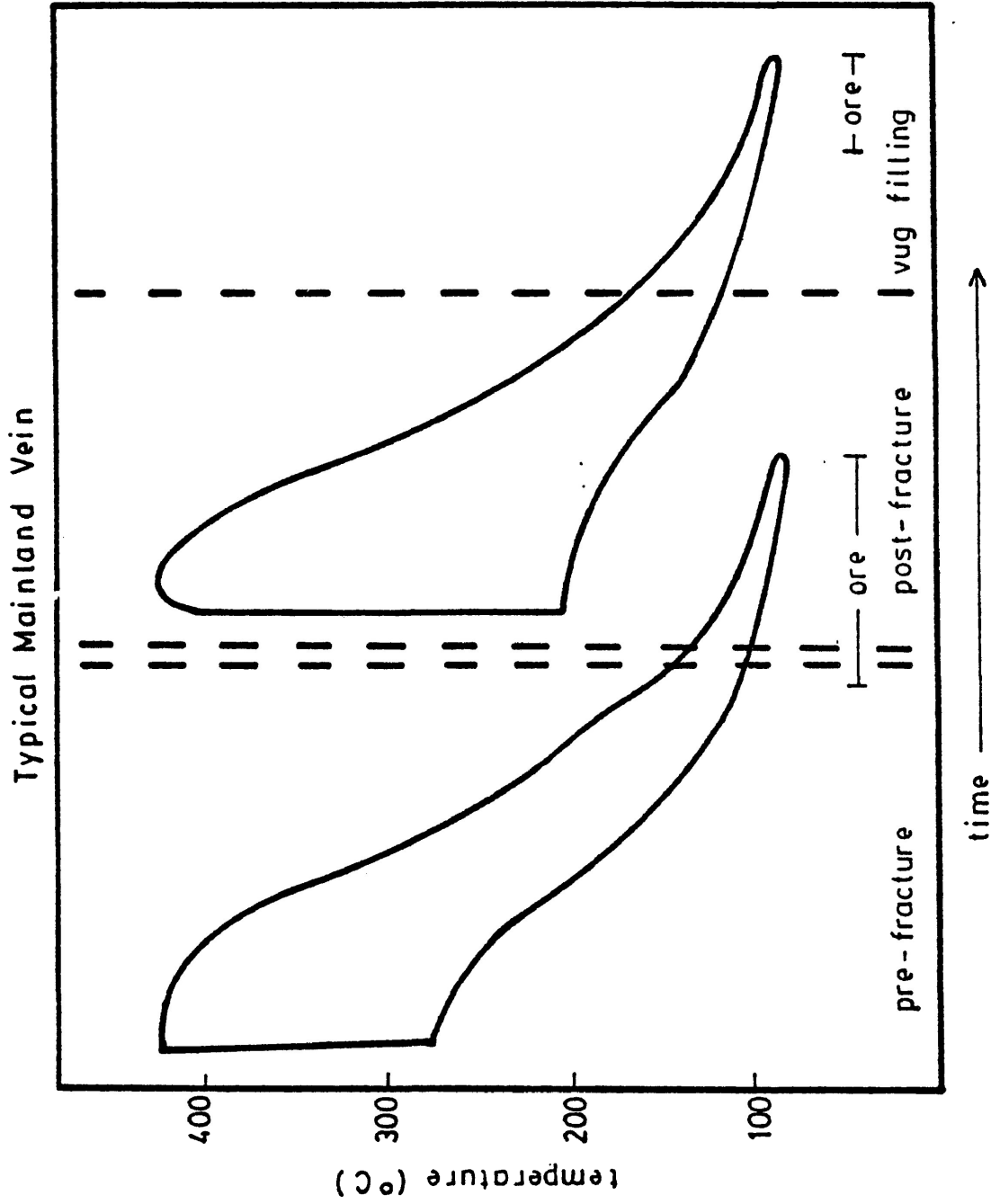


Figure 26: Relationship between depositional temperature and time at a typical Mainland vein. Fracturing and post-fracture depositional period absent in Port Arthur Group. Periods of ore deposition as indicated.

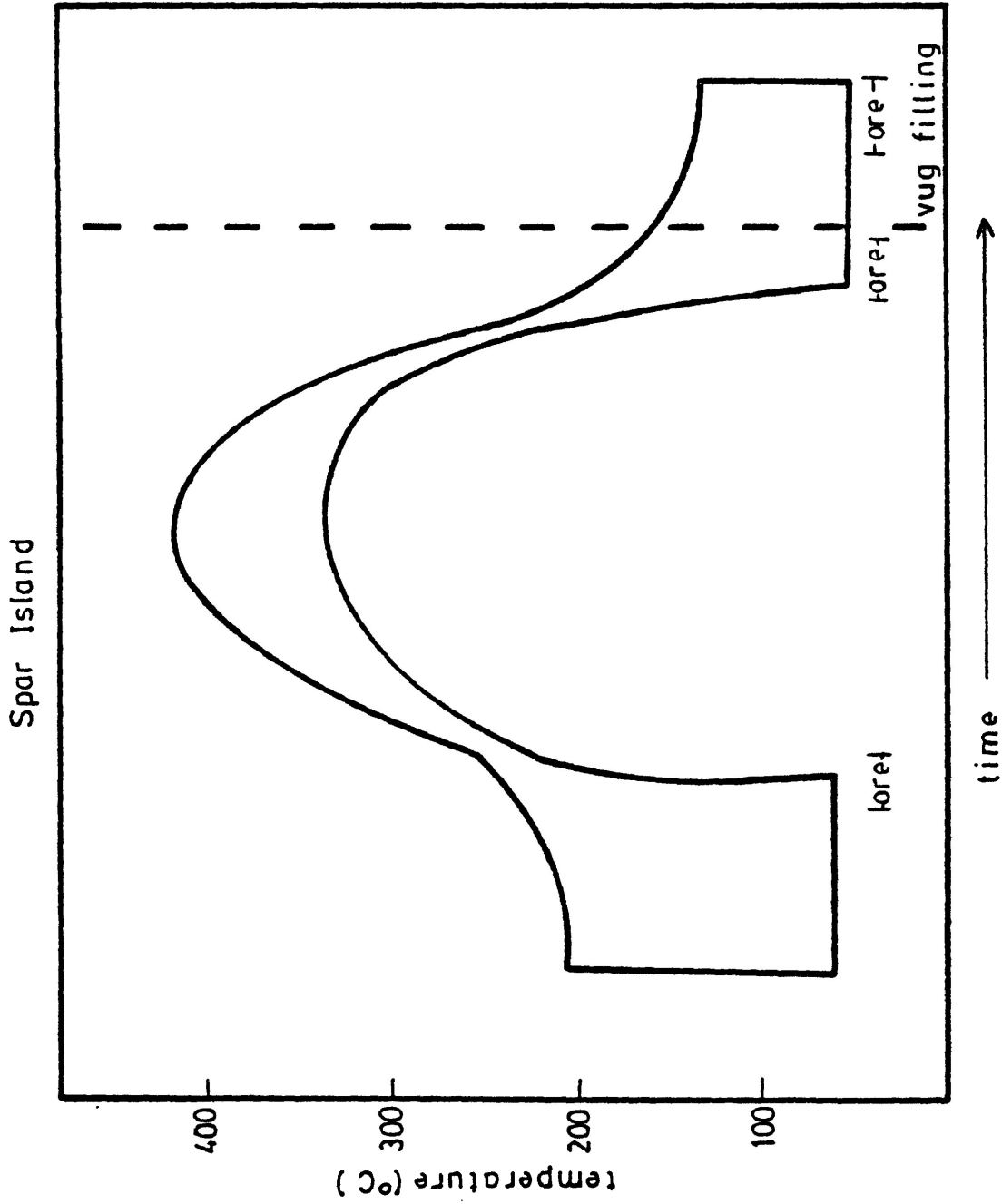


Figure 27: Relationship between depositional temperature and time at Spar Island. Periods of ore deposition as indicated.

sphalerite suggest that sulfur content of the fluids may have been an important control for ore deposition.

One possible explanation for the precipitation of sulfides after fracturing is that metals in the newly introduced, perhaps relatively oxidized, fluids mixed with residual fluids where sulfur concentrations had been increased by boiling.

Information regarding the salinity of the hydrothermal fluids indicated they ranged from weak to moderately strong salinity (1-30 equiv. wt.% NaCl). The dominant salt in the solution was  $\text{CaCl}_2$ , with undetermined amounts of NaCl, KCl, and  $\text{MgCl}_2$  also probably present. There is no apparent relationship between salinity and the temperature of the fluids (Figure 28). Variability in solution salinity might be caused by a variably saline source, inhomogeneity in the fluid within the fracture system due to boiling, or mixture of two fluids from different sources. At present there is insufficient data to choose amongst these possibilities.

Sulfur isotopic composition of mineral pairs demonstrates that processes of deposition did not occur during isotopic equilibrium. This could be a result of turbulence and convection within the hydrothermal system. In the Rabbit and Silver Mountain Groups this could be the result of a strong pulse of hydrothermal activity after the fracturing event. In the case of the Island Belt and the Port Arthur Group where the fracturing event is not in evidence and

where evidence of boiling is rare, convection of the fluids due to cooling is a possible mechanism.

Neither the fluid inclusion nor the sulfur isotopic data has particularly clarified the question of fluid source. It has been suggested that the larger intrusions, such as are found at Silver Islet or Spar Island, generated higher temperatures in convective cells formed in the Rove Shale, producing more complex metal assemblages (Franklin 1970, Smyk 1984, Franklin et al., in press). This idea is not supported by fluid inclusion behaviour at mines of varying complexity; however, their homogenization temperatures are representative only of depositional conditions. Hence temperatures of the hydrothermal fluids are still open to speculation.

Susak and Crerar (1985) present experimental data on the behaviour of metal complexes at elevated temperatures that would give a theoretical basis for the presence of Ni and Co only in deposits generated from higher temperature connate fluids. They demonstrate that the solubility of metals is affected by the co-ordination of the complexes they are found in; in relatively low temperature, low salinity solutions they occur in octahedral co-ordination, at increased temperature and salinity they occur in tetrahedral co-ordination. The solubility of the metal increases sharply as the transition is made from octahedral to tetrahedral co-ordination.

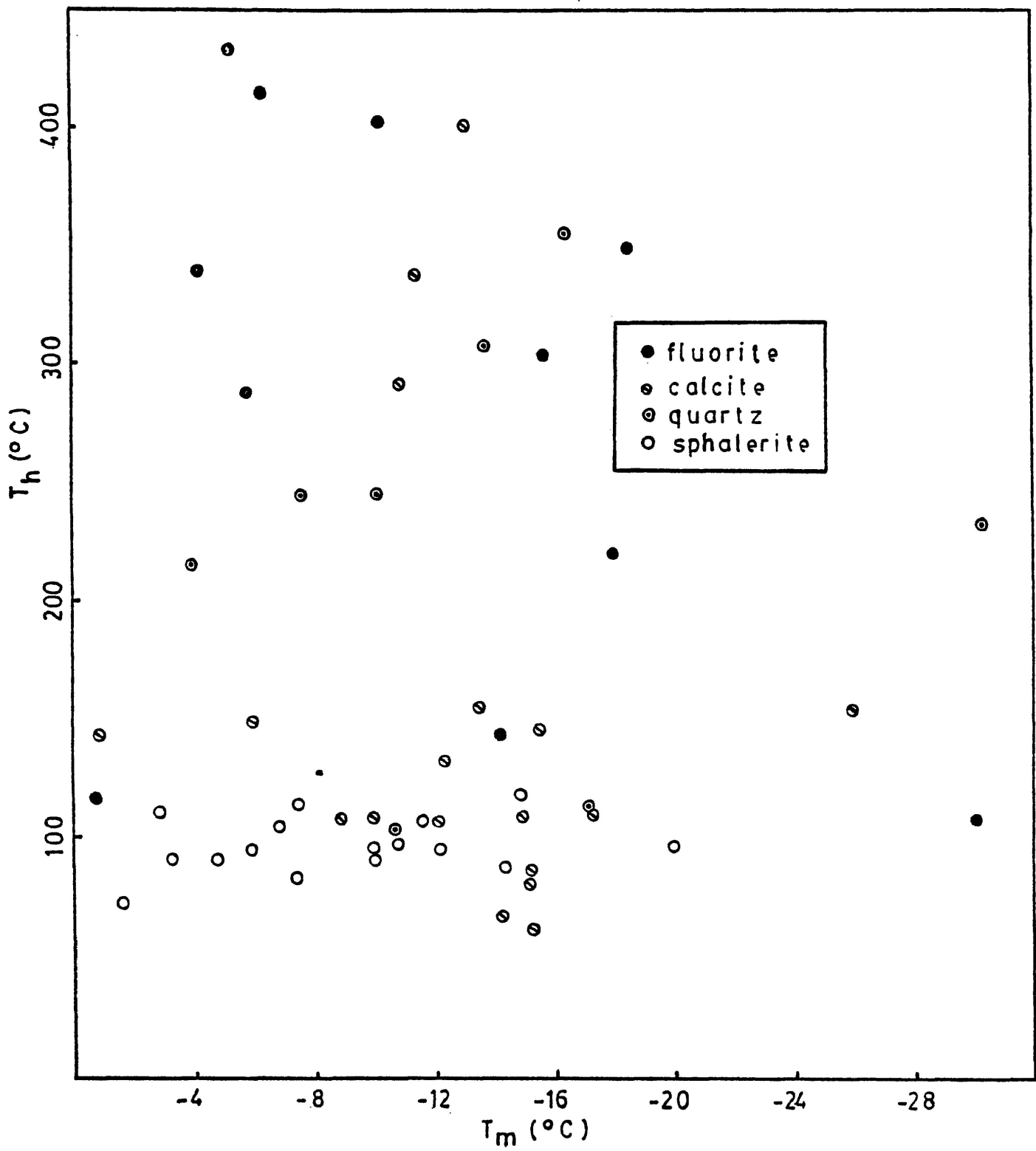


Figure 28:  $T_h$  vs  $T_m$  plot. No correlation between salinity and homogenization temperature was observed.

In the case of the silver veins the transition zone between these co-ordination states for Ni, Co, and Cu (common only in the Island Belt) occurs at a higher temperature than for Fe. Geological evidence suggests that Zn and Pb also have a relatively low temperature transition zone.

The anomalous presence of Ni and Co arsenides at the Big Harry vein and the 3A mine in the Rabbit Mountain and Port Arthur Groups, respectively, could be accounted for by this solubility effect, if it were assumed that short pulses of very high temperature ( $>400^{\circ}\text{C}$ ) hydrothermal fluids leached these elements from the shales, volcanics, or the solidified sills. In contrast, if the hydrothermal fluids were released solely from the mafic magmas, it is difficult to account for the presence of Ni and Co only in two of the veins spatially associated with Logan Sills.

The presence of the "fifth element", arsenic, in the 5-element association systems may be limited by the amount of sulfur in hydrothermal fluids. Metals can be efficiently transported in the form of chloride complexes in saline solutions (Barnes 1979); however, the dominant As complexes appear to be  $\text{H}_2\text{As}_2\text{S}_4$ ,  $\text{HAs}_2\text{S}_4^-$  and  $\text{As}_2\text{S}_4^{2-}$  (Mironova and Zotov 1980).

Sulfur isotopic composition points towards a source of lighter sulfur (+4.7%) than the Rove Shale (+16%), suggestive of a magmatic source for the fluids or the sulfur in the fluids. This

could be achieved either through direct entry of hydrous residual fluids from the sills and dykes entering the fracture system, or through reaction of an intrusion generated convection cell in the Rove Shale entering the intrusions and scavenging sulfur. In the latter case, metals might be leached from shale, and sulfur from the igneous intrusions.

As has been previously discussed, problems of system closure lead to some questioning of the source isotopic composition of +4.7% derived from the  $\delta^{34}\text{S}$  versus  $\Delta$  diagram. To try to clarify this problem a large number of analyses from a single vein are needed.

### CONCLUSIONS

The veins of the Thunder Bay Silver District can be divided into three groups mineralogically: the barren, the silver bearing, and the S-element association. The veins occur in two curvilinear belts, forming the Mainland Belt (Rabbit Mountain, Silver Mountain, Port Arthur Groups) and the Island Belt.

Gangue mineralogy of the Rabbit Mountain and Silver Mountain Groups is dominated by calcite, green and purple fluorite, and quartz. Precipitation occurred initially at relatively high temperatures (250°-400°C); temperature decreased with time. Homogenization of some fluid inclusions to a vapour phase is evidence of sporadic boiling through the vein systems in the early high temperature phase. A period of fracturing/faulting interrupted vein deposition. Ore deposition, sulfides, native silver, and acanthite, is associated with this fracturing episode. Sphalerite inclusion homogenization temperatures indicate ore precipitation occurred between 80°-115°C. Coeval calcite and fluorite were deposited over a broad temperature range, 80°-450°C, suggesting great inhomogeneity in the vein systems perhaps due to the mixing of residual initial fluids with a fresh influx of sulfur-rich hydrothermal fluids. Temperature of deposition again shows a general decrease with time.

In the Port Arthur Group gangue mineralogy is dominated by quartz and to a lesser extent calcite. Depositional temperatures range from 75°–300°C. A weak trend of decreasing temperature with time is indicated.

The deposits of the Island Belt are diverse in nature. At Silver Islet early deposition of dolomite and quartz is dominantly low temperature (70°–90°C) although some quartz is precipitated as high as 330°C. The dolomite deposition is associated with pyrite and argentite mineralization. As gangue mineralogy becomes dominated by calcite and quartz a general increase in temperature is observed (160°–300°C) accompanied by sporadic boiling. Sphalerite–native silver–Ni–Co arsenide/sulpharsenide deposition associated with this stage occurs between 75°–90°C.

At Spar Island initial deposition was low temperature; a period of high temperature (250°–325°C) deposition of barite ± quartz and calcite was preceded and followed by copper sulfide and silver deposition.

In all veins low temperatures (~100°C) characterize ore deposition.

With the exception of Victoria Island, which showed no evidence of high temperature deposition, the temperature range observed in veins of the barren, silver-bearing, and S-element association was similar (75°–450°C).

The salinity of hydrothermal fluids is quite variable in all the veins studied, ranging from 21.1-27.2 equiv. wt.% NaCl. The dominant salt in the fluids was  $\text{CaCl}_2$ . No correlation between salinity and fluid temperature or paragenesis was observed.

Iron content of sphalerite indicates low  $a_{\text{S}_2}$  in the ore-forming fluids ( $10^{-10}$ - $10^{-20}$ ) for the Mainland Belt and Silver Islet. Slightly higher sulfur activities are indicated by the sulfide minerals found at Spar Island.

Sulfur isotopic composition in hypogene sulfides from all veins varied from -1.7 to +12.2% with the exception of one galena sample from Rabbit Mountain (-9.3%). Barite sulfur isotopic composition fell within this range (+6.5 to +8.7%) with one exception from Silver Mountain (+30.7%). Paired data indicate deposition of sulfides generally occurred in isotopic disequilibrium, suggesting turbulence in the hydrothermal fluids.

The consistency of fluid inclusion, sulfur activity, and sulfur isotopic data suggest that both depositional environment and hydrothermal fluid source were similar for all veins in the silver district. Heterogeneity of the deposits appears to be a result of differences in the evolution of the fluids between their inception and entry into the depositional environment.

The source of the fluids is still enigmatic. Sulfur isotopic evidence suggests a magmatic source for the sulfur in the fluids ( $\delta^{34}\text{S} = +4.7\%$ ); however, a more comprehensive study of sulfur isotopic composition from single vein systems is needed to confirm this.

Conversely, if the interpretation that heterogeneity of the deposits is a result of fluid evolution is correct, a lateral secretion model allows the most freedom of variability between vein systems.

These two lines of evidence could be reconciled either by the assumption of:

- 1) a lateral secretion model, in which the convection cell passes both through the Rove shale (Gunflint or Archean strata for the Port Arthur Group) and the nearby mafic intrusions, or
- 2) a mixture of primary magmatic fluids containing sulfur  $\pm$  metals and convection connate waters from surrounding strata occurred in the open fractures and faults.

Clarification of fluid source might be gained through more comprehensive fluid inclusion and stable isotope studies of typical veins such as Silver Islet and Silver Mountain.

REFERENCES

- Arne, D. C. (1985); A Study of Zonation at the Nanisivik Zn-Pb-Ag Mine, Baffin Island, Canada; M.Sc. Thesis (unpublished) Lakehead University.
- Badham, J. P. N. (1976); Orogenesis and metallogenesis with reference to the silver-nickel-cobalt-arsenide ore association; in Metallogeny and Plate Tectonics, ed. D. F. Strong, Geological Association of Canada Special Paper; vol. 14 pp 559-569.
- Badham, J. P. N., Robinson, B. W. and Morton, R. D. (1972); The geology and genesis of the Great Bear Lake Silver Deposits; 24th International Geological Congress (Montreal); Section 4, pp 541-548.
- Barnes, H. L. (1979); Solubility of Ore Minerals in Geochemistry of Hydrothermal Ore Deposits. 2nd Edition; ed. H. L. Barnes; Wiley Interscience Publication; John Wiley & Sons; Toronto, pp 404-460.
- Barton, P. B. and Skinner, B. J. (1967); Sulfide Stabilities in Geochemistry of Hydrothermal Ore Deposits 1st edition; ed. H. L. Barnes; New York: Holt, Rinehard, and Winston pp 236-333.
- Barton, P. B. and Skinner, B. J. (1979); Sulfide Mineral Stabilities in Geochemistry of Hydrothermal Ore Deposits 2nd edition; ed. H. L. Barnes; Wiley Interscience Publication; John Wiley and Sons; Toronto pp 278-390.
- Birks, L. S. (1969); X-ray Spectrochemical Analysis, 2nd edition; Interscience Publishers, New York, p 143.
- Blackadar, R. G. (1956); Differentiation and assimilation in the Logan Sills, Lake Superior District, Ontario; American Journal of Science; vol. 254, pp 623-655.
- Bodnar, R. J. and Bethke, P. M. (1984); Systematics of fluid inclusions I: fluorite and sphalerite at 1 atmosphere confining pressure; Economic Geology; vol. 79, pp 141-161.
- Bowen, N. L. (1911); Silver in the Thunder Bay District. Annual Report, Ontario Bureau of Mines; vol. 20, pt. 2, pp 119-132.
- Boyle, R. W. and Dass, A. S. (1971); Origin of the Native Silver Veins at Cobalt, Ontario; in The Silver-Arsenide Deposits of the Cobalt-Gowganda Region, Ontario; The Canadian Mineralogist; vol. 11 pt. 1, pp 414-417.

- Brumby, G. R. et al. (1978); Improved sample preparation for fluid inclusion studies; Mineralogical Magazine; vol. 42, no. 322, pp 297-298.
- Cameron, E. M. (1983); Genesis of Proterozoic iron-formations: Sulphur isotope evidence; Geochimica et Cosmochimica Acta; vol. 47, pp 1069-1074.
- Cameron, E. M. and Garrels, R. M. (1980); Geochemical compositions of some Precambrian shales from the Canadian Shield; Chemical Geology; vol. 28, pp 181-197.
- Card, K. D. et al (1972); The Southern Province; in Variations in tectonic styles in Canada; Geological Association of Canada Special Paper II pp 335-380.
- Chambers, B. (1986); Geology and Mineralogy of the Creswell Silver Deposits, Mainland Belt Silver Region, Thunder Bay District, H.B.Sc. Thesis (unpublished), Lakehead University.
- Changkakoti, A., Morton, R. D., and Gray, J. (1986); Hydrothermal environments during the genesis of silver deposits in the Northwest Territories of Canada: Evidence from Fluid Inclusions; Mineralium Deposita; vol. 21, pp 63-69.
- Cole, B. L. (1978); Geology and Mineralogy of the Beaver Junior Mine, Mainland Belt Silver Region, Thunder Bay District; H.B.Sc. Thesis, (unpublished), Lakehead University.
- Davis, D. W. and Sutcliffe, R. H. (1984); U-Pb ages from the Nipigon Plate (abst.) in GAC-MAC 1984 Program with Abstracts. Joint Annual Meeting; vol. 9, p 57.
- Franklin, J. M. (1970); Metallogeny of the Proterozoic rocks of Thunder Bay District, Ontario; Ph.D. Thesis, University of Western Ontario, London, Ontario.
- Franklin J. M. (1978); Rubidium-strontium age determinations of the Rove formation shale. In "Rubidium-strontium isochron age studies, report 2" R. K. Wanless and W. D. Loveridge, editors; Geological Survey of Canada paper 77-14 pp 35-39.
- Franklin, J. M. (1982); Introduction to Proterozoic Geology of the Northern Lake Superior Area; in Proterozoic Geology of the Northern Lake Superior Area; ed. J. M. Franklin et al.; Geological Association of Canada Field Trip Guide Book, pp 1-13.
- Franklin, J. M., Kissin, S. A., Smyk, M.C., and Scott, S.D. (in press); Silver Deposits Associated with the Proterozoic Rocks of the Thunder Bay District, Ontario. Canadian Journal of Earth Sciences.

- Geul, J. C. C. (1970); Geology of Devon and Pardee Townships and the Stuart Location, District of Thunder Bay; Ontario Department of Mines, Geological Report 87, p 52.
- Geul, J. C. C. (1973); Geology of Crooks Township, Jarvis and Prince Locations, and Offshore Islands, District of Thunder Bay; Ontario Department of Mines, Geological Report 102, p 46.
- Giordano, T. H. and Barnes, H. L. (1981); Lead transport in Mississippi Valley type ore solutions; Economic Geology; vol. 76, pp 2200-2211.
- Goodwin, A. M. (1956); Facies relations in the Gunflint Iron formation; Economic Geology; vol. 51, pp 656-695.
- Hall, S. C. and Stumpfl, E. F. (1972); The five elements (Ag-Bi-Co-Ni-As) - a critical appraisal of the geological environments in which it occurs and of the theories affecting its origin; 24th International Geological Congress (Montreal); Section 4, p 540.
- Hanson, G. N. and Malhotra, R. (1971); K-Ar Ages of Mafic Dikes and Evidence of Low-Grade Metamorphism in Northeastern Minnesota; Geological Society of America Bulletin; vol. 82, pp 1107-1114.
- Harvey, P. L. (1985); A test of the Lateral Secretion Hypothesis at the Rabbit Mountain Mine, Mainland Belt Silver Region, Thunder Bay District, Ontario H.B.Sc. Thesis (unpublished), Lakehead University.
- Holland, R. A. G., Bray, C. J., and Spooner, E. T. C. (1978); A method for preparing doubly-polished thin sections suitable for microthermometric examination of fluid inclusions; Mineralogical Magazine; 42, pp 407-408.
- Hurley, P. M., Fairbairn, H. W., Pinson, Jr., W. H., and Hower, J. (1962); Unmetamorphosed minerals in the Gunflint Formation used to test the age of the Animikie; Journal of Geology; vol. 70, pp 489-492.
- Ingall, E. D. (1888); Report on mines and mining on Lake Superior; Geological and Natural History Survey of Canada Annual Report for 1887-8; New Series 3, pt. 1, pp 1-131.
- Kovack, J., and Faure, G. (1969); The age of the Gunflint Iron Formation of Animikie series in Ontario, Canada; Geological Society of America Bulletin; vol. 80, pp 1725-1736.

- Lawler, J. P. and Crawford, M. L., (1983); Stretching of fluid inclusions resulting from a low-temperature microthermometric technique; *Economic Geology*; vol. 78, pp 527-529.
- MacFarlane, T. (1880); Silver Islet; *Transactions of the American Institute of Mining Engineers*; vol. 8, pp 226-253.
- Manuala, T. L.. (1979); *Geology and Mineralogy of the Little Pig Vein, Mainland Belt Silver Region, Thunder Bay District*, H.B.Sc. Thesis (unpublished), Lakehead University.
- Mironova, G. D. and Zotov, A. V. (1980); Solubility studies of the stability of As(III) sulfide complexes at 90°C; *Geochemistry International*; vol. 17, pp 46-54.
- Moorehouse, W. W. (1960); Gunflint Iron Range in the vicinity of Port Arthur; *Ontario Department of Mines Annual Report*; vol. 69, part 7, pp 1-40.
- Morey, G. B. (1969); The geology of the Middle Precambrian Rove Formation in northeastern Minnesota; *Minnesota Geological Survey spec. pub., SP7, Special Publication series*; University of Minnesota, Minneapolis, p 62.
- Morey, G. B. (1972); Gunflint Range; in *Geology of Minnesota: A Centennial Volume*; ed. P. K. Sims and G. B. Morey; *Minnesota Geological Survey*, pp 218-225.
- Mosley, E. B. (1977); *Geology and Mineralogy of the Rabbit Mountain Mine, Mainland Belt Silver Region, Thunder Bay District, Ontario*; H.B.Sc. Thesis (unpublished), Lakehead University.
- Ohmoto, H. (1972); Systematics of sulfur and carbon isotopes in hydrothermal ore deposits; *Economic Geology*; vol. 67, pp 551-578.
- Ohmoto, H. and Rye, R. O. (1979); *Isotopes of Sulfur and Carbon in Geochemistry of Hydrothermal Ore Deposits 2nd edition*; ed. H. L. Barnes; *Wiley Interscience Publication*; John Wiley and Sons; Toronto, pp 509-567.
- Peterman, Z. E. (1966); Rb-Sr dating of Middle Precambrian metasedimentary rocks of Minnesota; *Geological Society of America Bulletin*; vol. 77, pp 1031-1044.
- Petruk, W. and Jambor, J. L. (1971); in *The silver-arsenide deposits of the Cobalt-Gowganda region, Ontario*; *Canadian Mineralogist*; vol. 11, part 1, pp 1-429.

- Pinckney, P. M. and Rafter, T. A. (1972); Fractionation of sulfur isotopes during ore deposition in the Upper Mississippi Valley zinc-lead district; *Economic Geology*; vol. 67, pp 315-328.
- Potter, R. W. (1977); Pressure corrections for fluid inclusion homogenization temperatures based on the volumetric properties of the system NaCl-H<sub>2</sub>O; *U.S. Geological Survey Journal of Resources*; vol. 5, pp 603-607.
- Potter, R. W., Clyne, M. A., and Brown, D. L. (1978); Freezing point depression of aqueous sodium chloride solutions; *Economic Geology*; vol. 73, pp 284-285.
- Robertson, W. A. and Fahrig, W. F. (1971); The great paleomagnetic loop - the polar wandering path from Canadian Shield rocks during the Neohelikian Era; *Canadian Journal of Earth Sciences*; vol. 8, pp 1355-1372.
- Robinson, B. W. and Ohmoto, H. (1973); Mineralogy, fluid inclusions, and stable isotopes of the Echo Bay U-Ni-Ag-Cu deposits, Northwest Territories, Canada; *Economic Geology*; vol. 68, pp 635-656.
- Roedder, E. (1984); Fluid inclusions; *Mineralogical Society of America Reviews in Mineralogy*; vol. 12.
- Sakai, H. (1968); Isotopic properties of sulfur compounds in hydrothermal processes; *Geochemical Journal*; vol. 2, pp 29-49.
- Scott, S. D. (1972); The Ag-Co-Ni-As ores of the Siscoe metals of Ontario mine, Gowganda, Ontario, Canada; 24th International Geological Congress; Sect. 4, pp 528-538.
- Scott, S. D. (1983); Chemical behaviour of sphalerite and arsenopyrite in hydrothermal and metamorphic environments; *Mineralogical Magazine*; vol. 47, pp 427-435.
- Seward, T. M. (1976); The stability of chloride complexes of silver in hydrothermal solutions up to 350°C.; *Geochimica et Cosmochimica Acta*; vol. 40, pp 1329-1341.
- Shegelski, R. J. (1982); The Gunflint Formation in the Thunder Bay Area; in *Proterozoic Geology of the Northern Lake Superior Area*; ed. J. M. Franklin et al; Geological Association of Canada; pp 15-31.
- Smyk, M. C. (1984); A Comparative Study of Silver Occurrences, Island Belt Silver Region, Thunder Bay District, Ontario; H.B.Sc. Thesis (unpublished), Lakehead University.

- Stille, P. and Clauer, N. (1986); Sm-Nd isochron-age and provenance of the argillites of the Gunflint Iron Formation in Ontario, Canada; *Geochimica et Cosmochimica Acta*; vol. 50, pp 1141-1146.
- Susak, N. J. and Crerar, D. A. (1985); Spectra and coordination changes of transition metals in hydrothermal solutions: Implications for ore genesis; *Geochimica et Cosmochimica Acta*; vol. 49, pp 555-564.
- Vine, J. P. and Tourtelot, E. B. (1970); Geochemistry of black shale deposits - a summary report; *Economic Geology*; vol. 65, pp 253-272.
- Weiblen, P. W., Mathez, E. A., and Morey, G. B. (1972); Logan Intrusions; in *Geology of Minnesota: A Centennial Volume*, ed. P. K. Sims and G. B. Morey; Minnesota Geological Survey.

## APPENDIX 1.

**Preparation of Doubly Polished Thin Sections with Heating  
From D. Arne (1985)**

1. Take specimens provided and trim to fit the interior dimensions of a 1" Bakelite polished section mounting ring. Leave enough ease around specimen for some movement. Be careful that sample depth will not catch on Bakelite lug depressions.
2. Grind sample surface on 400 grit carborundum to give a smooth working surface. Clean well to remove all carborundum. Dry thoroughly. Never heat specimen above 100°C as this will denature the fluid inclusions rendering the specimen useless.
3. Take blank Bakelite mounts and lightly skim surface to insure a smooth inclusive surface. Clean rings.
4. Have ready for use, a clean teflon surface big enough to hold all specimens. Using vaseline or other suitable product, carefully apply a light coating to the outer rim of the mounting rings. This will help to make a seal between the ring and the teflon when mounting takes place. Place specimens, flat side down, far enough apart to allow for mounting rings. Be sure that markings are visible, or that a specific order is maintained.
5. Place rings down over specimens. Mix or have on hand a cool setting epoxy such araldite. Fill rings up to the bottom of lug depressions. Using a dissecting pin or other instrument slightly agitate specimens to help air bubbles trapped around specimen to release. Be careful not to move mount.
6. When epoxy has set, lift mounted specimens and grind on a 400 grit carborundum to remove epoxy leaving a free sample surface. Clean thoroughly, then examine each surface carefully for pits or holes using a binocular microscope. Holes will have to be roughed out and filled with more epoxy, reground and re-examined. It is important to maintain a clean uncontaminated surface for diamond polishing on a Duren polishing machine.
7. Prior to the final grind, slightly level the edge of the bakelite holder. This will help to reduce surface drag and allows the free passage of the specimen on the polishing media.
8. When the surface of the specimen has a satisfactory bond it should be ground with a slurry of 5 micron alumina or a "fine-grained" cast iron lap especially machined to fit the "Duren" machine. The samples should rotate until the

surfaces are very smooth, almost to matte polish, and most importantly, free from as many cavities as possible. This stage of the polished surface is for the specimen in the Bakelite ring ONLY, not for a P.T.S. Remove samples and clean as previously stated. The surface will be smooth therefore there will be no need to use 6 or 3 micron diamond. If the lead lap is flat, 1 micron diam. will give a quick and satisfactory polish.

9. When the surface has reached a stage of clear areas the wanted mineral is showing 1 micron scratches - a hand polish using a slurry .03 micron alumina and distilled water with a soft tissue or pad; held in the hand will produce a clean satisfactory polish, - for P.S. and P.T.S. with NO surface relief.
10. When surface is satisfactory, clean specimens and place on a cool hotplate (less than 100°C) to warm. Using 1" circular glass discs and a cool melting thermal plastic (e.g. Crystalbond ND509. Lakeside 70°C) mount the polished surface on the glass discs being careful that the bond is flat. Mount the discs on regular petrographic slides by the same method.
11. Carefully offcut specimens being careful to maintain the identifying marking in some manner. Grind samples to translucence as per thin section techniques. This varies from specimen to specimen.
12. Leaving specimens mounted on glass, apply polish to the second side as previously explained.
13. When the samples are ready for use, they can be floated from the glass discs by using a suitable solvent.

#### Cold Mounting Modification

To prepare double polished thin sections for the Area 14 Orebody without heating, Lepage's Miracle Mender was substituted for thermal plastic cement when bonding the first polished surface to the 1" glass disc. As Miracle Mender does not bond two glass surfaces very well, an aluminum template with a 1" diameter hole was used for cutting and grinding instead of cementing the glass disc to a rectangular glass slide. Sections prepared with Miracle Mender required submersion in acetone for up to 8 hours to separate the thin section from the glass disc.

## APPENDIX 2.

X-ray Diffraction Identification of Intergrowth from Silver Islet

Ref <sup>1</sup>	Int <sup>2</sup>	d-spacing	S.D. <sup>3</sup>	galena	nickeline	annaberqite
1	S	3.1320	0.0946		10 $\bar{1}$ 0	
2	S	2.9210	0.2365	002		201 $\bar{3}$ 11
3	W	2.6468	0.0237		10 $\bar{1}$ 1	330
4	S	2.0942	0.1183	022		
5	VW	1.9466	0.0946		10 $\bar{1}$ 2	
6	M-S	1.8985	0.1183			132
7	M	1.7882	0.2365	113		
8	W	1.7073	0.0473	222		
9	W-M	1.6302	0.0237			511 460
10	VW	1.4846	0.5913	004		
11	VW	1.3544	0.1656	113		
12	W	1.3228	0.1656	024		
13	VW	1.2375	0.0946		0004	
14	W	1.2321	0.0473	442		
15	VW	0.9981	0.0237	531		
16	VW	0.9886	0.8987	244 or	006 $\bar{1}$	
17	W	0.9501	0.8286		10 $\bar{1}$ 5	
18	VVW	0.9142	0.9697		? $\bar{1}$	
19	VW	0.8572	0.8571	444	3141	
20	VVW	0.7950	0.5913	246		

---

<sup>1</sup> Reflection

<sup>2</sup> Intensity where S-strong; M-moderate; W-weak; V-very

<sup>3</sup> Standard Deviation

## APPENDIX 3.

Mineralogy of the Silver Islet Mine (modified after Tanton, 1931)

native elements	
silver .....	Ag
arquerite (mercurian silver)*.....	(Hg, Ag)
arsenic .....	As
sulfides	
argentite .....	Ag <sub>2</sub> S
chalcopyrite .....	CuFeS <sub>2</sub>
galena .....	PbS
marcasite .....	FeS <sub>2</sub>
millerite* .....	NiS
sphalerite .....	(Zn, Fe)S
bismuthinite .....	Bi <sub>2</sub> S <sub>3</sub>
arsenides and sulfarsenides	
chloanthite .....	(Ni, Co, Fe)As <sub>3-x</sub>
cobaltite .....	CoAsS
domeykite .....	Cu <sub>3</sub> As
nickeline .....	NiAs
smaltite .....	CoAsS
gersdorffite .....	NiAsS
safflorite .....	(Co, Fe, Ni)As <sub>2</sub>
antimonides	
breithauptite* .....	NiSb
sulfosalts	
tetrahedrite .....	Cu <sub>12</sub> Sb <sub>4</sub> S <sub>13</sub>
halides	
fluorite .....	CaF <sub>2</sub>
oxides	
quartz .....	SiO <sub>2</sub>
carbonates	
calcite .....	CaCO <sub>3</sub>
dolomite .....	CaMg(CO <sub>3</sub> ) <sub>2</sub>
rhodochrosite .....	MnCO <sub>3</sub>
sulfates	
barite .....	BaSO <sub>4</sub>
others	
annabergite .....	(Ni, Co) <sub>3</sub> (AsO <sub>4</sub> ) <sub>2</sub> ·8H <sub>2</sub> O
erythrite .....	(Co <sub>3</sub> (AsO <sub>4</sub> ))·8H <sub>2</sub> O

---

\* Not observed but presence inferred on the basis of chemical data.